How can the James Webb Space Telescope Measure First Light, Reionization, & Galaxy Assembly?

Rogier Windhorst (Arizona State University)

Collaborators: S. Cohen, R. Jansen, N. Hathi (ASU), C. Conselice (UK), & H. Yan (Carnegie)

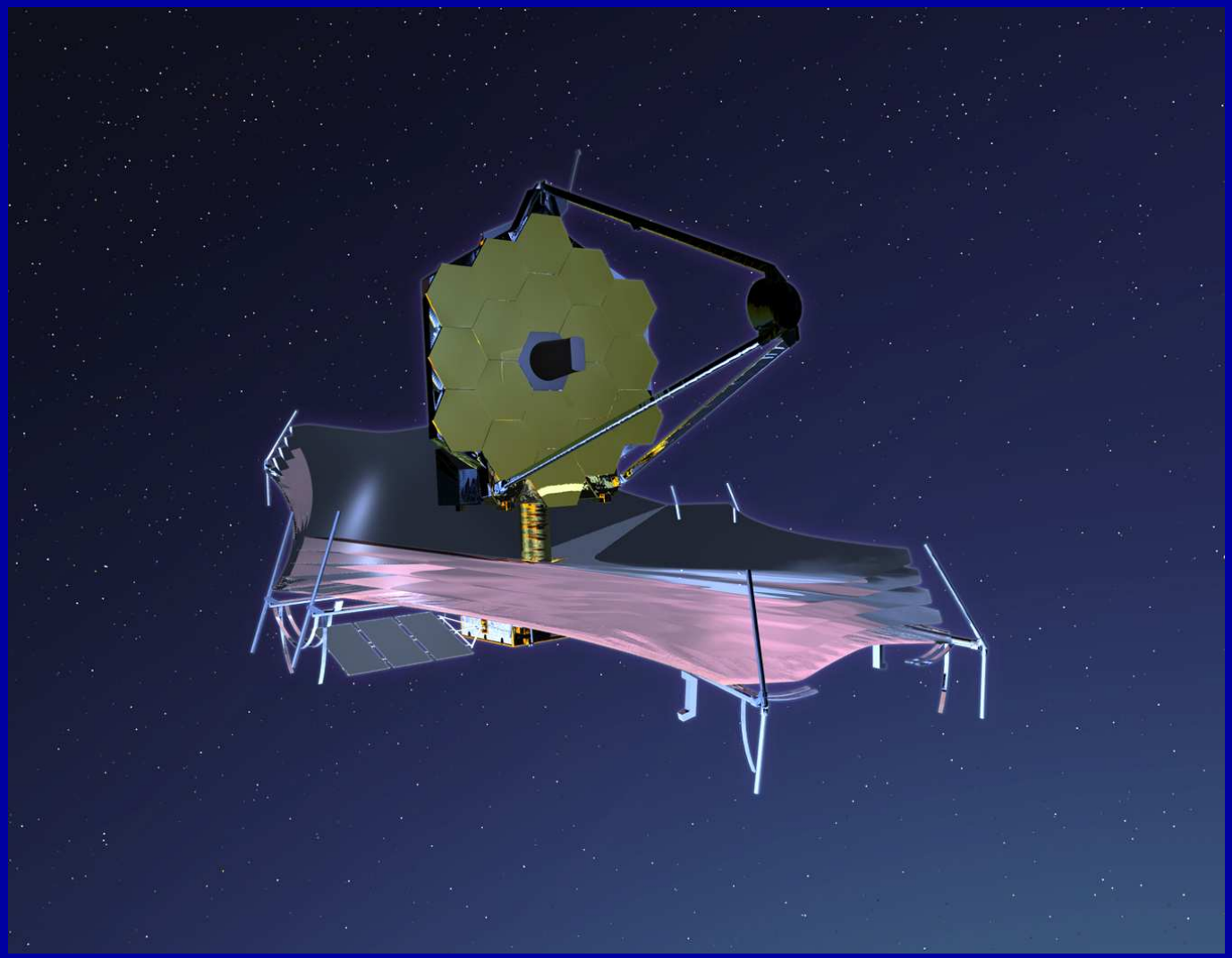

Colloquium at the Carnegie Institution of Washington, Pasadena, CA — Tuesday April 3, 2007

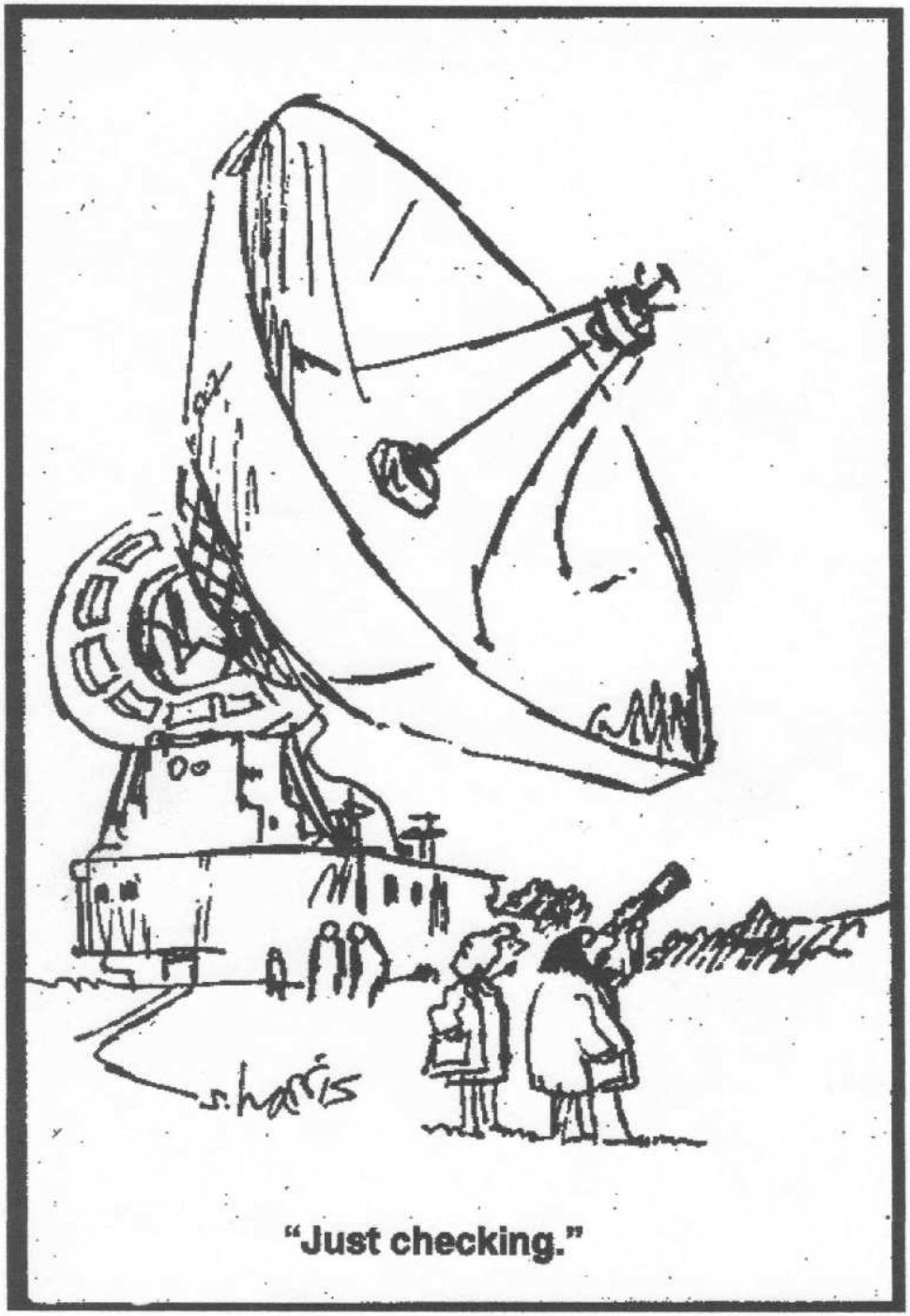

HST and JWST changed the career of this radio astronomer ...

Outline

- (1) What is JWST and how will it be deployed?
- (2) What instruments and sensitivity will JWST have?
- (3) How JWST can measure First Light and Reionization
- (4) How JWST can measure Galaxy Assembly
- (5) Predicted Galaxy Appearance for JWST at z$\simeq$1–15
- (6) Summary and Conclusions
- (7) Appendix: will JWST (& SKA) reach the Natural Confusion Limit?

Sponsored by NASA/JWST

ASU Arizona State University

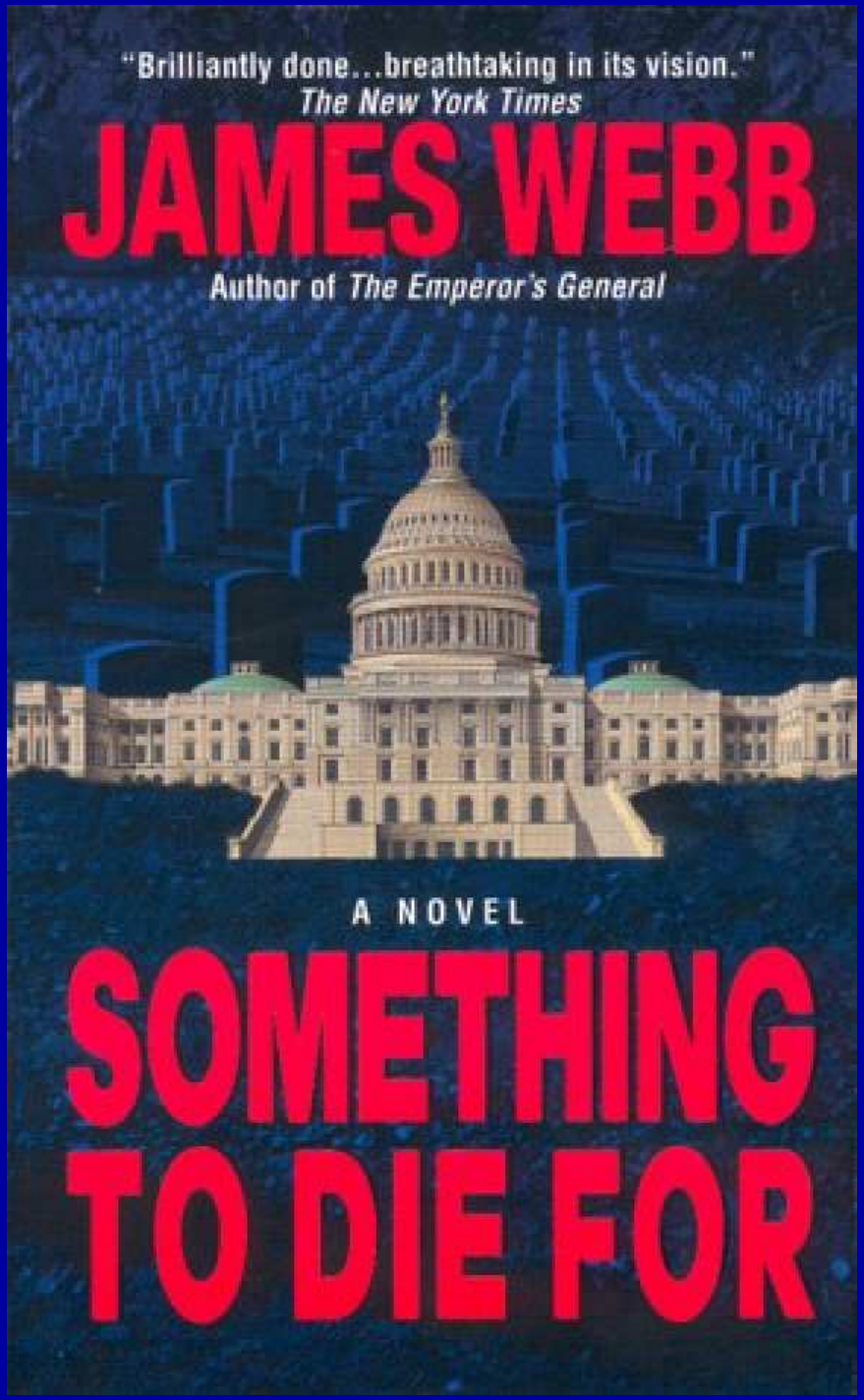

Need hard-working grad students & postdocs in $\gtrsim$2013 ... It'll be worth it!

James Webb Space Telescope

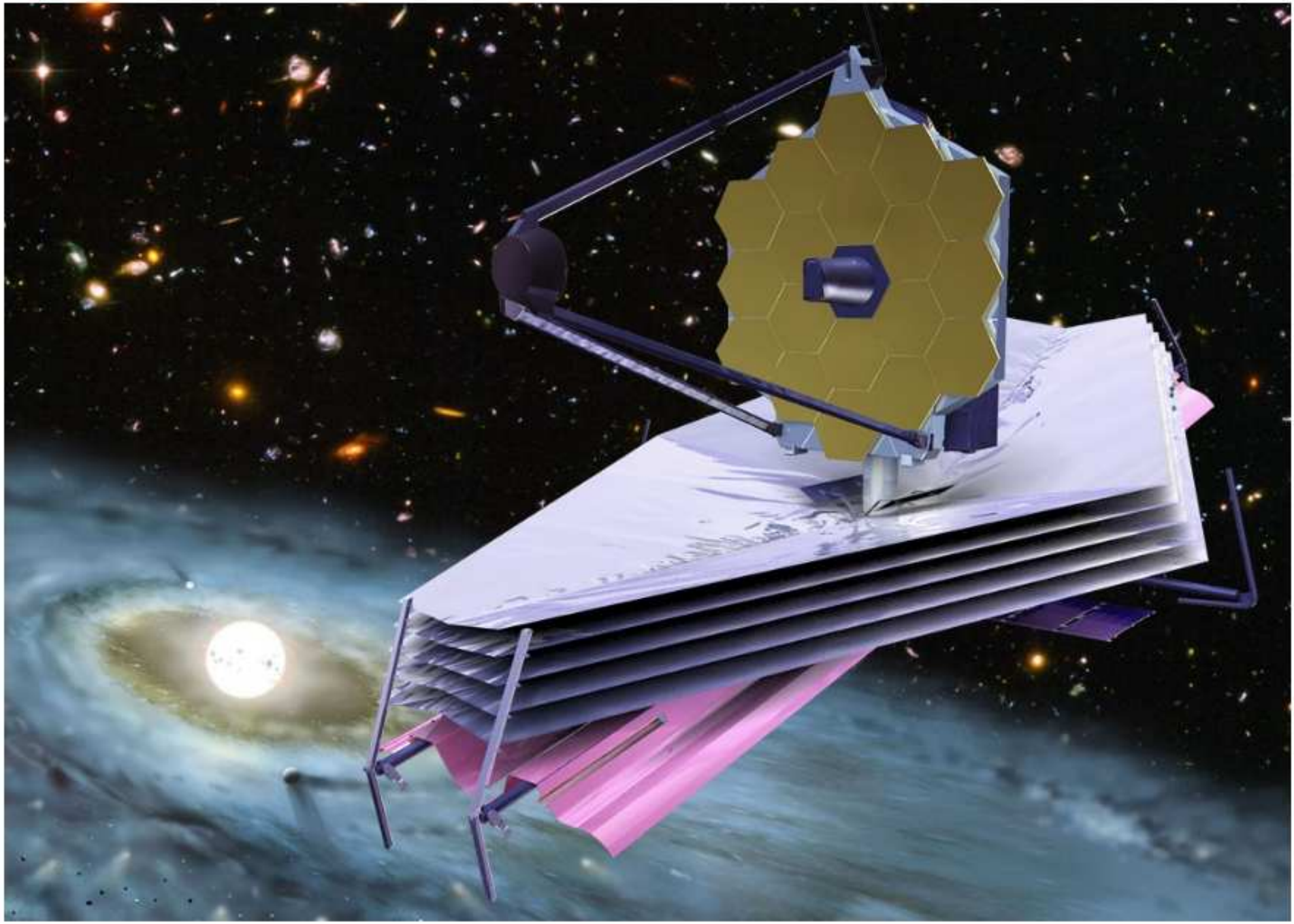

- (1) What is the James Webb Space Telescope (JWST)?

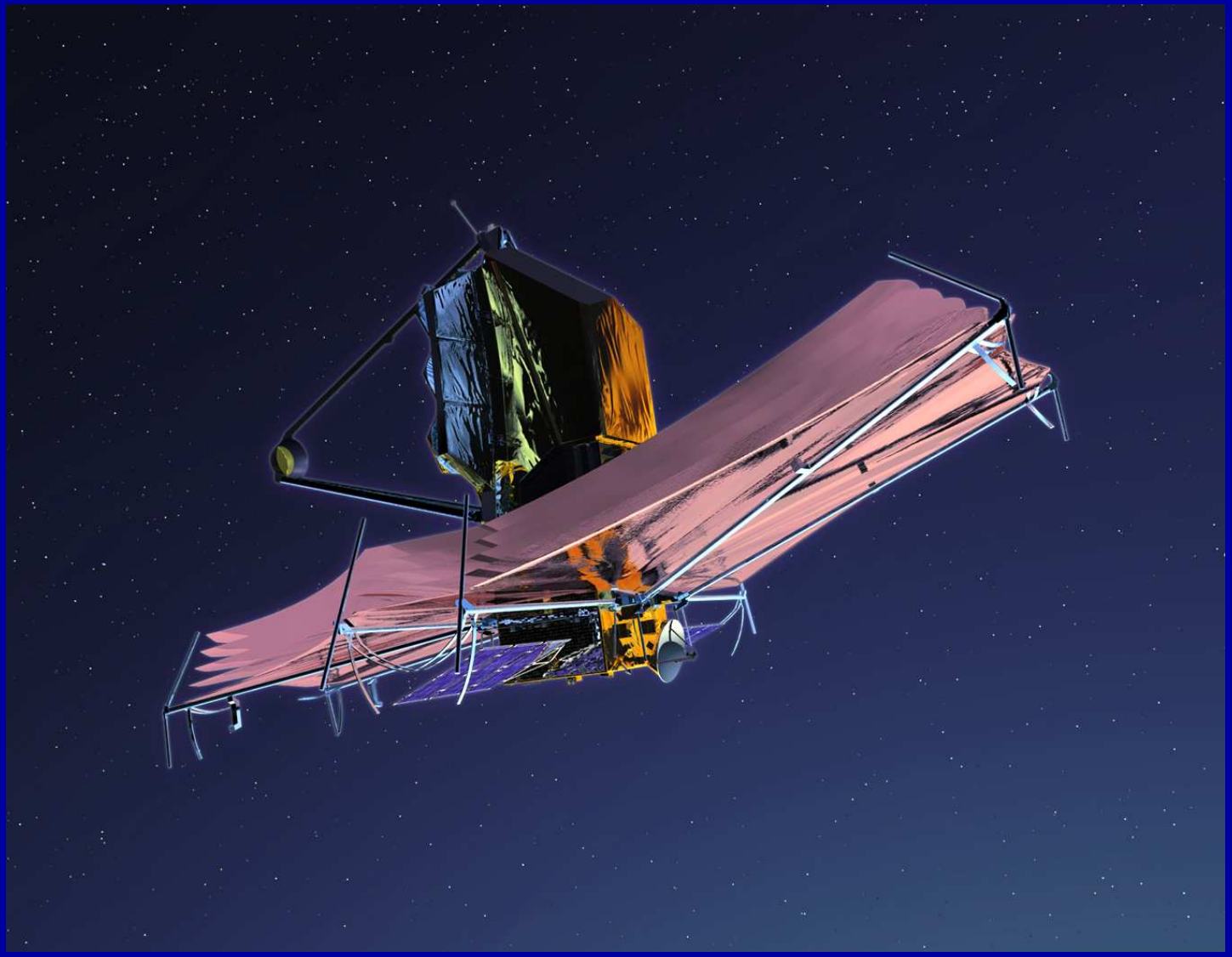

- A fully deployable 6.5 meter (25 m^2) segmented IR telescope for imaging and spectroscopy from 0.6 to 28 μm, to be launched by NASA $\gtrsim$2013. It has a nested array of sun-shields to keep its ambient temperature at 35-45 K, allowing faint imaging (AB$\lesssim$31.5) and spectroscopy (AB$\lesssim$29 mag).

Life size model of JWST: displayed at the Jan. 2007 AAS mtg in Seattle.

Life-sized model of JWST, used to test the deployment of its sun-shield.

Life-sized model of JWST, at NASA/GSFC Friday afternoon after 5 pm ...

- (1) How will JWST travel to its L2 orbit?

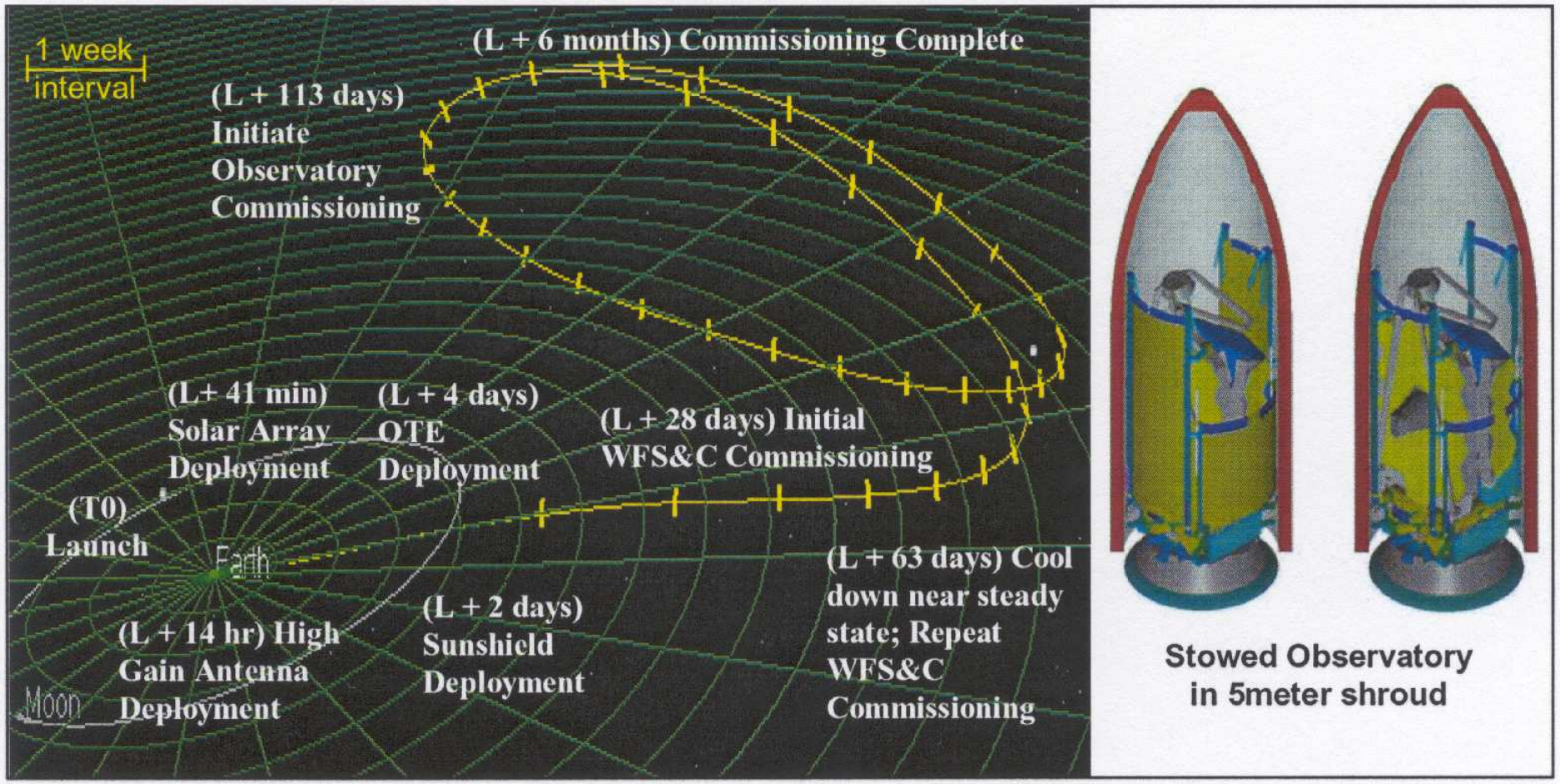

Figure 52. JWST orbit and trajectory to L2, and stowed view in 5 meter shroud.

After launch in $\gtrsim$2013 with an Ariane V vehicle, JWST will orbit around the the Earth–Sun Lagrange point L2. From there, JWST can cover the whole sky in segments that move along in RA with the Earth, have an observing efficiency $\gtrsim$70%, and send data back to Earth every day.

- (1) How will the JWST be automatically deployed?

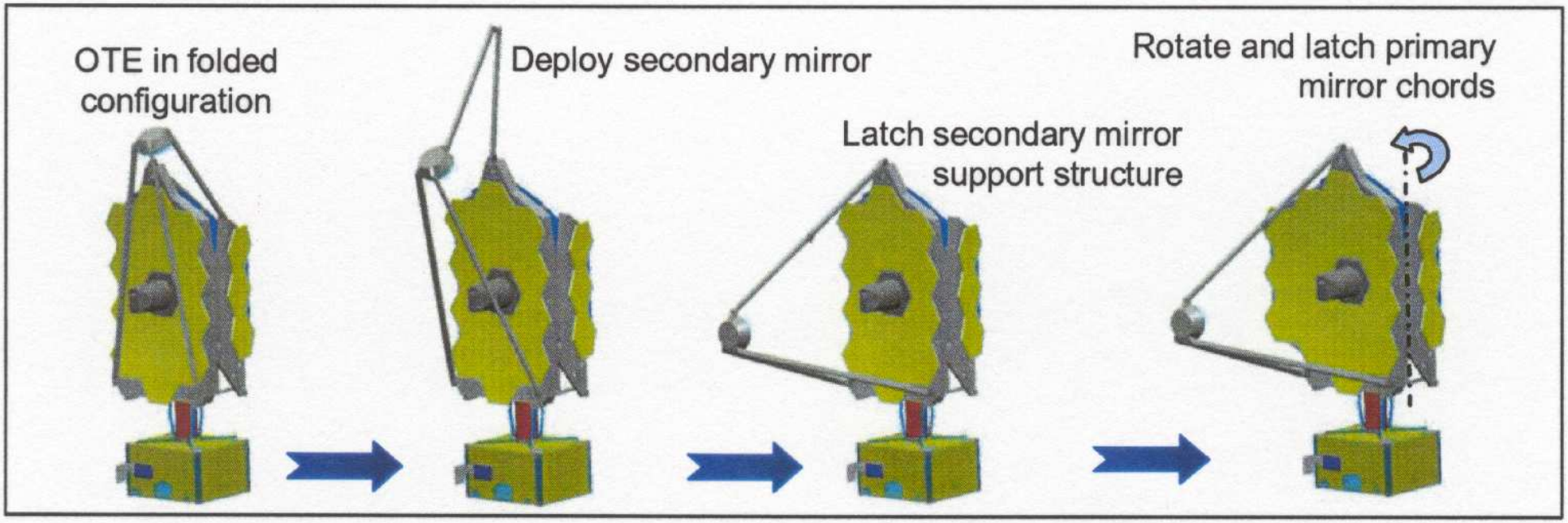

Figure 53. Telescope Deployment Sequence (Deployment steps 4 and 5)

During its several month journey to L2, JWST will be automatically deployed in phases, its instruments will be tested and calibrated, and it will then be inserted into an L2 halo orbit.

From an orbit around the the Earth–Sun Lagrange point L2, JWST can cover the whole sky in segments, have an observing efficiency $\gtrsim 70\%$, and send data back to Earth every day.

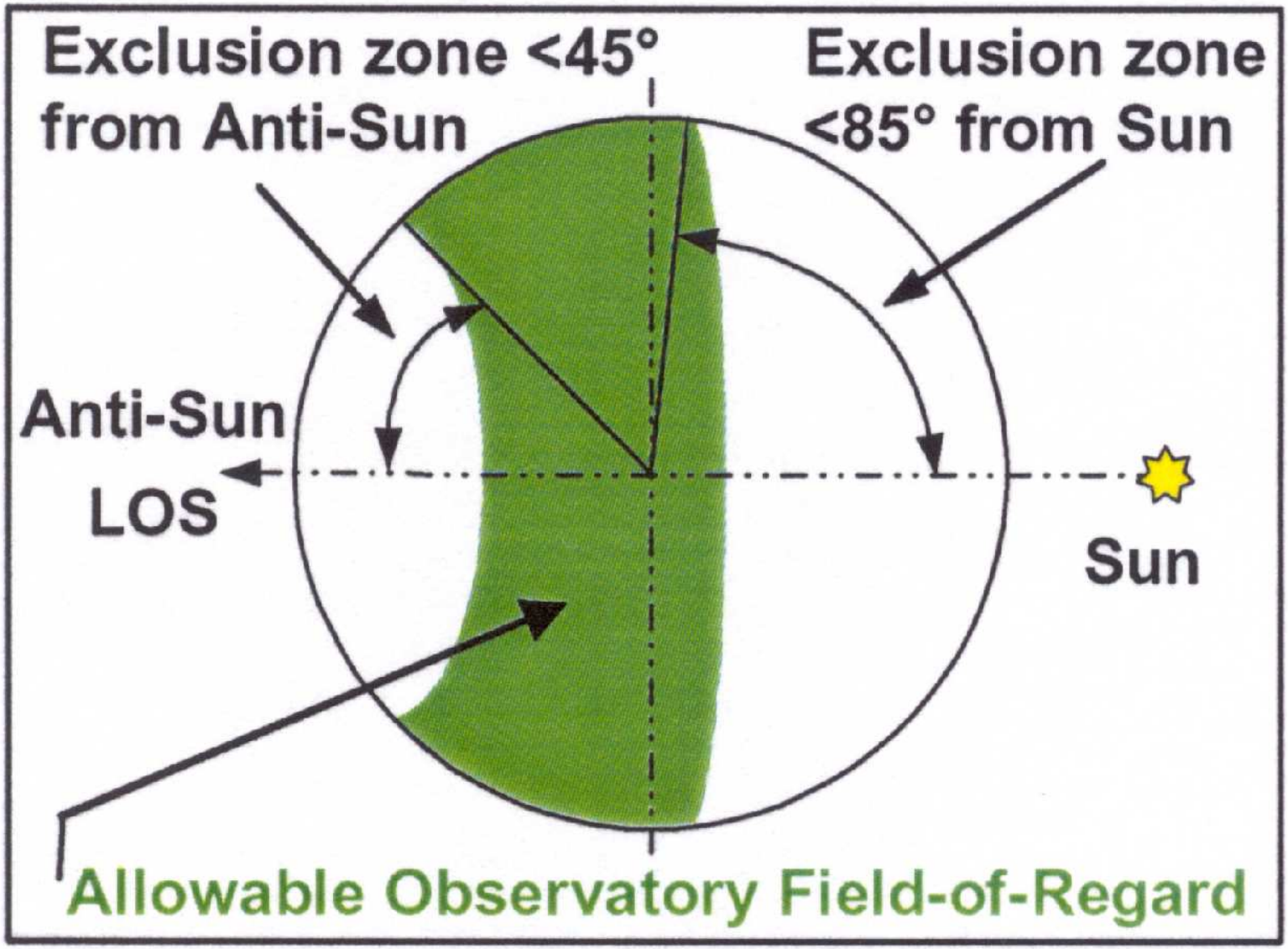

Figure 30. Observatory field of regard (FOR).

JWST can observe segments of sky that move around as it orbits the Sun.

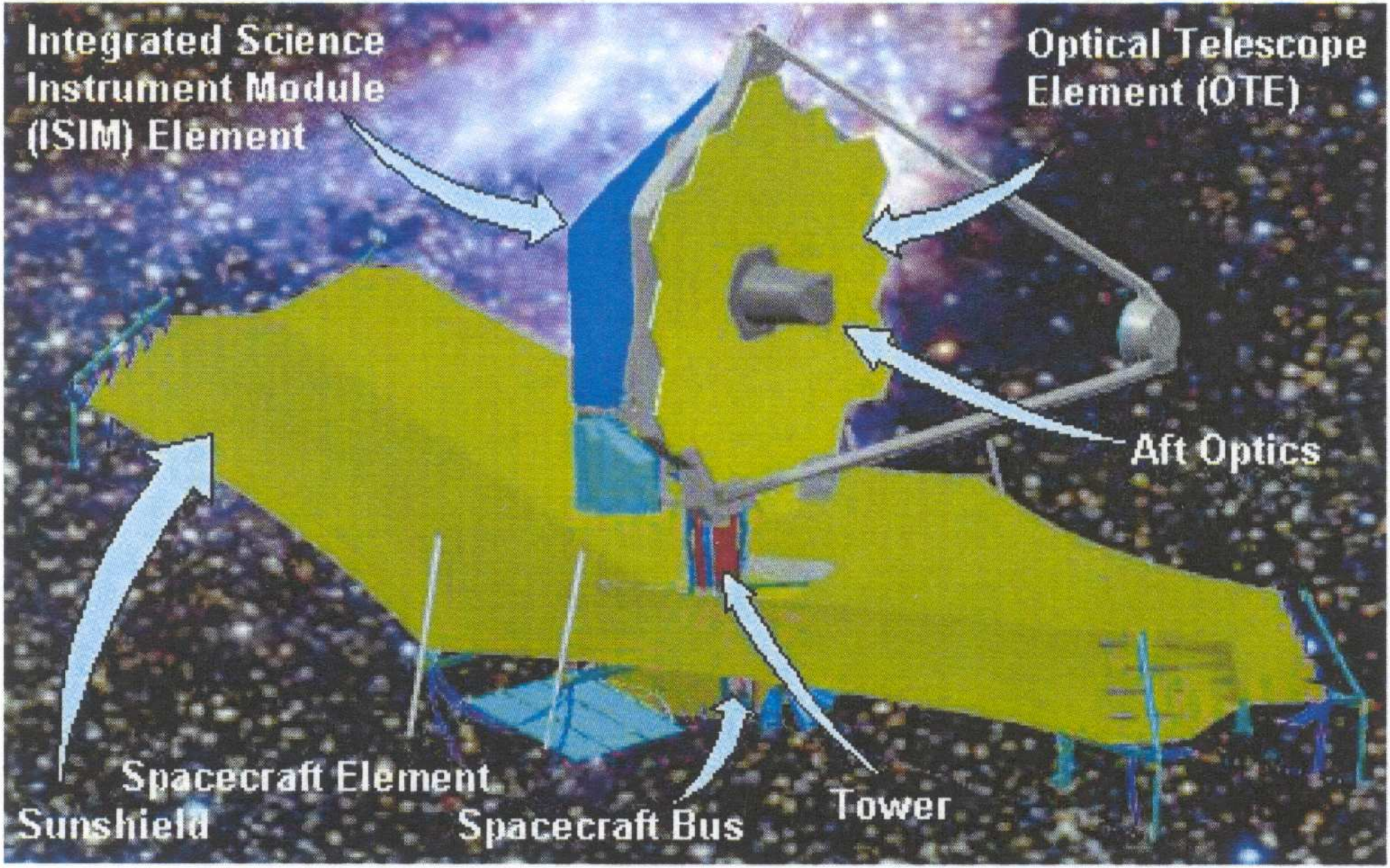

JWST mission reviewed in Gardner, J. P., et al. 2006, Space Science Reviews, Vol. 123, pg. 485–606 (astro-ph/0606175)

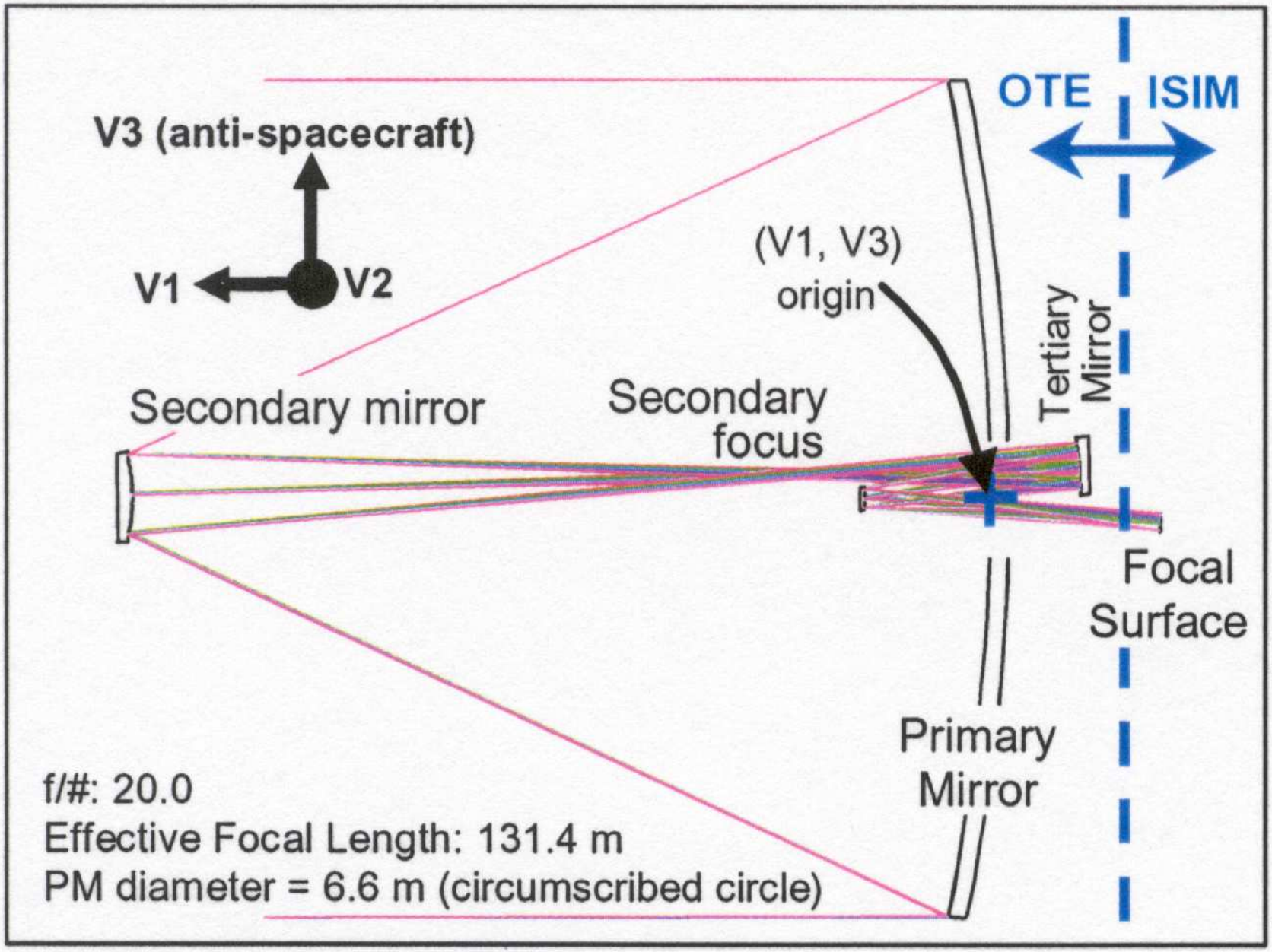

Figure 33. OTE optical layout

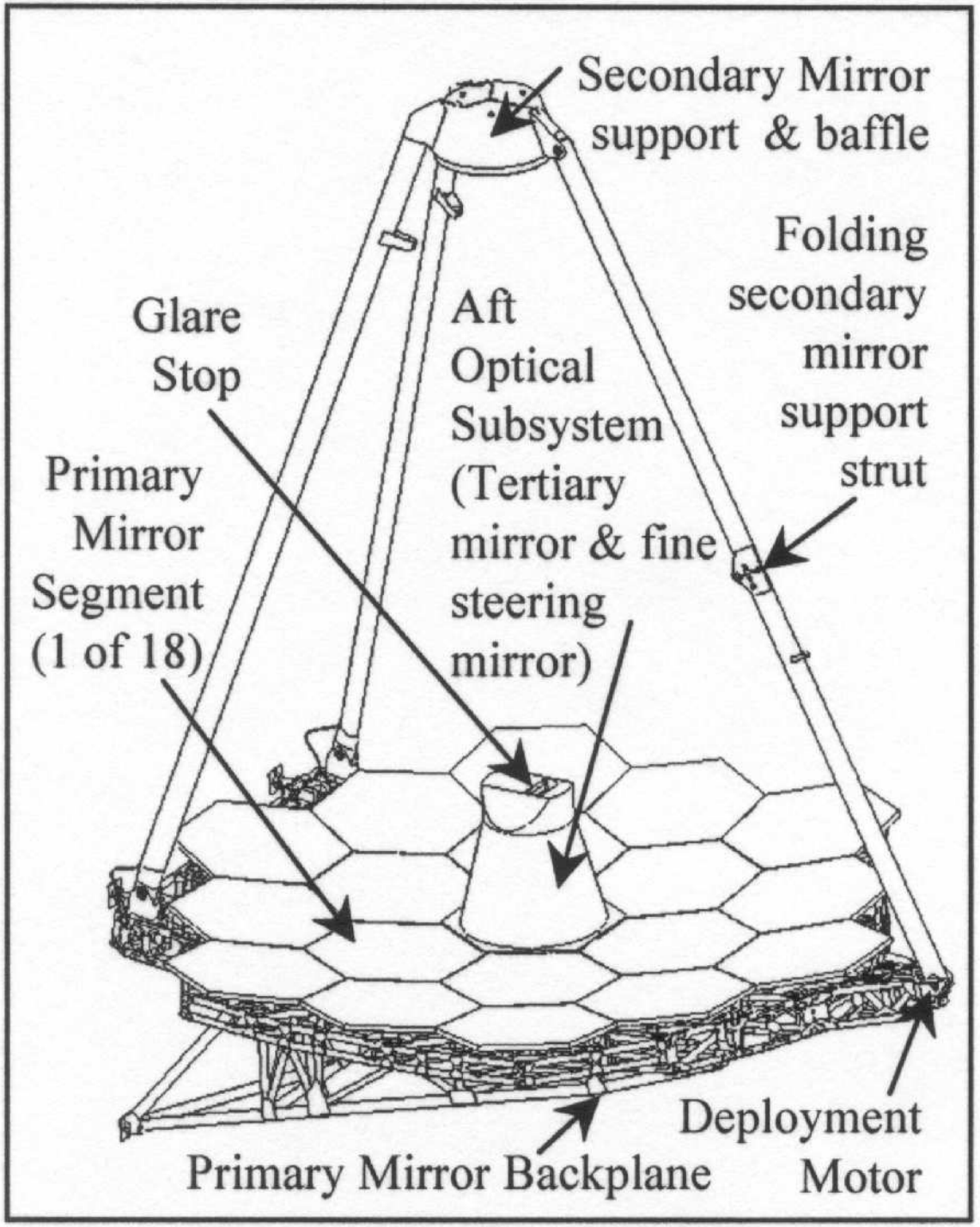
Secondary Mirror
support & baffle
Folding
secondary
mirror
support
strut
Glare
Stop
Aft
Optical
Subsystem
(Tertiary
mirror & fine
steering
mirror)
Primary
Mirror
Segment
(1 of 18)
Deployment
Motor
Primary Mirror Backplane

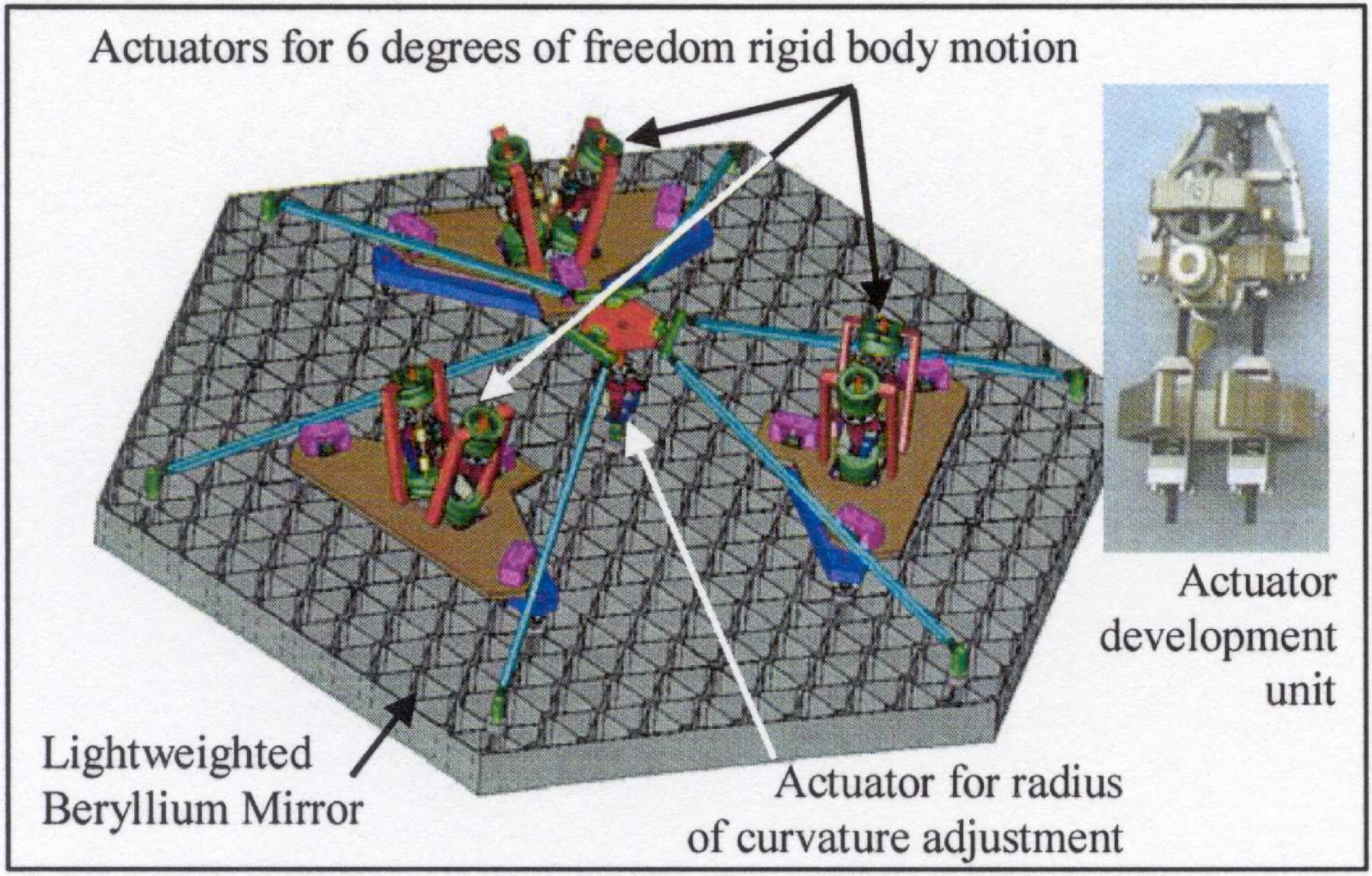

Figure 36. Rear view of a primary mirror segment.

Active mirror segment support through hexapods, similar to Keck.

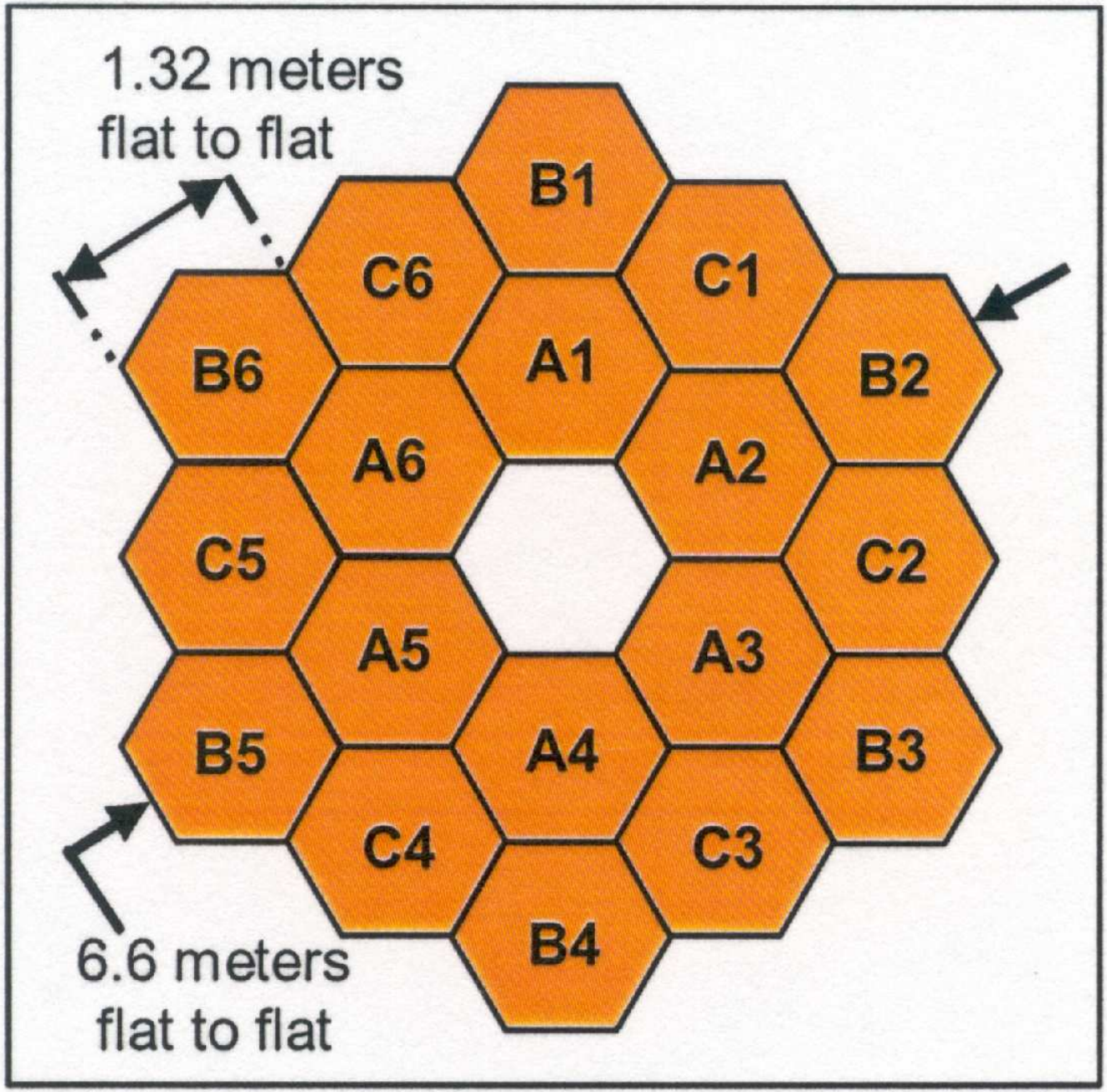

Edge-to-edge diameter is 6.60 m, but effective circular diameter is 5.85 m.

Cannot cleanly descope aperture without doing major harm to PSF.

Despite NASA's CAN-do approach: Must find all the cans-of-worms ...

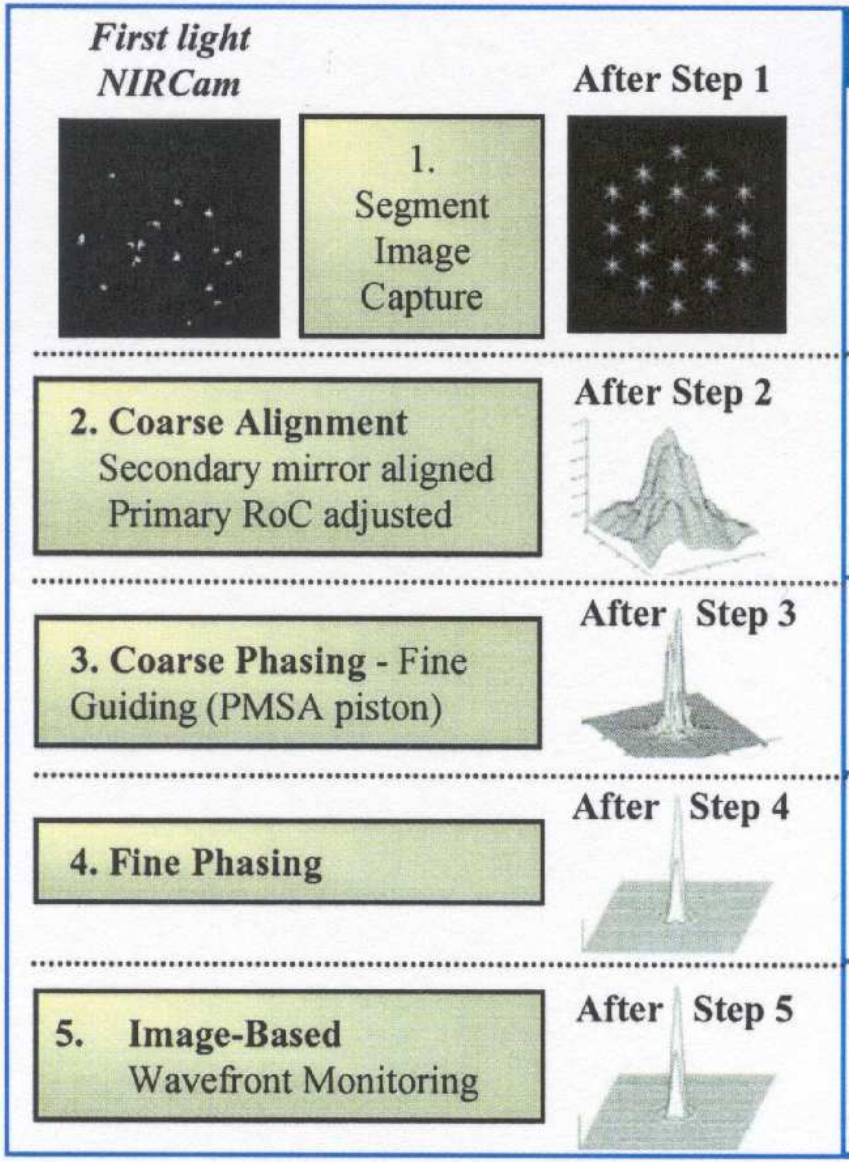

	Initial Capture	Final Condition
1. Segment Image Capture	18 individual 1.6-m diameter aberrated sub-telescope images PM segments: < 1 mm, < 2 arcmin tilt SM: < 3 mm, < 5 arcmin tilt	PM segments: < 100 μm, < 2 arcsec tilt SM: < 3 mm, < 5 arcmin tilt
2. Coarse Alignment Secondary mirror aligned Primary RoC adjusted	Primary Mirror segments: < 1 mm, < 10 arcsec tilt Secondary Mirror : < 3 mm, < 5 arcmin tilt	WFE < 200 mm (rms)
3. Coarse Phasing - Fine Guiding (PMSA piston)	WFE: < 250 μm rms	WFE < 1 μm (rms)
4. Fine Phasing	WFE: < 5 μm (rms)	WFE < 110 nm (rms)
5. Image-Based Wavefront Monitoring	WFE: < 150 nm (rms)	WFE < 110 nm (rms)

Figure 38. WFS&C commissioning and maintenance.

JWST's Wave Front Sensing and Control is similar to that at Keck and HET. Successful 2006 demo of H/W, S/W on 6/1 scale model (2μm-Strehl$\gtrsim$0.85).

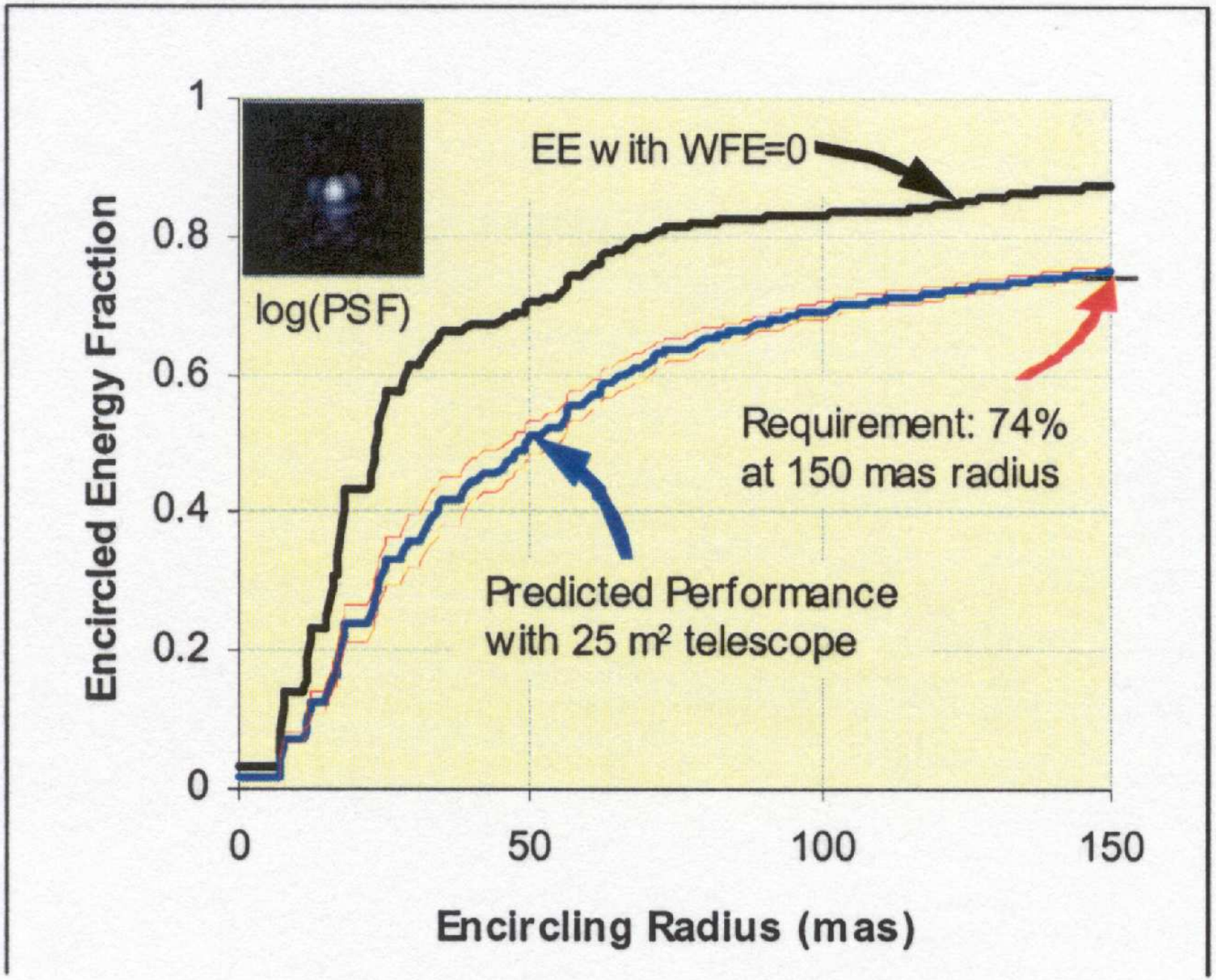

1/6 Scale model: system can produce diffraction limited images at 2.0μm.

• (2) What instruments will JWST have?

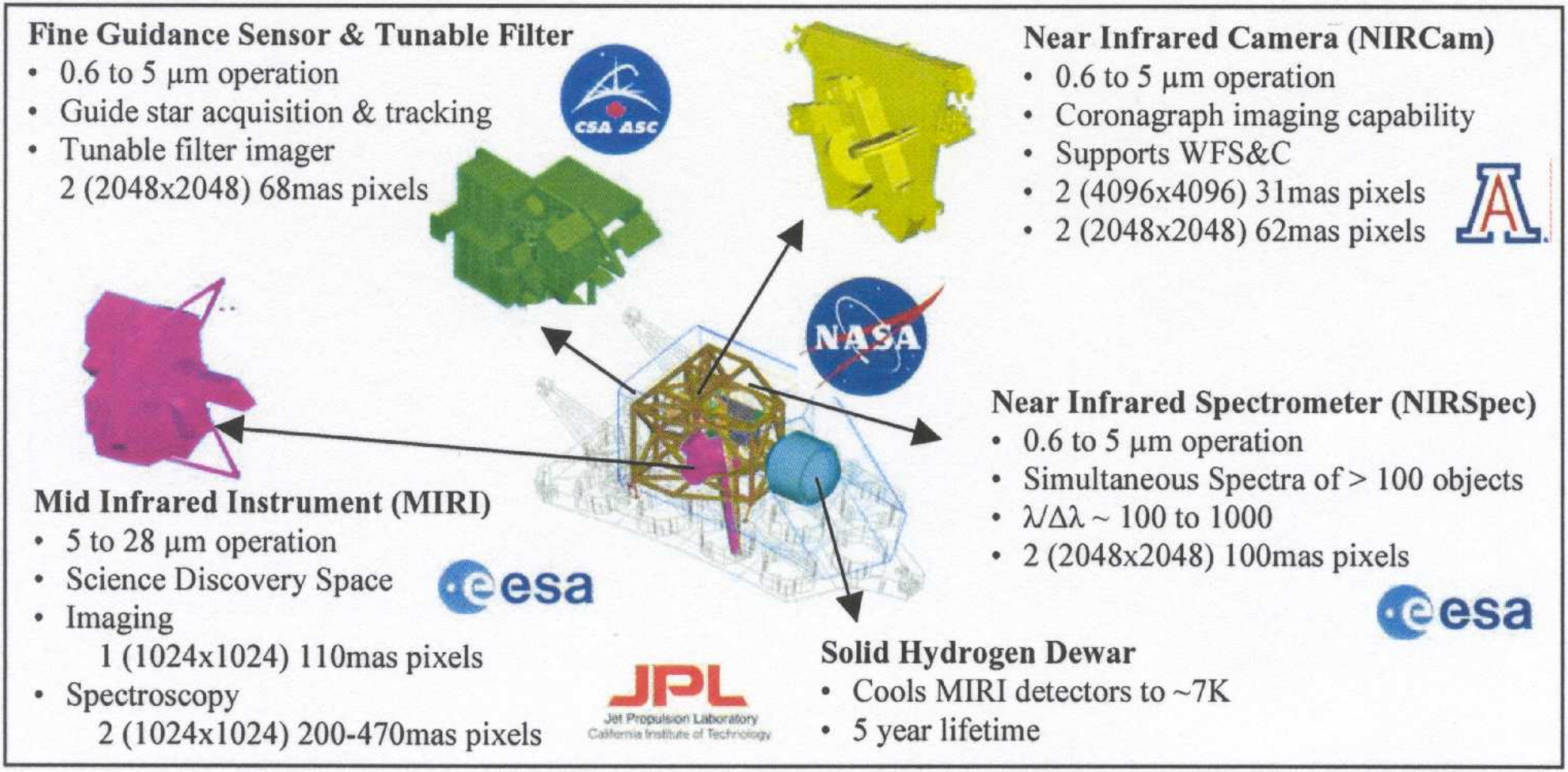

Figure 37. ISIM element and its science instrumentation.

The JWST instrument complement: US (UofA), ESA, and CSA.

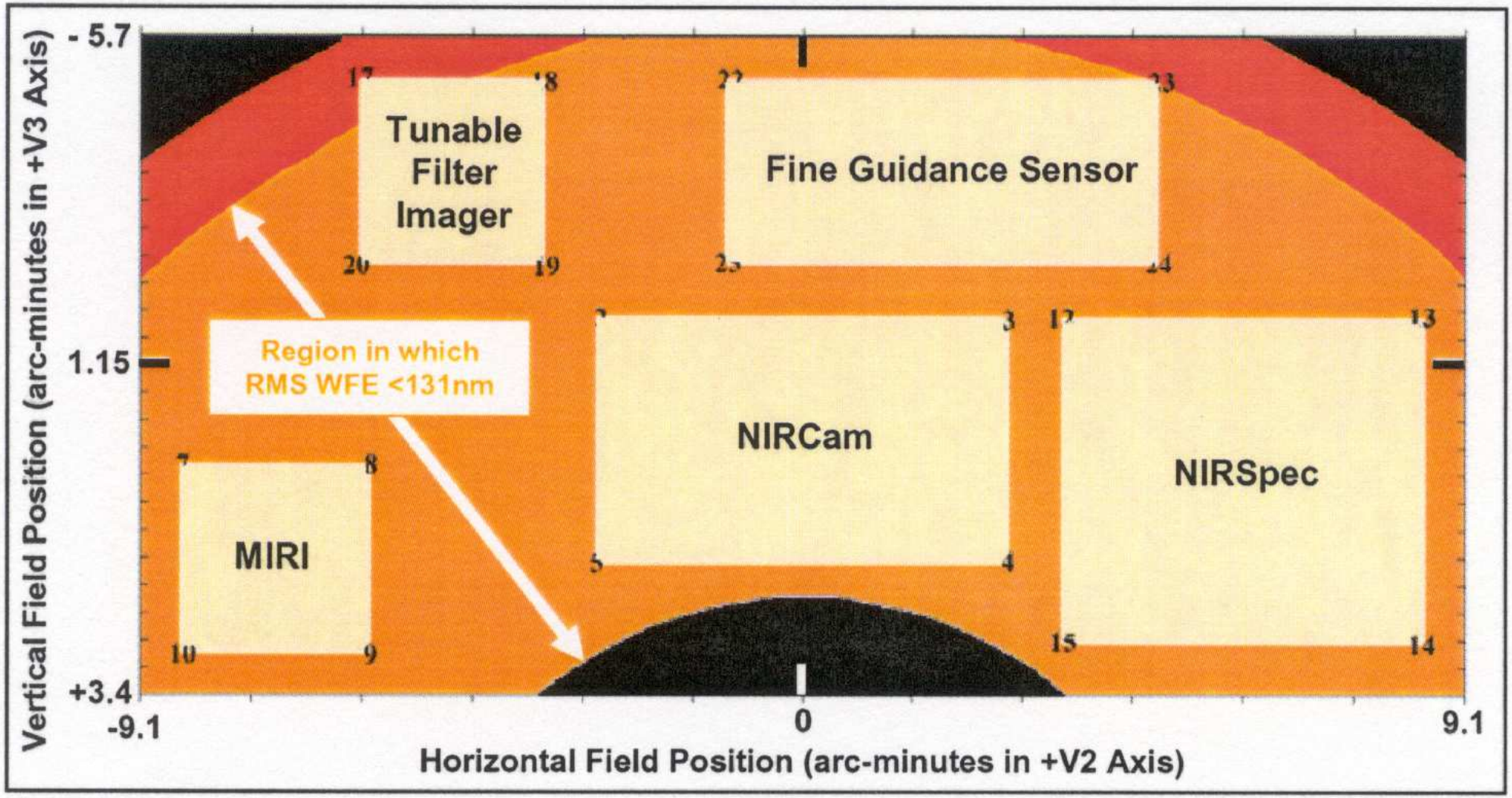

Figure 34. Placement of the ISIM instrument FPAs in the OTE field of view.

JWST instruments can in principle be used in parallel (not yet implemented).

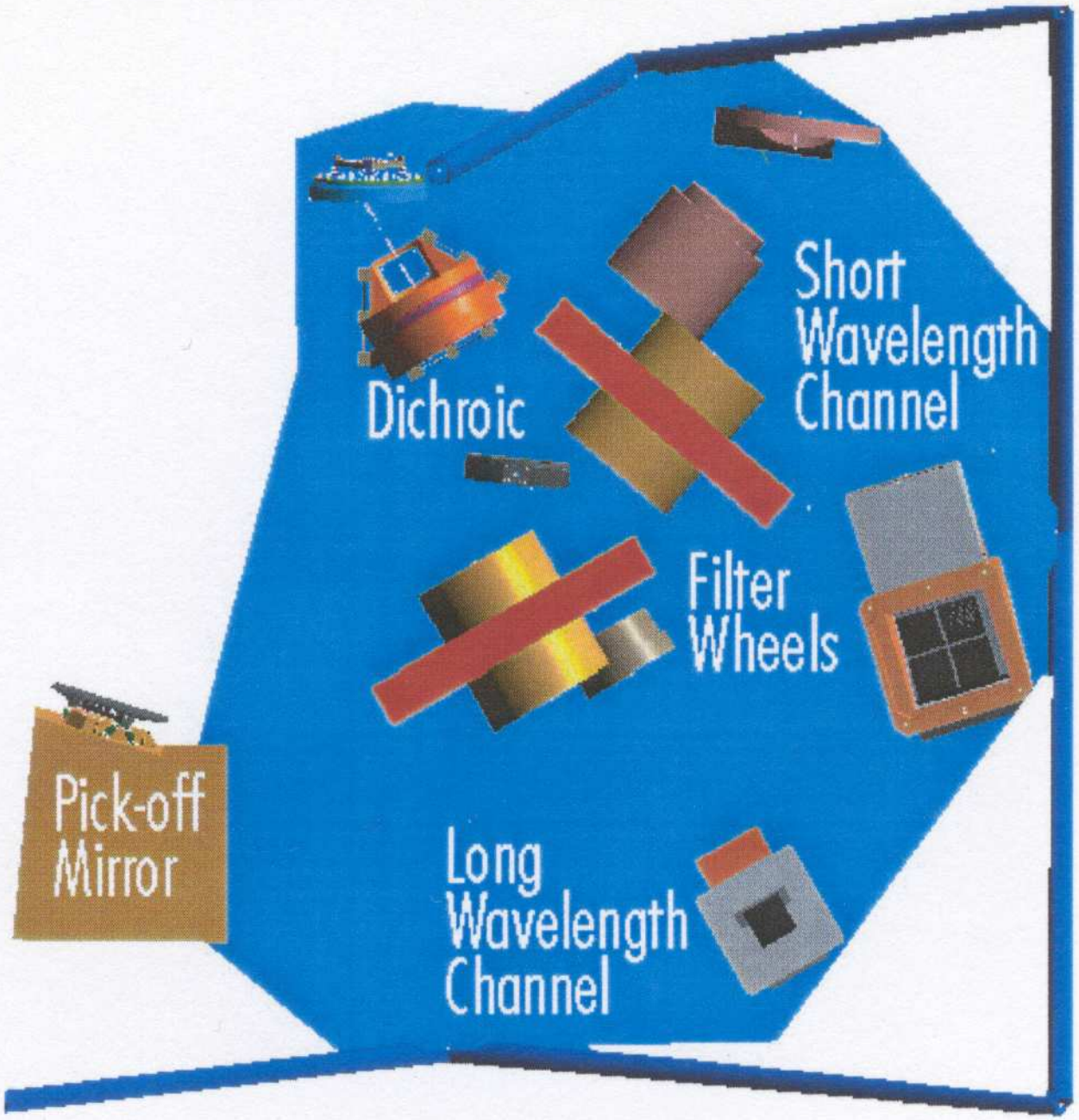

Figure 43. Optical layout of one of two NIRCam imaging modules.

- (2) What instruments will JWST have?

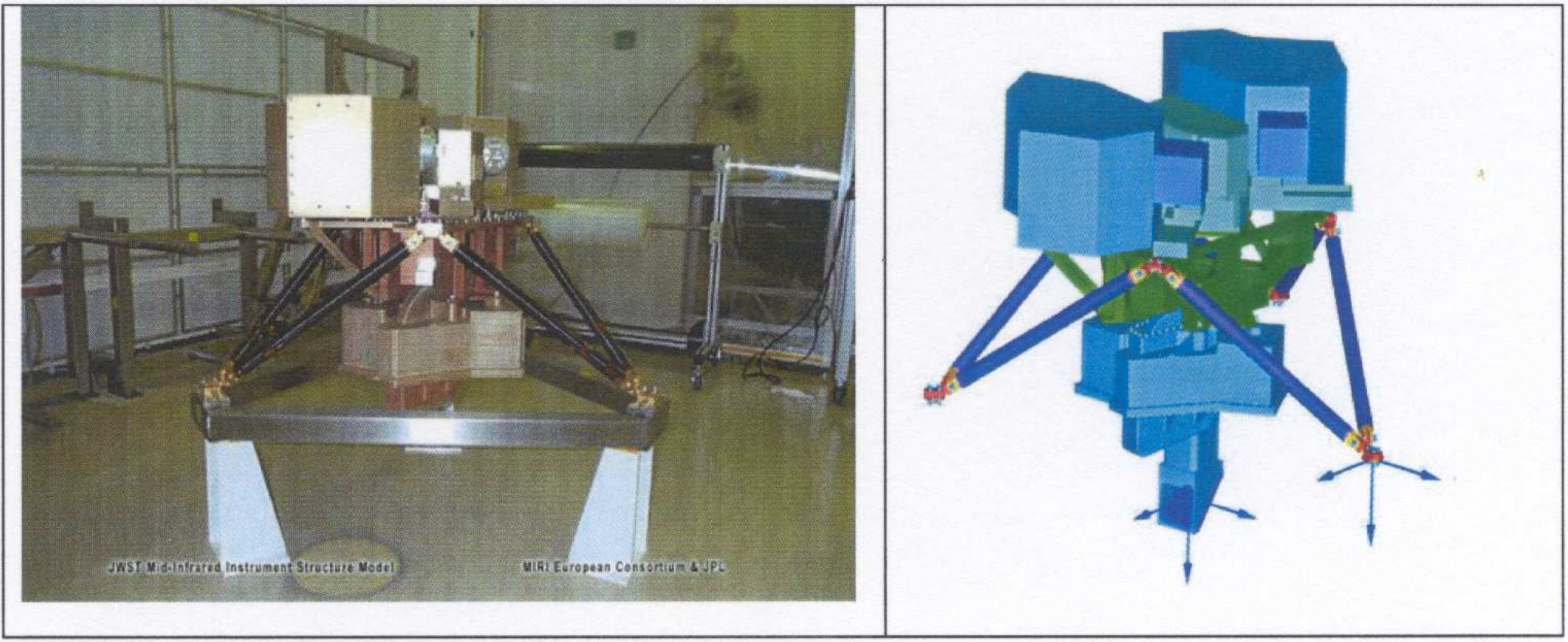

Figure 47. The MIRI structural and thermal model (left) compared to a computer design of the instrument (right).

The Mid-Infra-Red Instrument MIRI made by an UofA + JPL + ESA consortium will do imaging and spectroscopy from 5–28 μm. MIRI is actively cooled by a cryocooler, so that its lifetime is not limited by consumables.

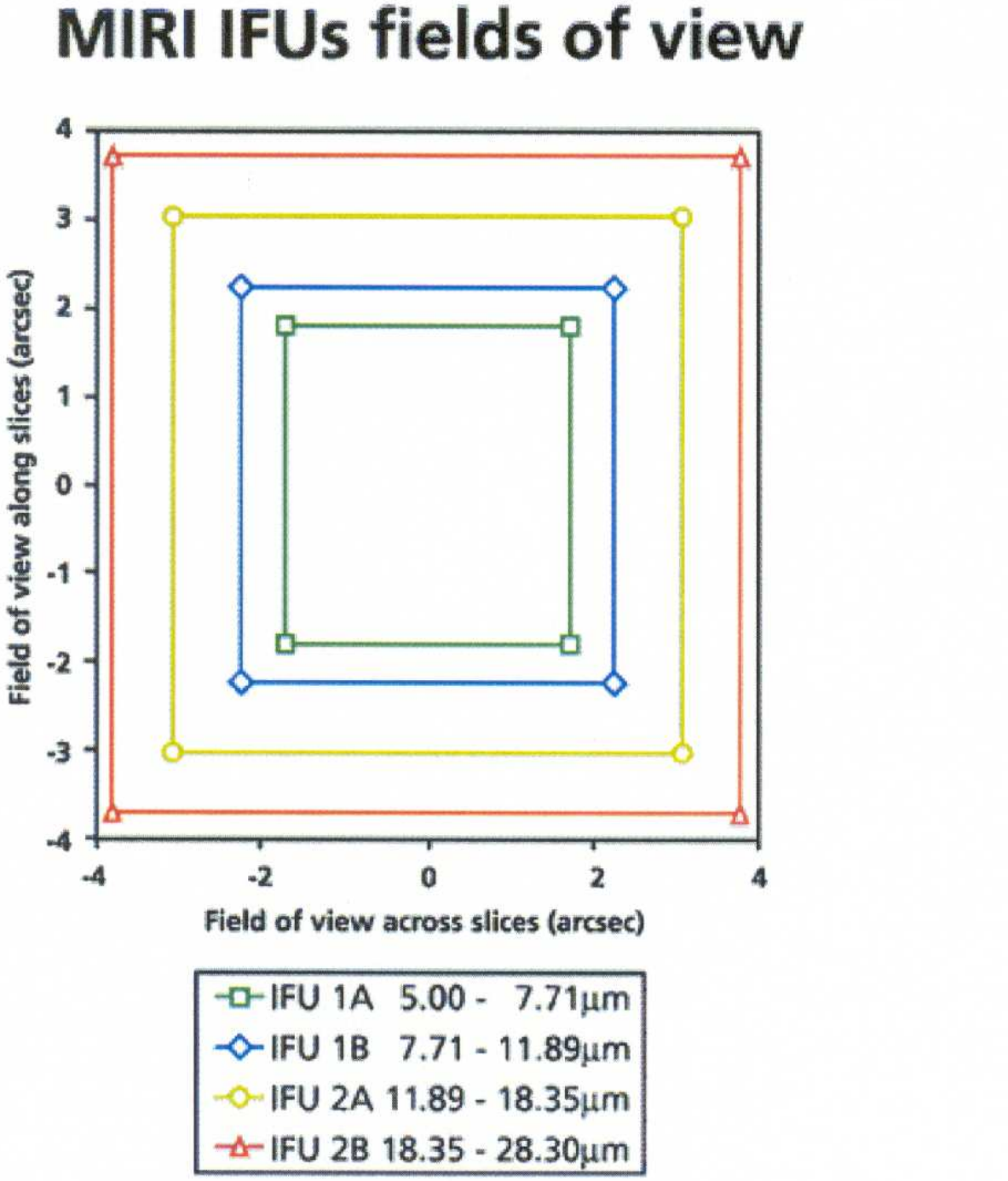

Figure 49. Fields of view of the MIRI IFU spectrograph.

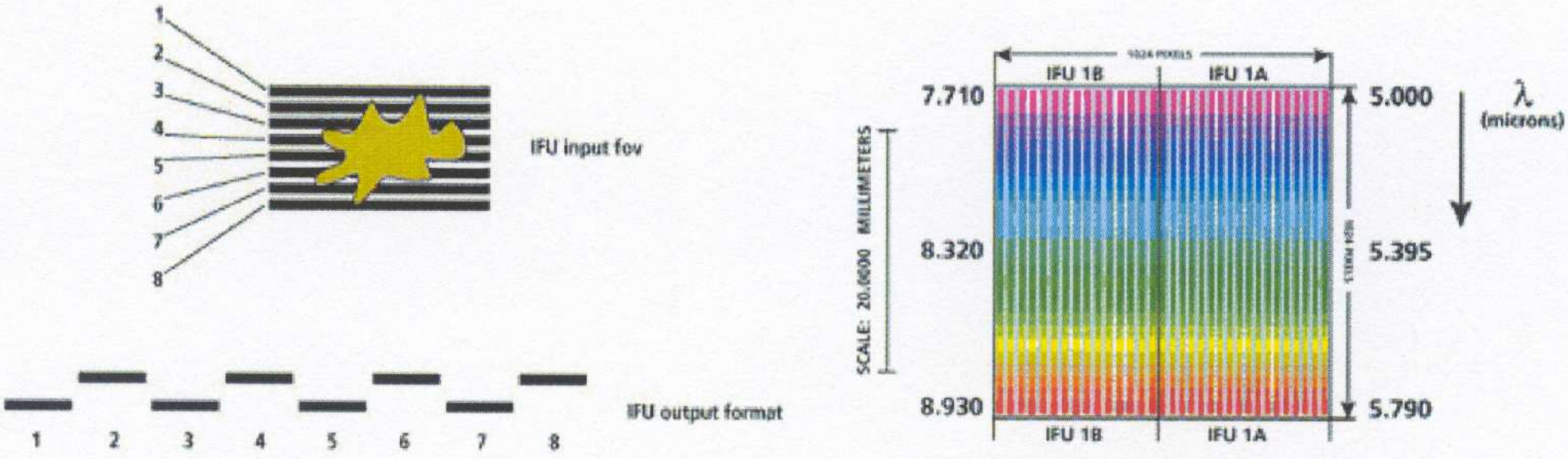

Figure 50. Schematic illustration of the MIRI IFU image slicer format (left) and dispersed spectra on detector (right)

The MIRI Integral Field Unit (IFU) has an image slicer that makes spatially resolved spectra at wavelengths 5 μm$\lesssim\lambda\lesssim$9 μm.

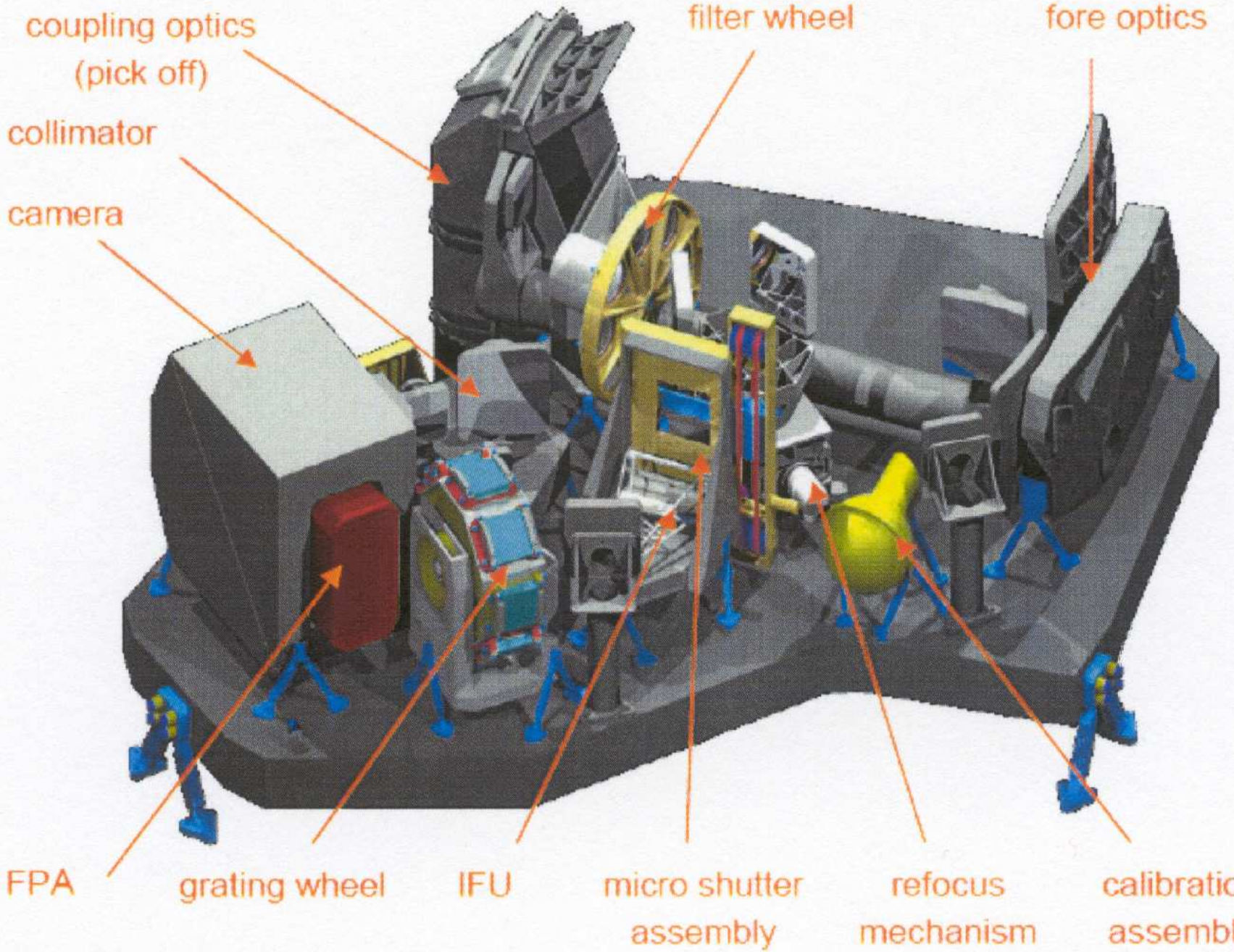

Figure 45. The NIRSpec instrument.

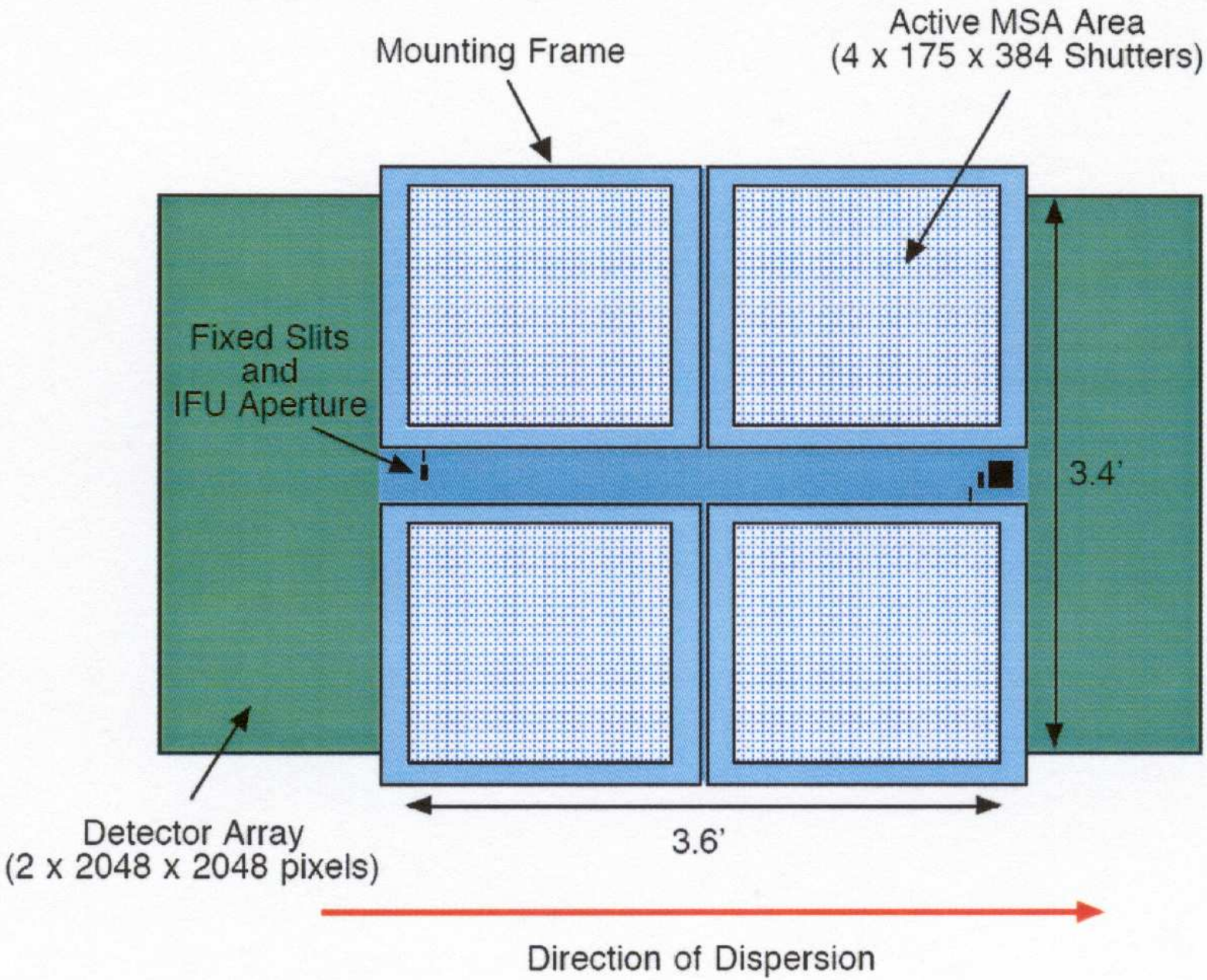

Figure 46. Schematic layout of the NIRSpec slit mask overlaid the detector array projected to the same angular scale.

• (2) What sensitivity will JWST have?

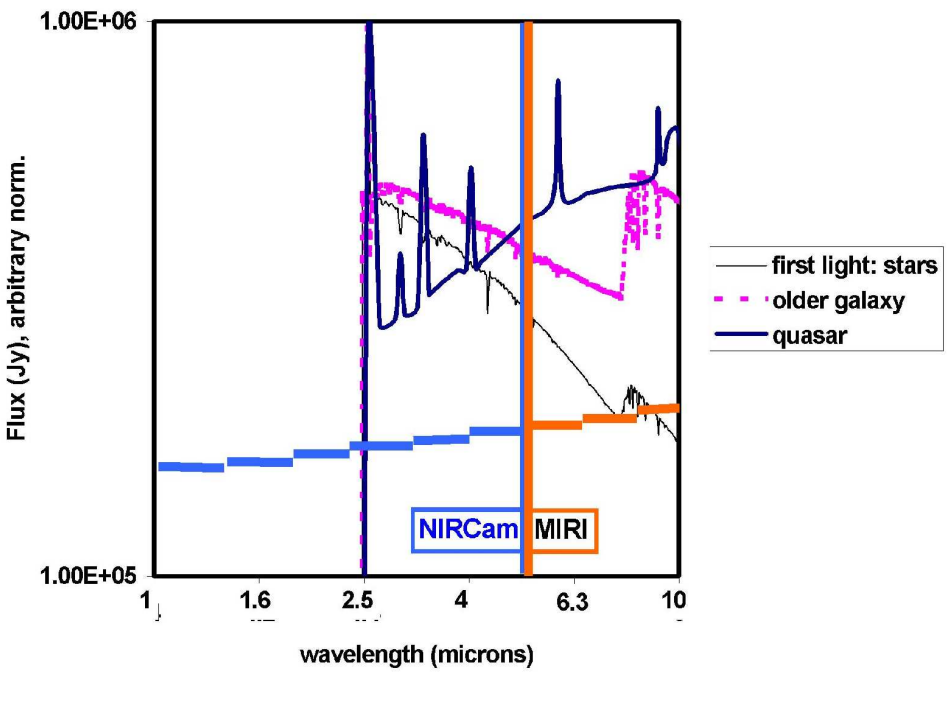

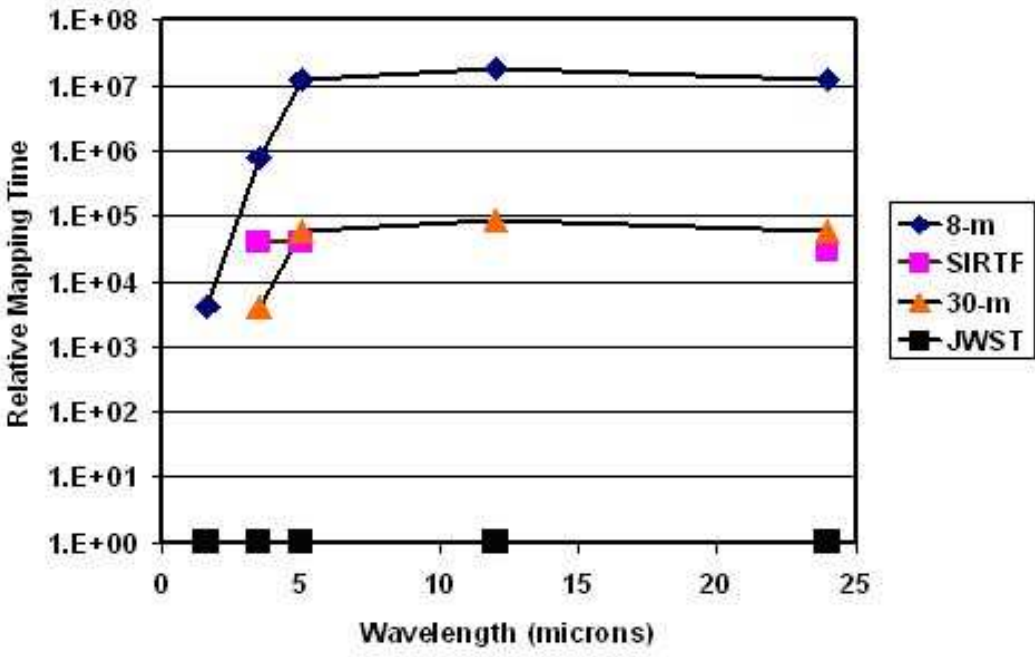

The NIRCam and MIRI sensitivity complement each other straddling 5 μm in wavelength, and together allow objects to be found to redshifts z=15–20 in $\sim 10^5$ sec (28 hrs) integration times.

The left panel shows the NIRCam and MIRI broadband sensitivity to a Quasar, a "First Light" galaxy dominated by massive stars, and a 50 Myr "old" galaxy, all at z=20. The right panel shows the relative survey time versus wavelength that Spitzer, a ground-based IR-optimized 8-m (Gemini) and a 30-m telescope would need to match JWST.

240 hrs HST/ACS in Vi'z' in the Hubble UltraDeep Field (HUDF)

6.5m JWST PSF's models (Ball Aerospace and GSFC):

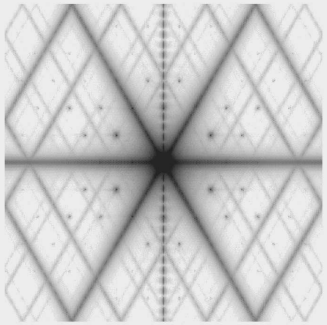

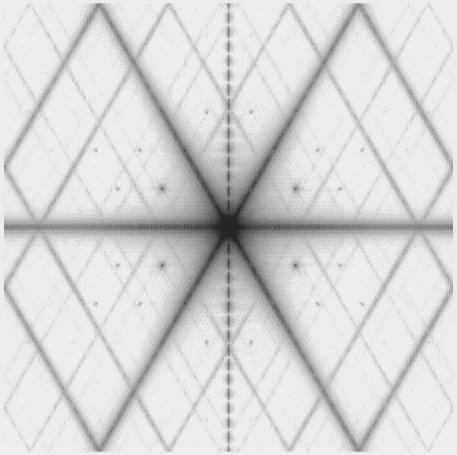

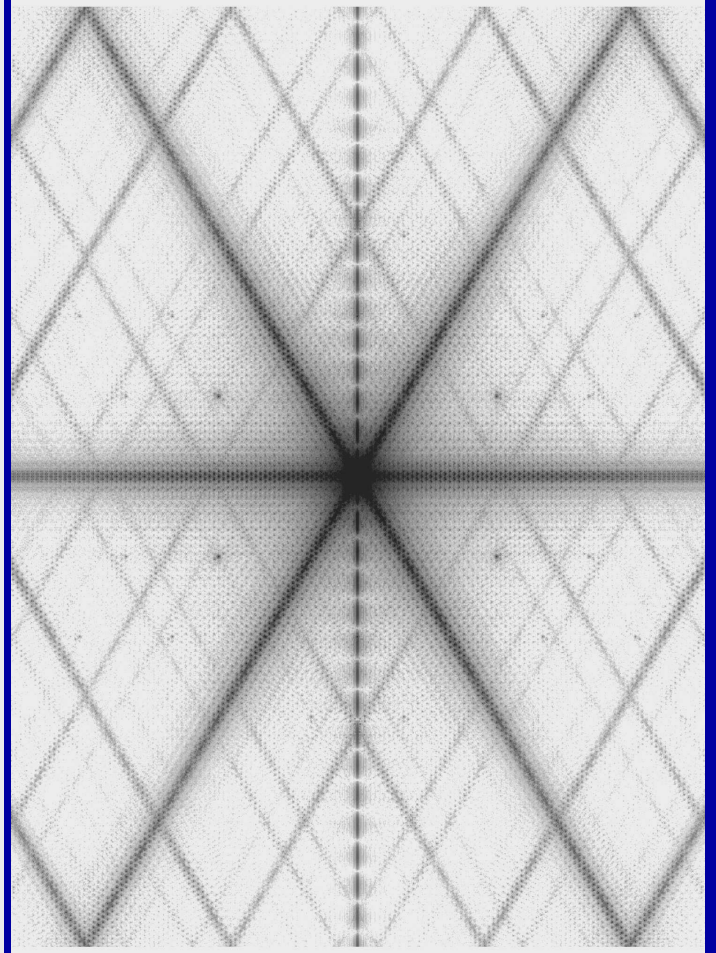

NIRCam 0.7 μm 1.0 μm ($<$150 nm WFE) 2.0 μm (diffr. limit)

Design PSF's are shown at logarithmic stretch: they have $\gtrsim$74% EE at r$\lesssim$0$''\!.$15 at 1.0μm, and are diffraction limited at 2.0μm (Strehl$\gtrsim$0.80).

$\lesssim$20 hrs JWST NIRCam at 0.7, 0.9, 2.0 μm in the HUDF

Truth≡240 hrs HUDF Vi'z' $\lesssim$20 hrs JWST 0.7, 0.9, 2.0 μm

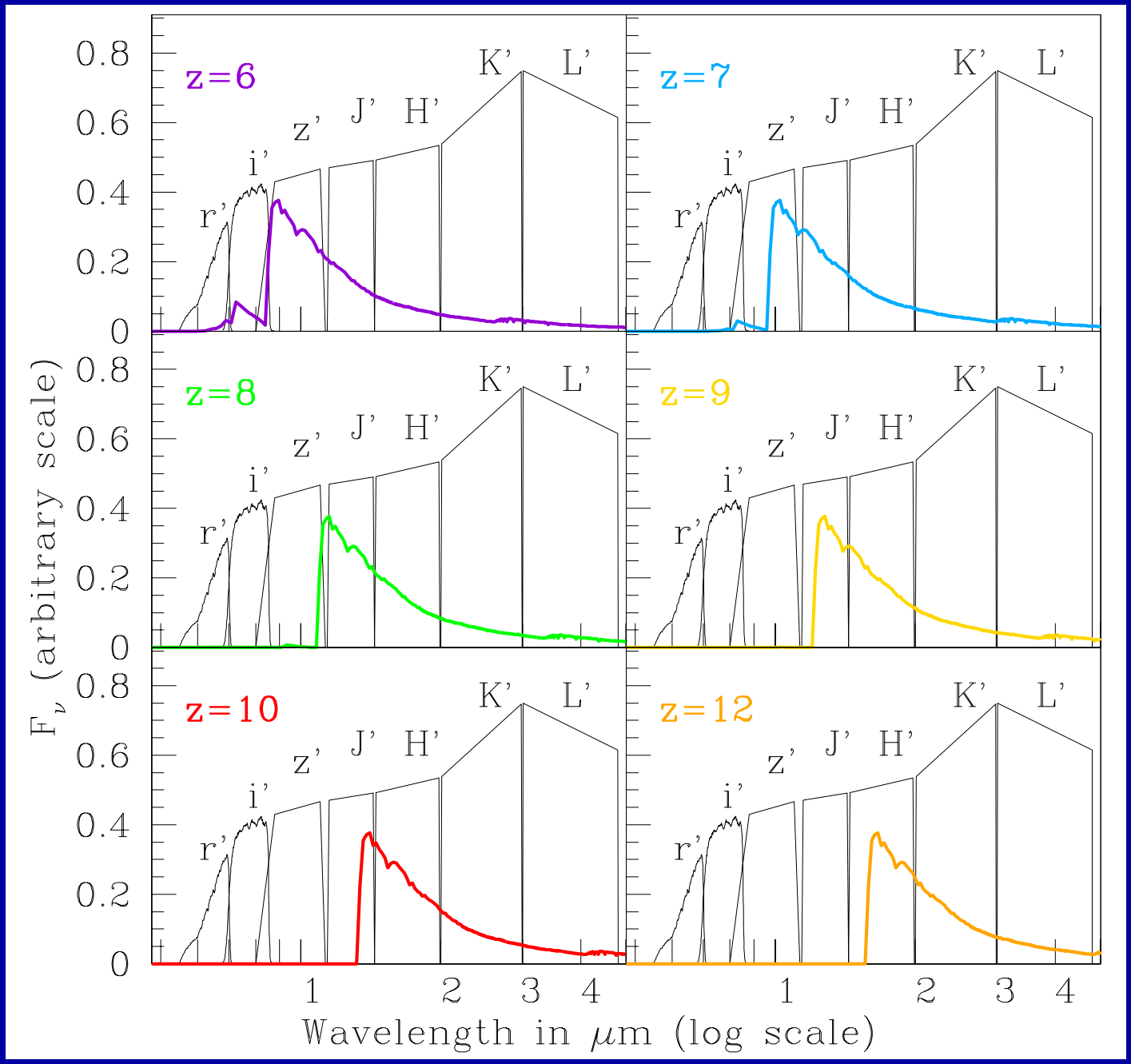

- Can't beat redshift: to see First Light, must observe near–mid IR.

$\Rightarrow$ This is why JWST needs NIRCam at 0.8–5 μm and MIRI at 5–28 μm.

(3a) What is First Light, Reionization, and Galaxy Assembly?

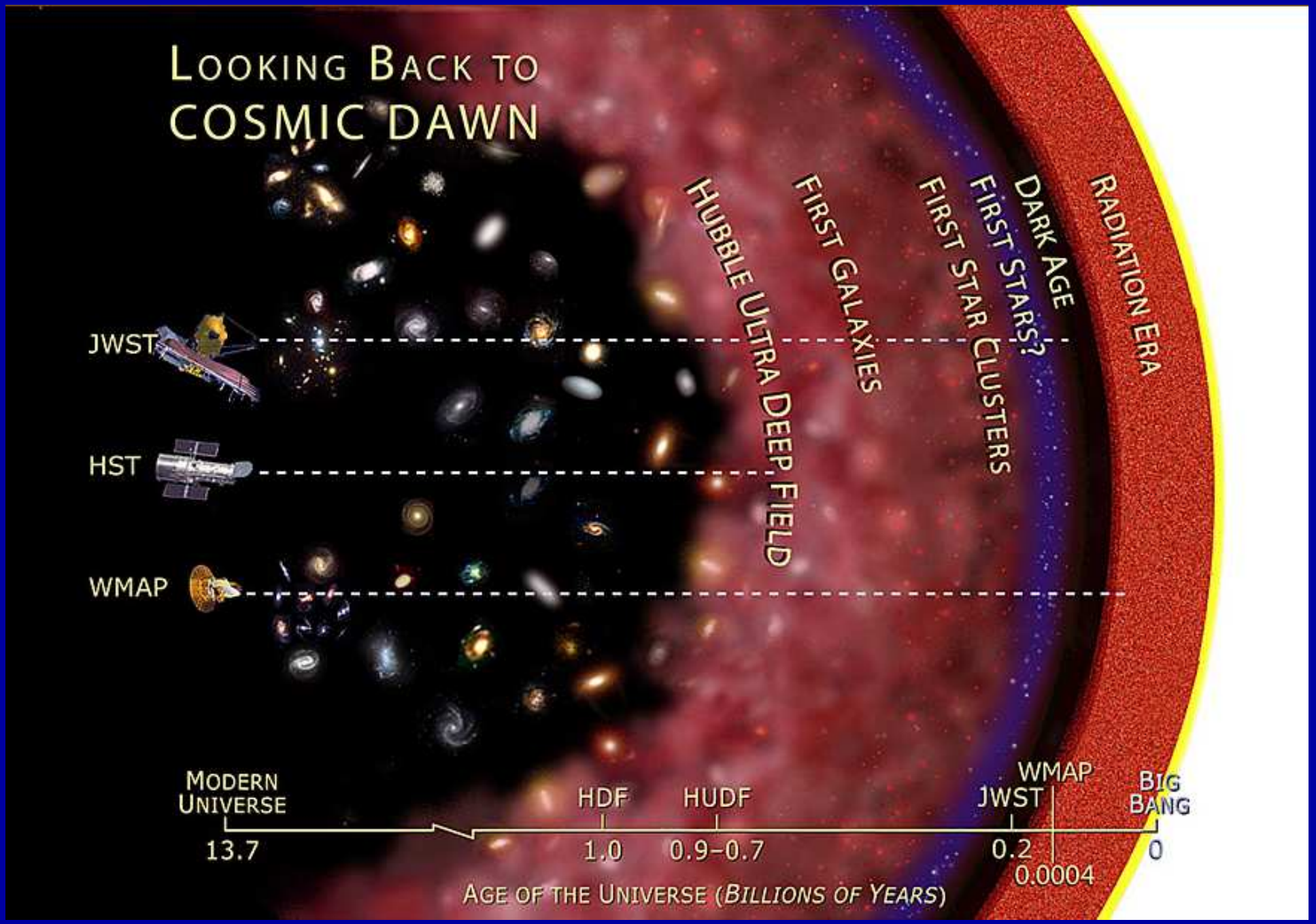

NASA telescopes penetrating Cosmic Dawn, First Light, & Recombination

- (3a) What is First Light and Reionization?

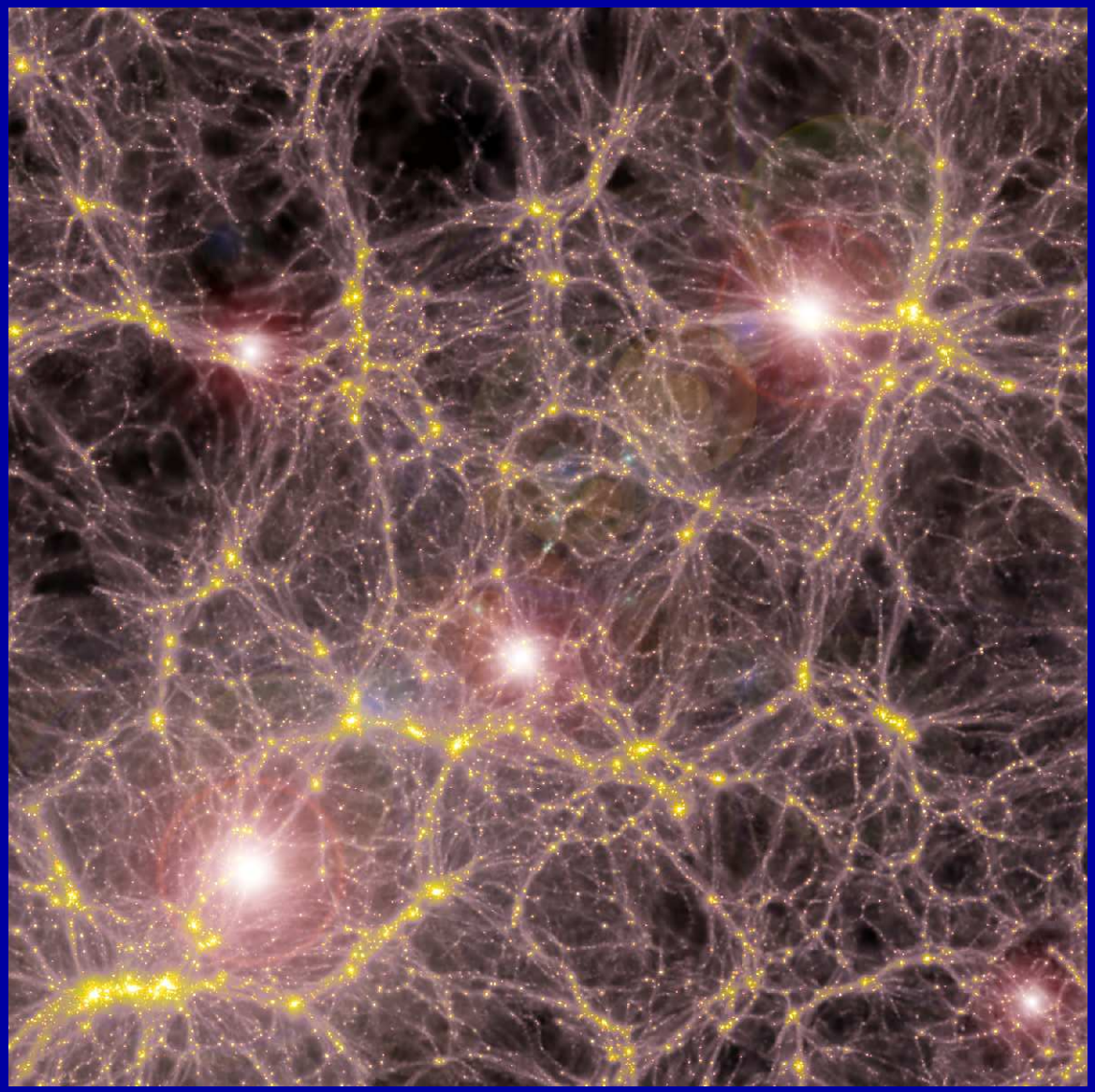

- Detailed Hydrodynamical models (V. Bromm) show that formation of Pop III stars reionized universe for the first time at $z \lesssim 10$–30 (First Light).
- A this should be visible to JWST as the first Pop III star clusters, and perhaps their extremely luminous supernovae at $z \simeq 10 \longrightarrow 30$.

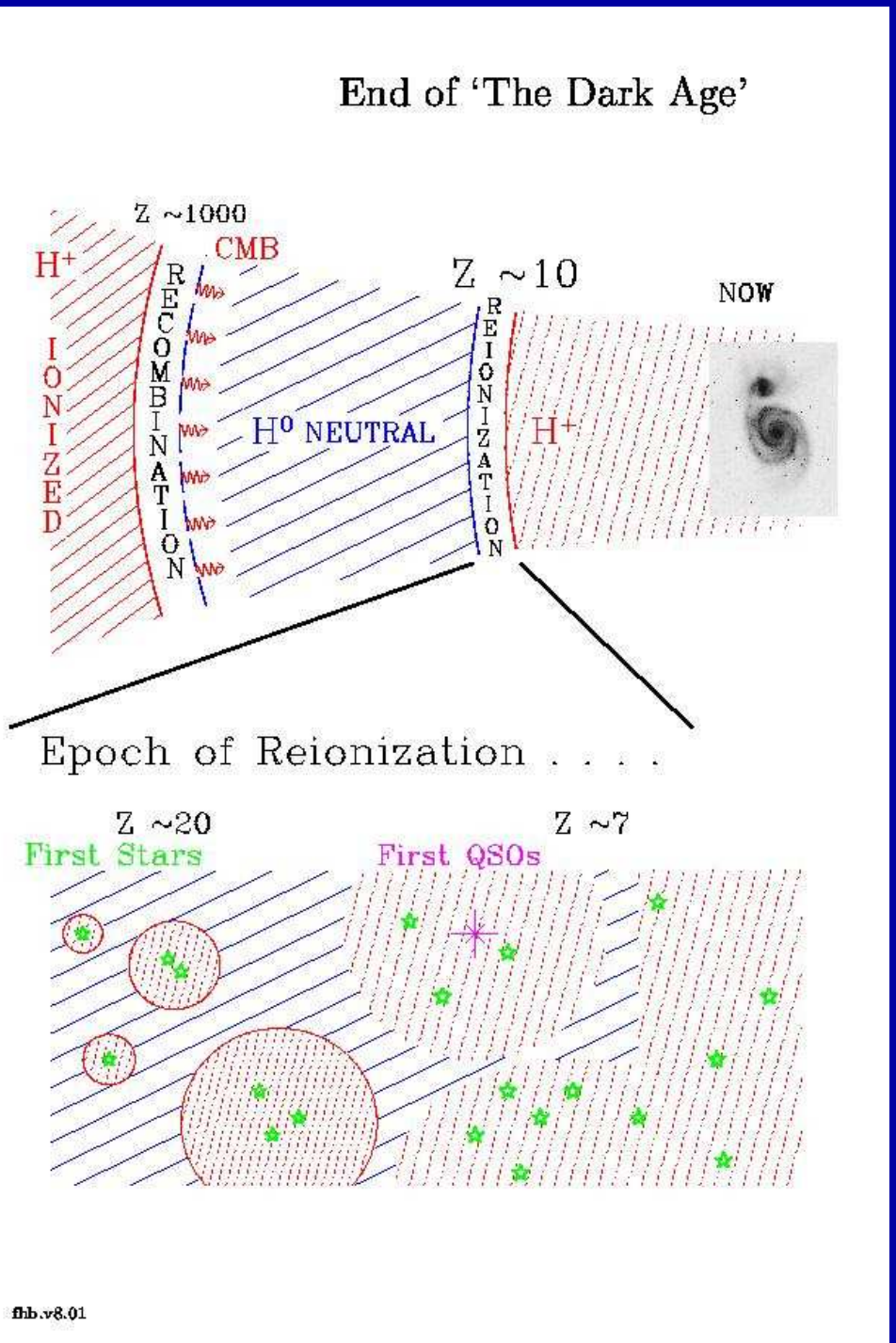

WMAP: First Light may have happened as following:

- (0) Dark Ages since recombination (z=1089) until First Light objects started shining (z=11–20).
- (1) First Light when Population III stars start shining with mass $\gtrsim$100–200 $M_\odot$ at z$\simeq$11–20.
- (2) Pop III supernovae heated IGM, which could not cool and form normal Pop II halo stars until z$\simeq$9–10.
- (3) This is followed by Pop II stars forming in dwarf galaxies (mass$\simeq 10^7$–10^9 $M_\odot$) at z$\simeq$6–9, ending the epoch of reionization.

(Fig. courtesy of Dr. F. Briggs)

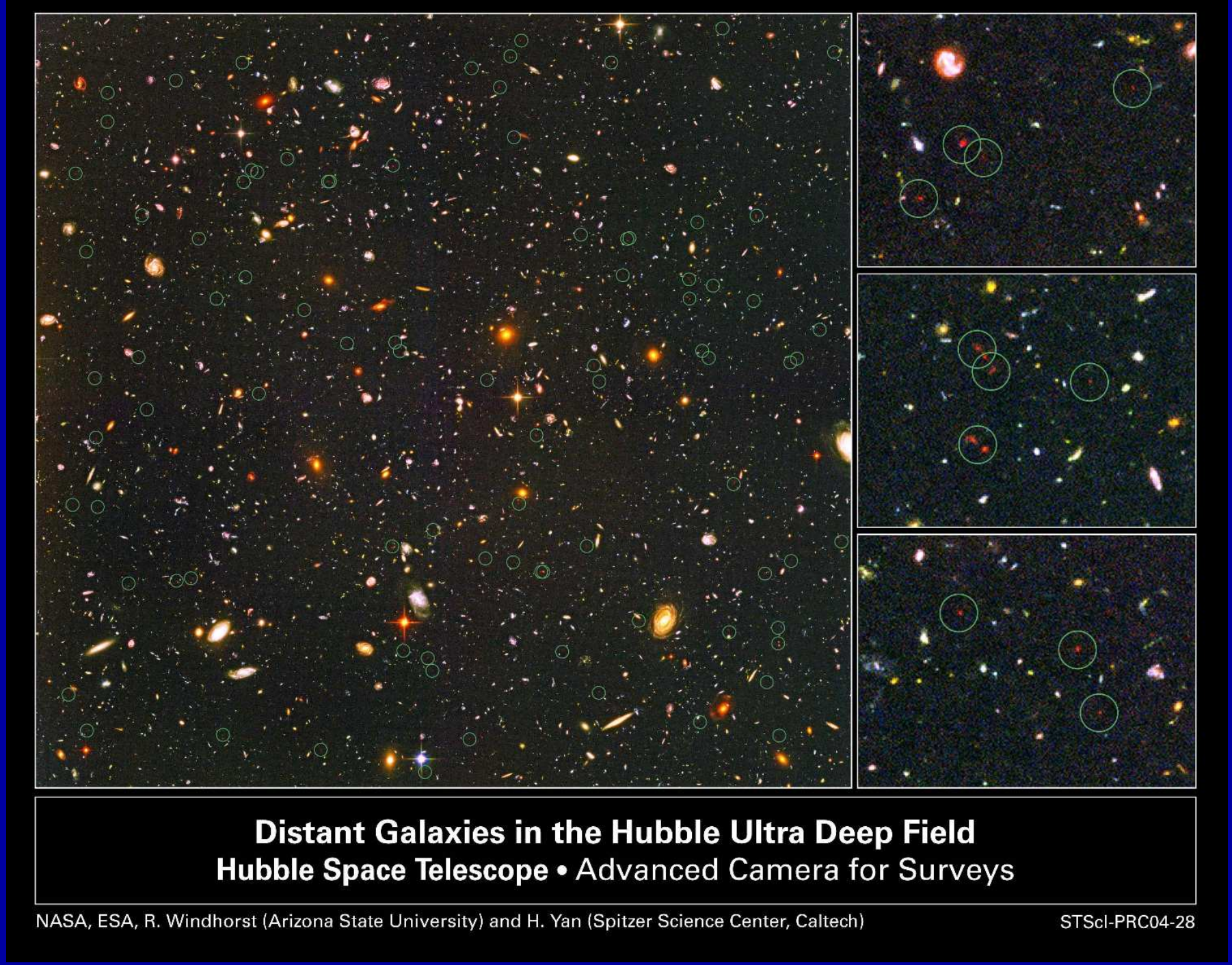

HUDF i-drops: faint galaxies at $z \simeq 6$ (Yan & Windhorst 2004), most spectroscopically confirmed at $z \simeq 6$ to AB $\lesssim 27.0$ mag (Malhotra et al. 2005).

- (3b) How JWST can measure First Light and Reionization

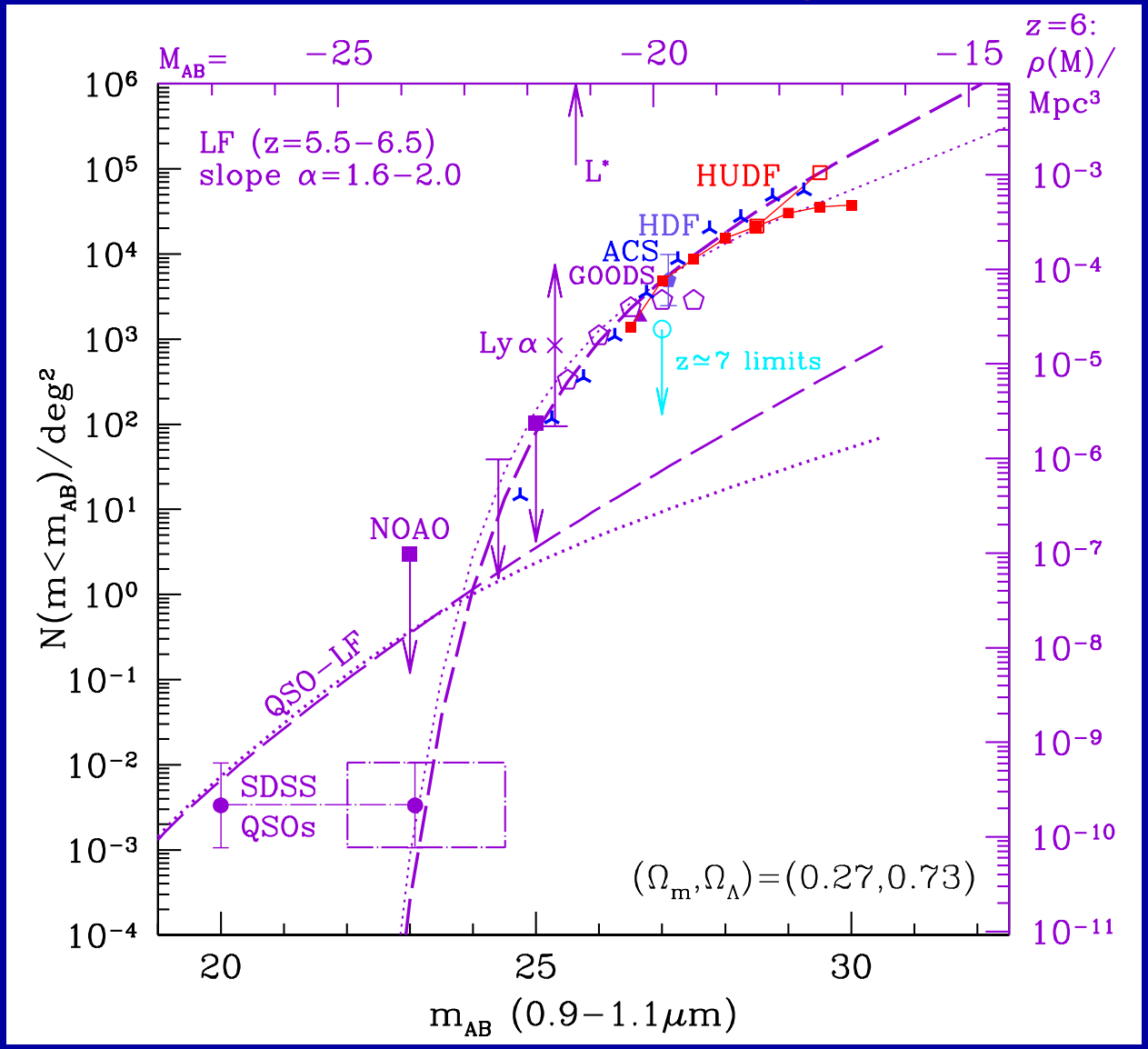

HUDF shows that luminosity function of z≃6 objects (Yan & Windhorst 2004a, b) may be very steep: faint-end Schechter slope $|\alpha|\simeq 1.6$–2.0.

$\Rightarrow$ Dwarf galaxies and not quasars likely completed the reionization epoch at z≃6. This is what JWST will observe in detail to z$\gtrsim$10–20.

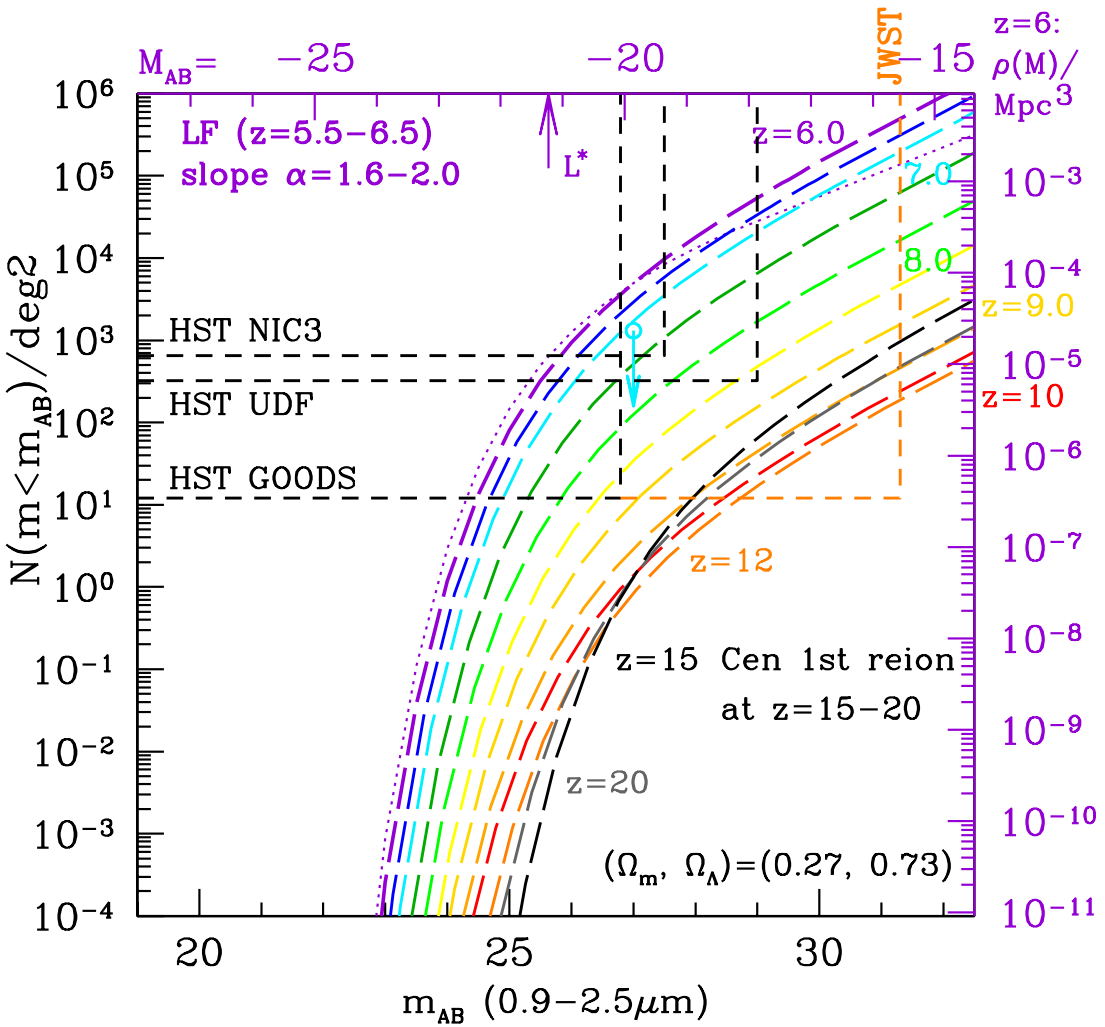

- With proper survey strategy (area AND depth), JWST can trace the entire reionization epoch and detect the first star-forming objects.
- Objects at $z \gtrsim 9$ are rare, since volume element is small and JWST samples brighter part of LF. JWST needs the quoted sensitivity/aperture (A), field-of-view (FOV$=\Omega$), and wavelength range (0.7-28 μm).

- (4) How JWST can measure Galaxy Assembly

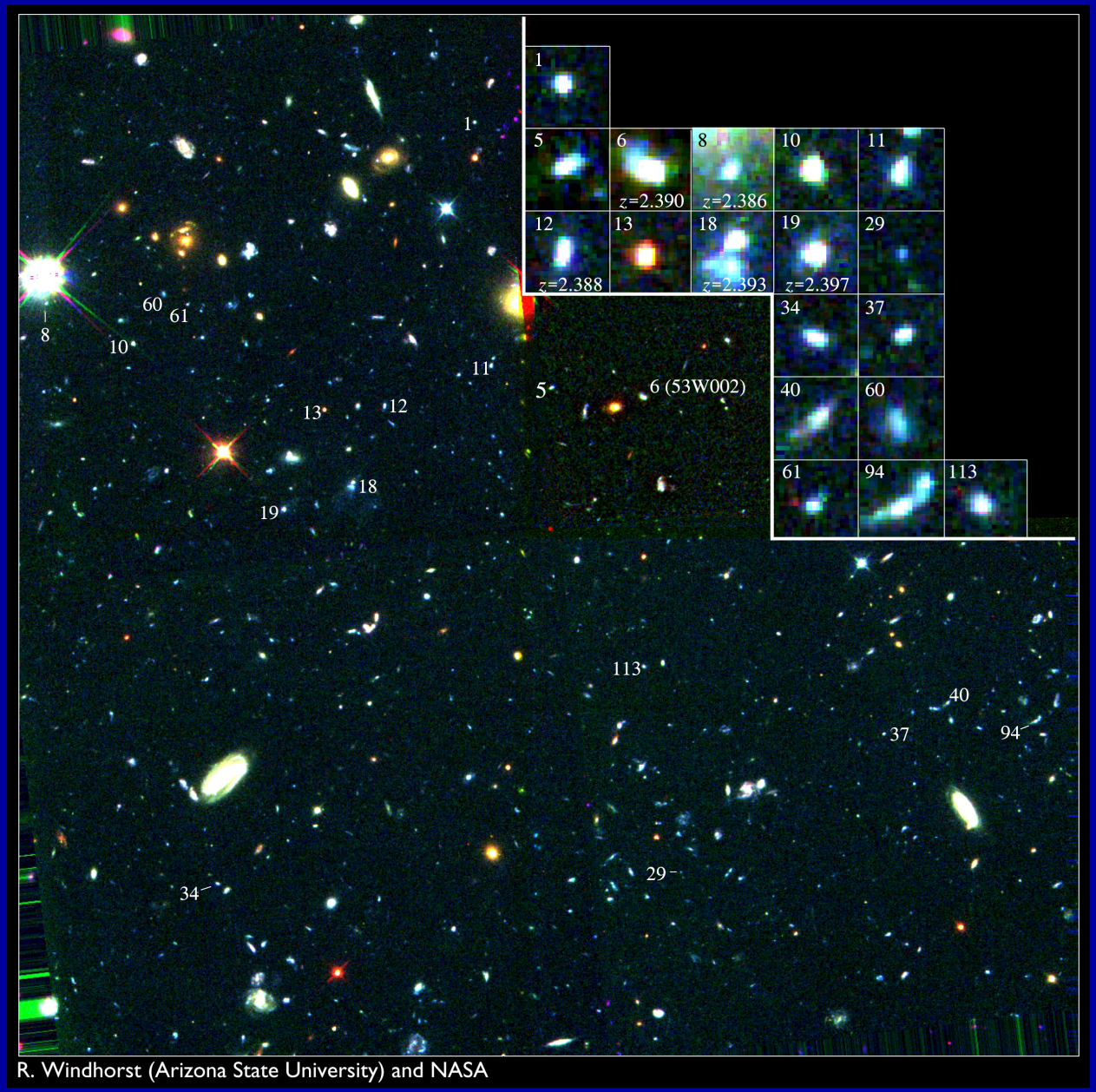

One of the remarkable discoveries of HST was how numerous and small faint galaxies are — the building blocks of the giant galaxies seen today.

THE HUBBLE DEEP FIELD CORE SAMPLE ($I < 26.0$)

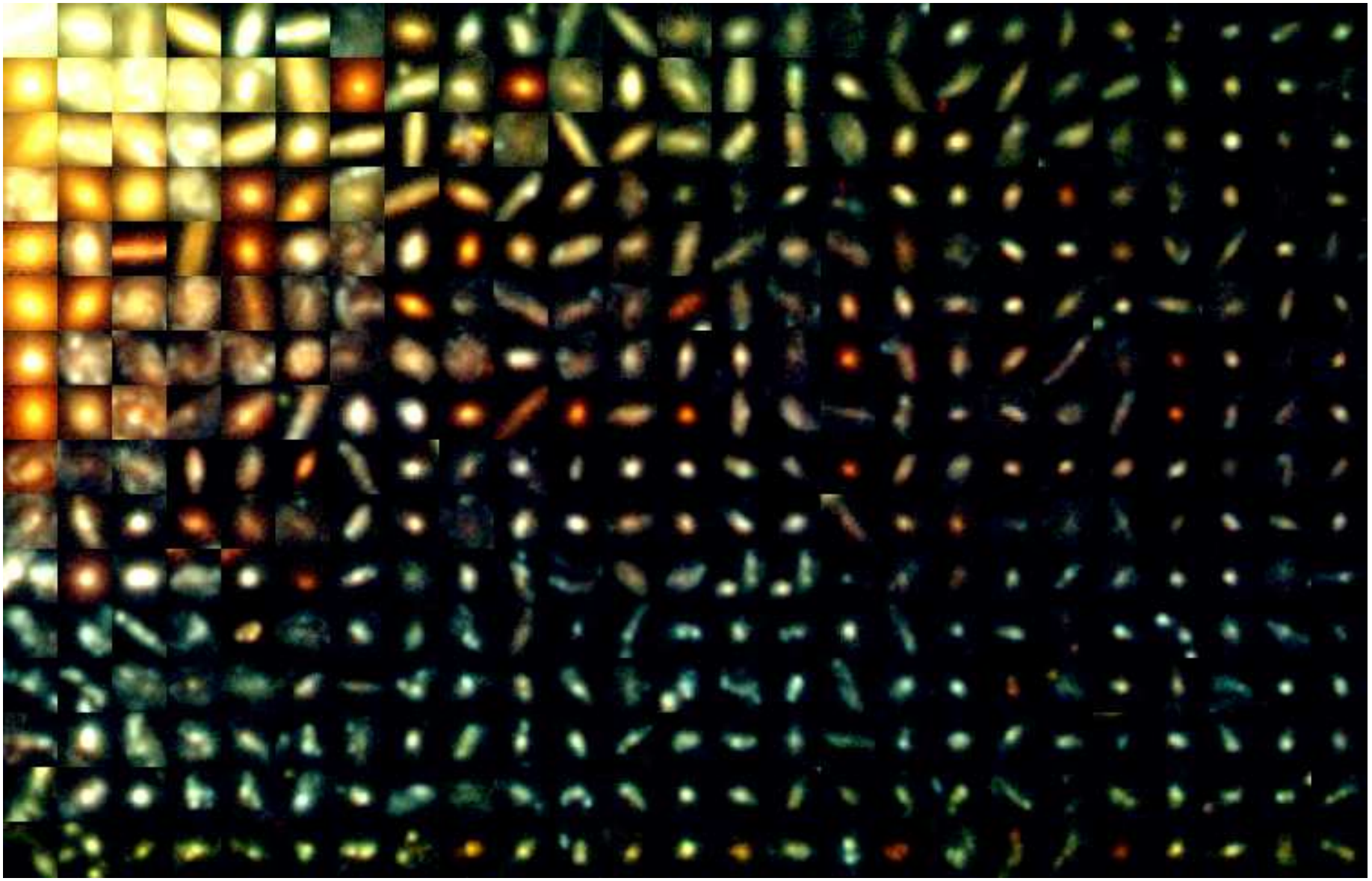

• (4) How JWST can measure Galaxy Assembly

• Galaxies of Hubble types formed over a wide range of cosmic time, but with a notable phase transition around $z \simeq 0.5$–1.0:

(1) Subgalactic units rapidly merge from $z \simeq 7 \longrightarrow 1$ to grow bigger units.

(2) Merger products start to settle as galaxies with giant bulges or large disks around $z \simeq 1$. These evolved mostly passively since then, resulting in the giant galaxies that we see today.

• JWST can measure how galaxies of all types formed over a wide range of cosmic time, by accurately measuring their distribution over rest-frame structure and type as a function of redshift or cosmic epoch.

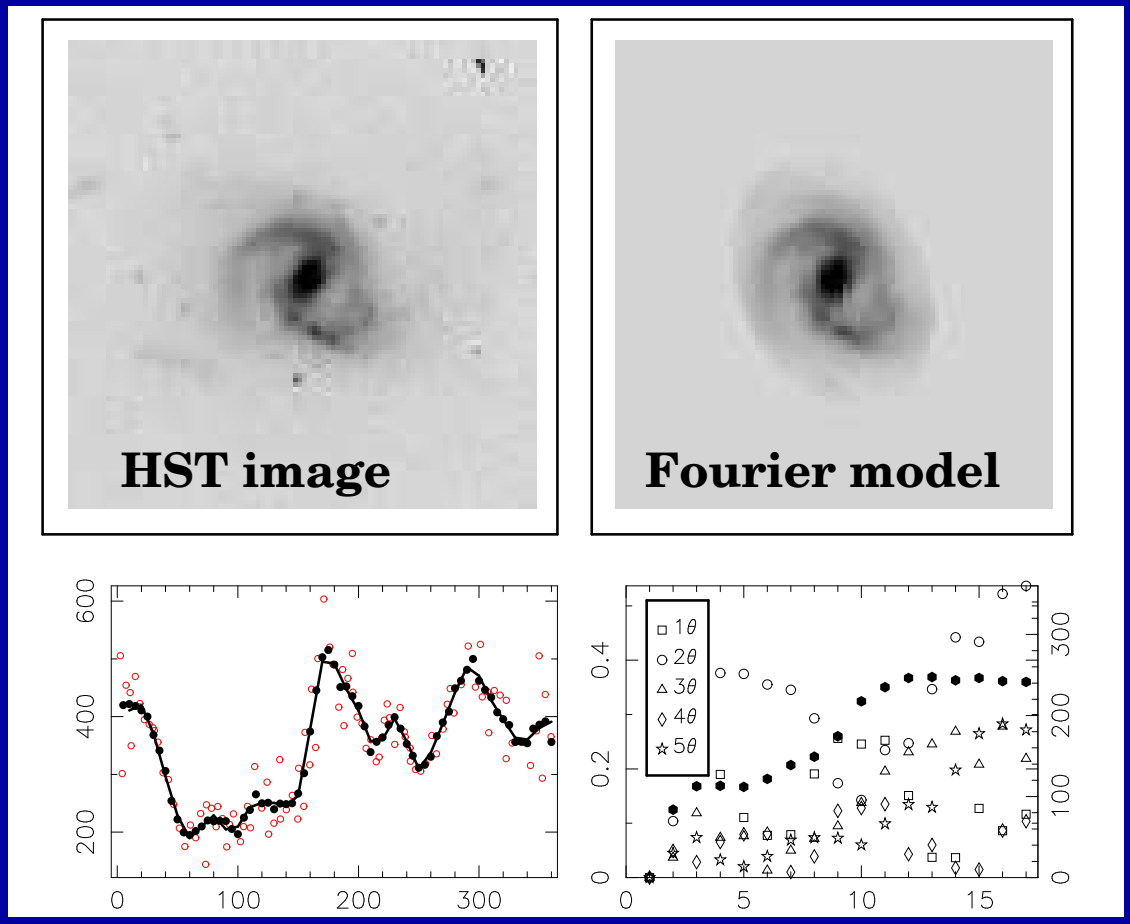

Fourier Decomposition is a robust way to measure galaxy morphology and structure in a quantitative way (Odewahn et al. 2002):

- (1) Fourier series are made in successive concentric annuli.
- (2) Even Fourier components indicate symmetric parts (arms, rings, bars).
- (3) Odd Fourier components indicate asymmetric parts (lopsidedness).
- (4) JWST can measure the evolution of each feature/class directly.

Total EII/S0 Sabc Irr/Mergers

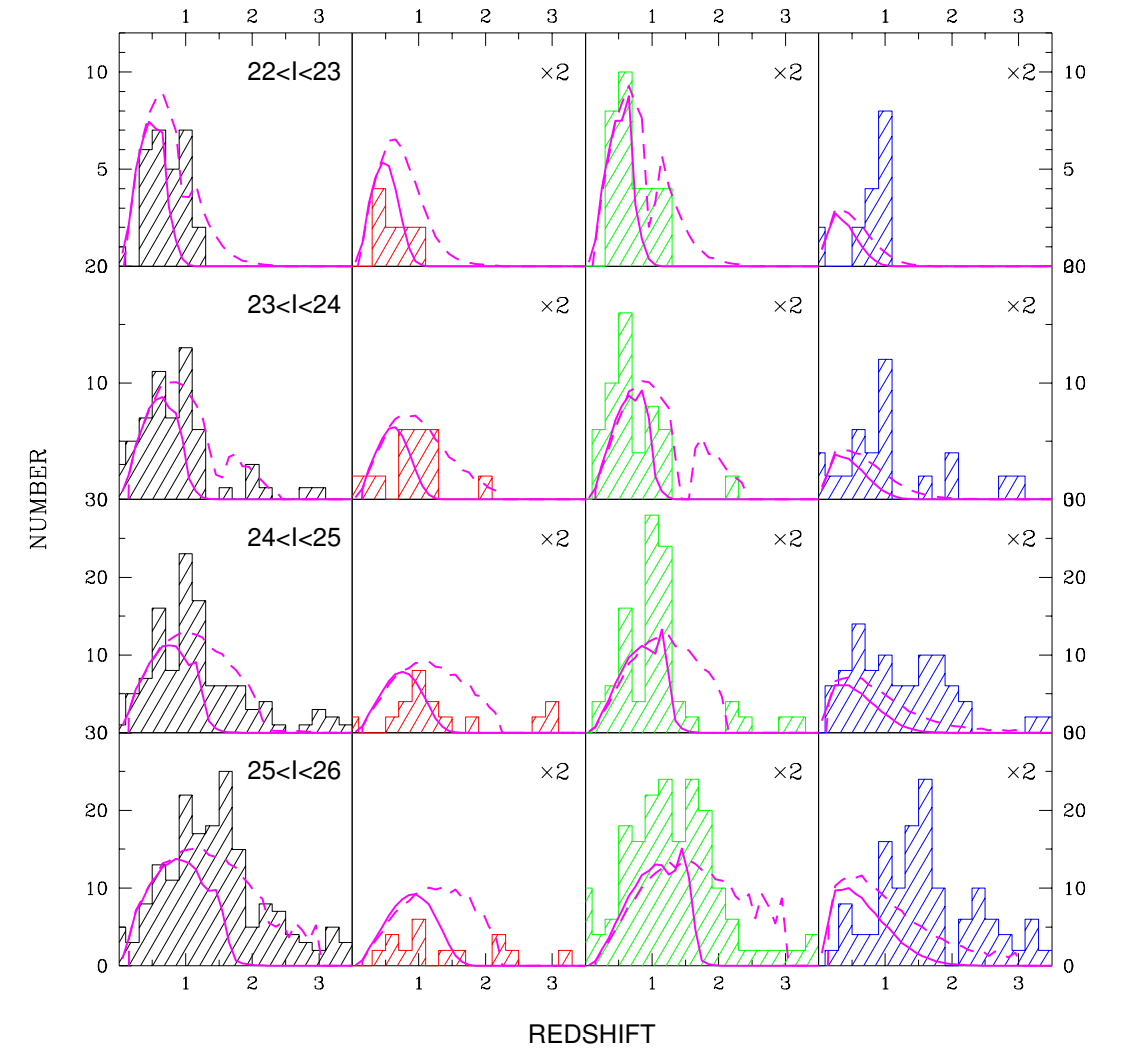

- JWST can measure how galaxies of all Hubble types formed over a wide range of cosmic time, by measuring their redshift distribution as a function of rest-frame type.
- For this, the types must be well imaged for large samples from deep, uniform and high quality multi-wavelength images, which JWST can do.

Driver et al. 1998, Astrophys. J. Letters, 496, L93

LF Faint-end Slope Evolution (fundamental, like local IMF)

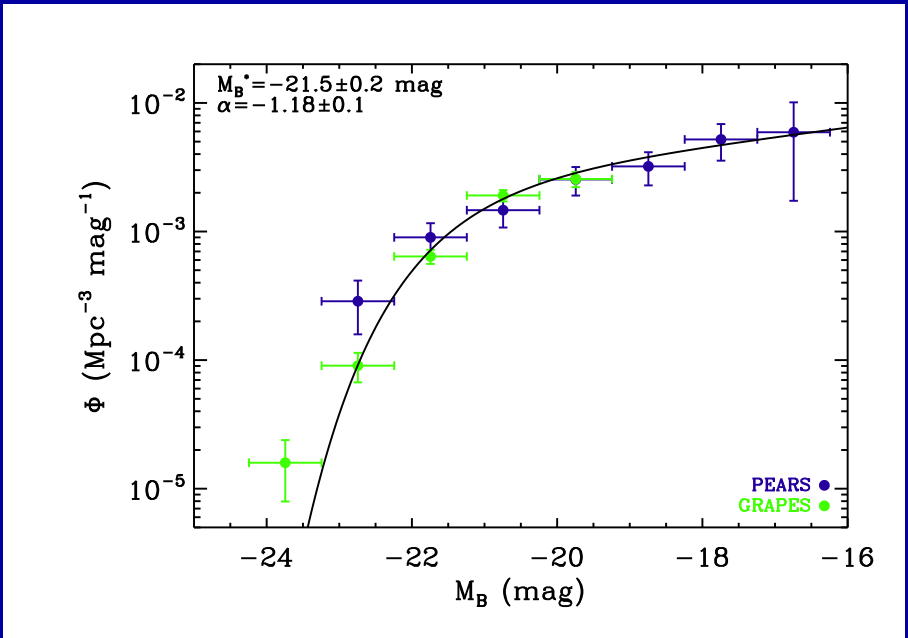

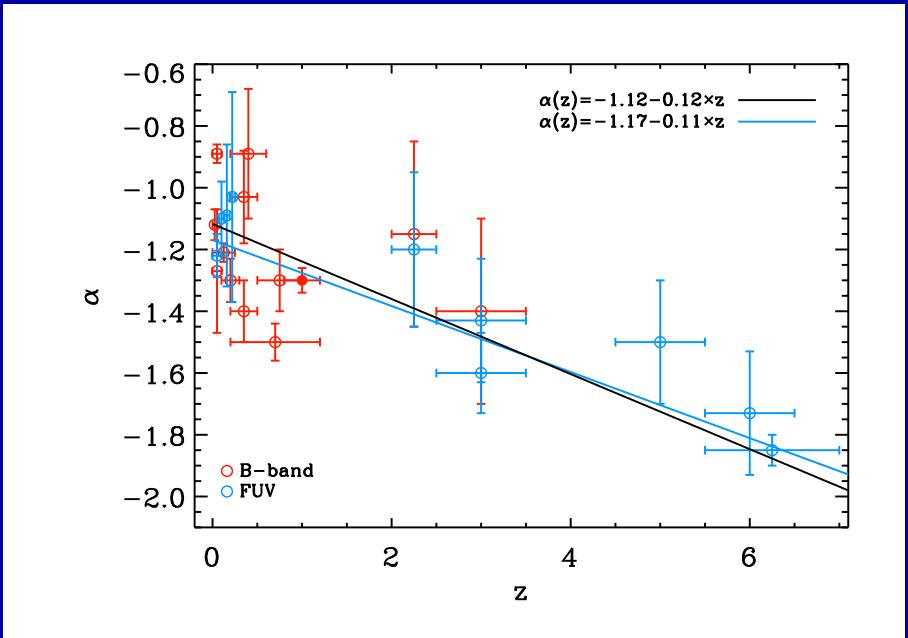

Measuring the faint-end of the LF at z≃2–10 with accurate z's to AB≲31 mag is a very important constraint to hierarchical formation theories. The HST/ACS PEARS project did this to AB=27.0 mag with lower spectral resolution than g-b spectroscopy (Ryan et al. 2007; astro-ph/0703743).

- JWST will fill in big data gap at 4≲z≲10–20 in different environments.
- Constraints to AGN and SF Feedback processes: these produce different faint-end slopes and slope-evolution, which JWST will measure.
- Measure environmental impact on LF faint-end slope directly: Significant (low-z) scatter is likely due to different clustering environments.

(5) Predicted Galaxy Appearance for JWST at z≃1–15

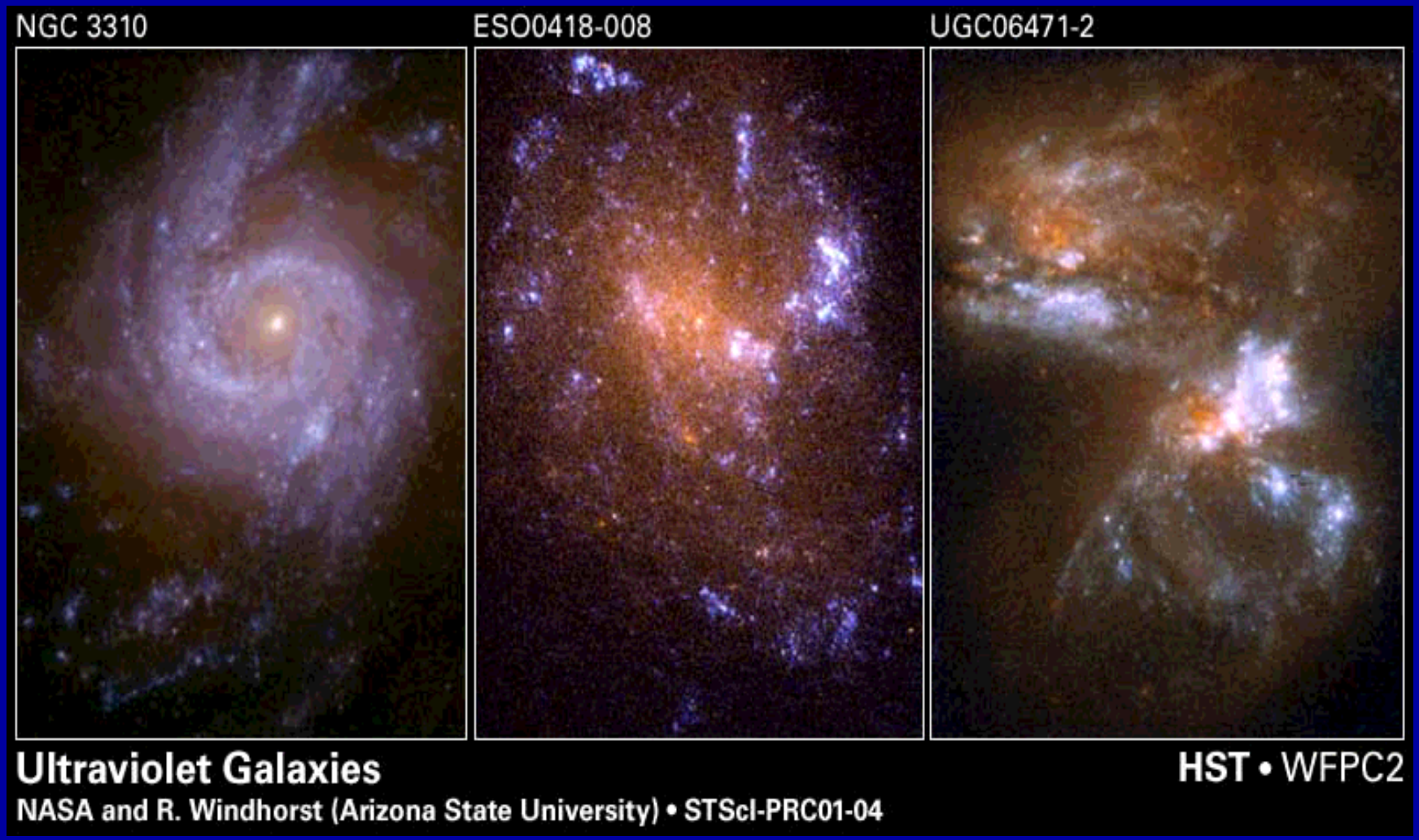

- The uncertain rest-frame UV-morphology of galaxies is dominated by young and hot stars, with often copious amounts of dust superimposed.
- This makes comparison with very high redshift galaxies seen by JWST complicated, although with good images a quantitative analysis of the restframe-wavelength dependent morphology and structure can be made.

(5) Predicted Galaxy Appearance for JWST at z≃1–15

HST z=0 JWST z=2 z=5 z=9 z=15

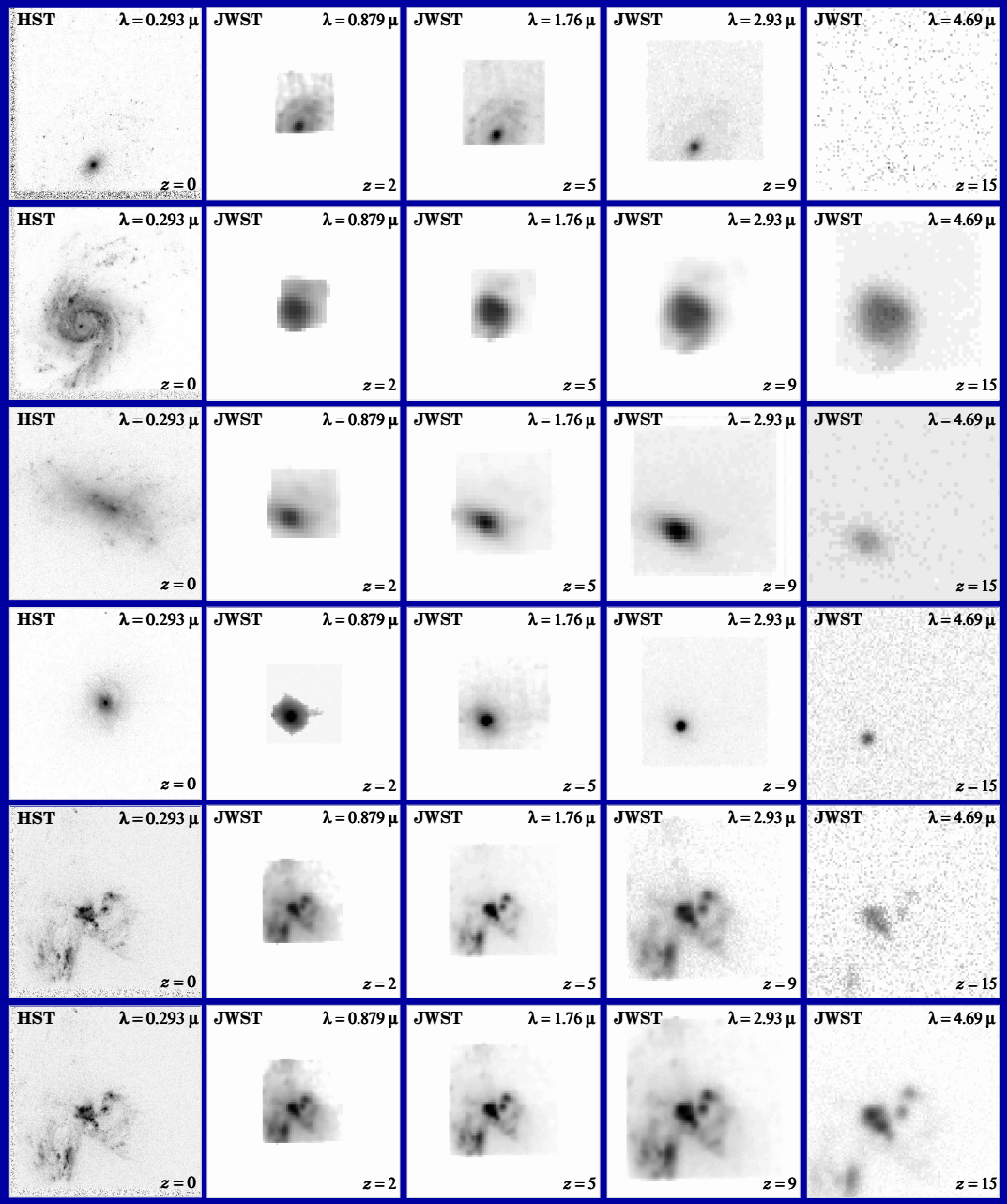

With proper restframe-UV training, JWST can quantitatively measure the evolution of galaxy morphology and structure over a wide range of cosmic time:

- (1) Most disks will SB-dim away at high z, but most formed at z≲1–2.
- (2) High SB structures are visible to very high z.
- (3) Point sources (AGN) are visible to very high z.
- (4) High SB-parts of mergers/train-wrecks are visible to very high z.

(6) Conclusions

(1) JWST Project is technologically front-loaded and well on track:

- Most items at Technical Readiness Level 6 (TRL-6) by Jan. 2007 ($i.e.$, demonstration in a relevant environment — ground or space).
- Technical Non-Advocate Review (T-NAR) in 2007 and Mission Preliminary Design Review (PDR) in March 2008.

(2) JWST will map the epochs of First Light, Reionization, and Galaxy Assembly in detail. It will determine:

- The formation and evolution of the first (reionizing) Pop III star-clusters.
- The origin of the Hubble sequence in hierarchical formation scenarios.

(3) JWST will have a major impact on astrophysics after 2013:

- Current generation of graduate students and postdocs will be using JWST during their professional career.
- JWST will define the next frontier to explore: the Dark Ages at $z \gtrsim 20$.

SPARE CHARTS

- References and other sources of material shown:

http://www.asu.edu/clas/hst/www/jwst/ [Talk, Movie, Java-tool]

http://wwwgrapes.dyndns.org/udf_map/index.html [Clickable HUDF map]

http://www.jwst.nasa.gov/ and http://www.stsci.edu/jwst/

http://www.jwst.nasa.gov/ISIM/index.html

http://ircamera.as.arizona.edu/nircam/

http://ircamera.as.arizona.edu/MIRI/

http://www.stsci.edu/jwst/instruments/nirspec/

http://www.stsci.edu/jwst/instruments/guider/

Gardner, J. P., Mather, J. C., Clampin, M., Doyon, R., Greenhouse, M. A., Hammel, H. B., Hutchings, J. B., Jakobsen, P., Lilly,S. J., Long, K. S., Lunine, J. I., McCaughrean, M. J., Mountain, M., Nella, J., Rieke, G. H., Rieke, M. J., Rix, H.-W., Smith, E. P., Sonneborn, G., Stiavelli, M., Stockman, H. S., Windhorst, R. A., & Wright, G. S. 2006, Space Science Reviews, 123, 485–606 (astro-ph/0606175)

Mather, J., Stockman, H. 2000, Proc. SPIE Vol. 4013, p. 2-16, in "UV, Optical, and IR Space Telescopes and Instruments", Eds. J. B. Breckinridge & P. Jakobsen (Berlin: Springer)

(7) Appendix: will JWST & SKA reach the Natural Confusion Limit?

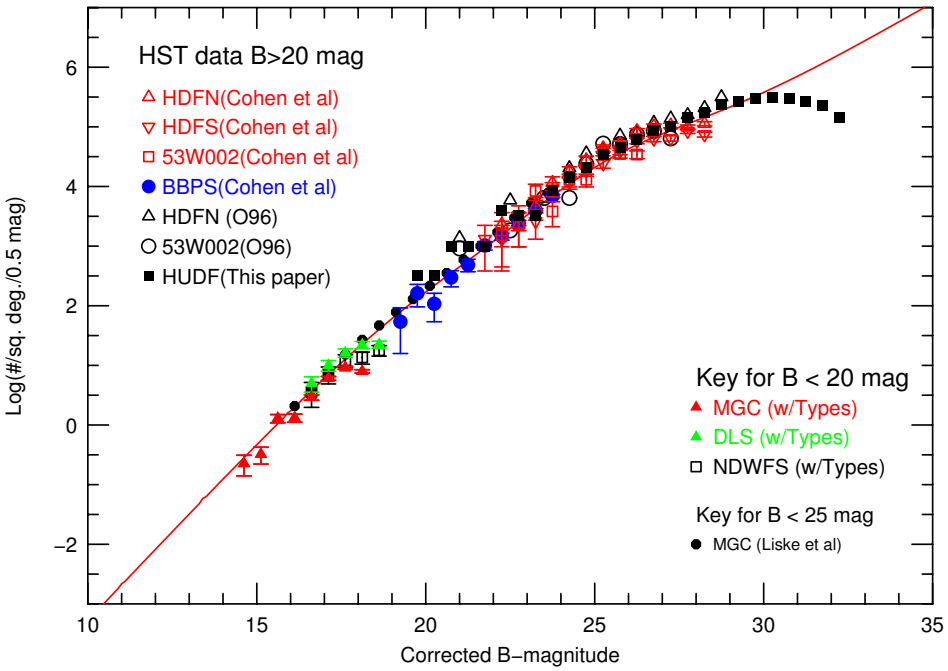

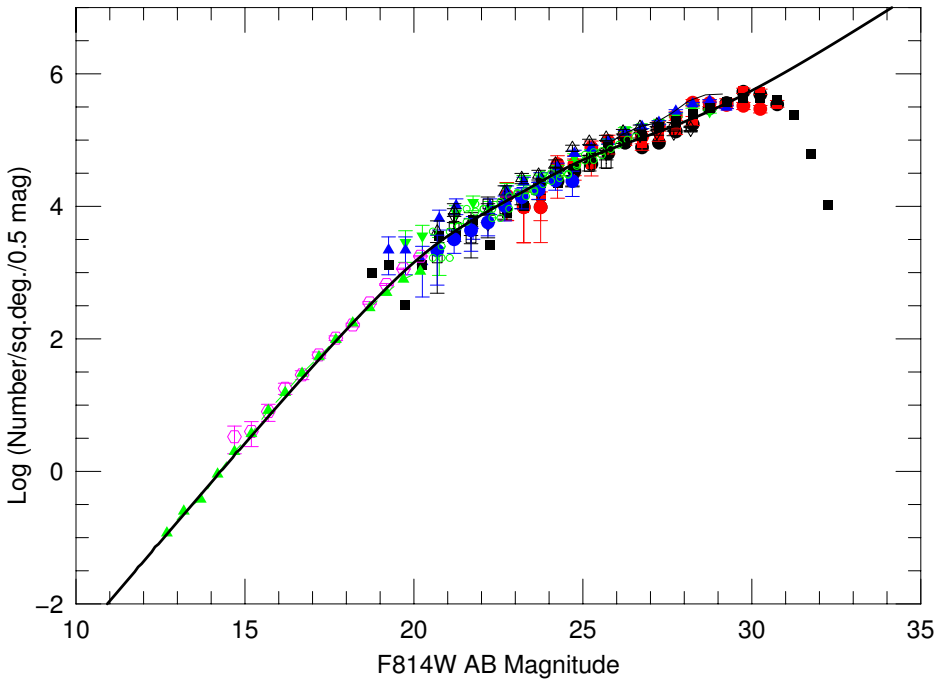

- HUDF galaxy counts (Cohen et al. 2006): expect an integral of $\gtrsim 2\times10^6$ galaxies/deg^2 to AB=31.5 mag ($\simeq$ 1 nJy at optical wavelengths). JWST and SKA will see similar surface densities to $\simeq$1 and 10 nJy, resp.
- $\Rightarrow$ Must carry out JWST and SKA nJy-surveys with sufficient spatial resolution to avoid object confusion (from HST: this means FWHM$\lesssim 0\farcs08$).
- $\Rightarrow$ Observe with JWST/NIRSpec/MEMS and SKA HI line channels, to disentangle overlapping continuum sources in redshifts space.

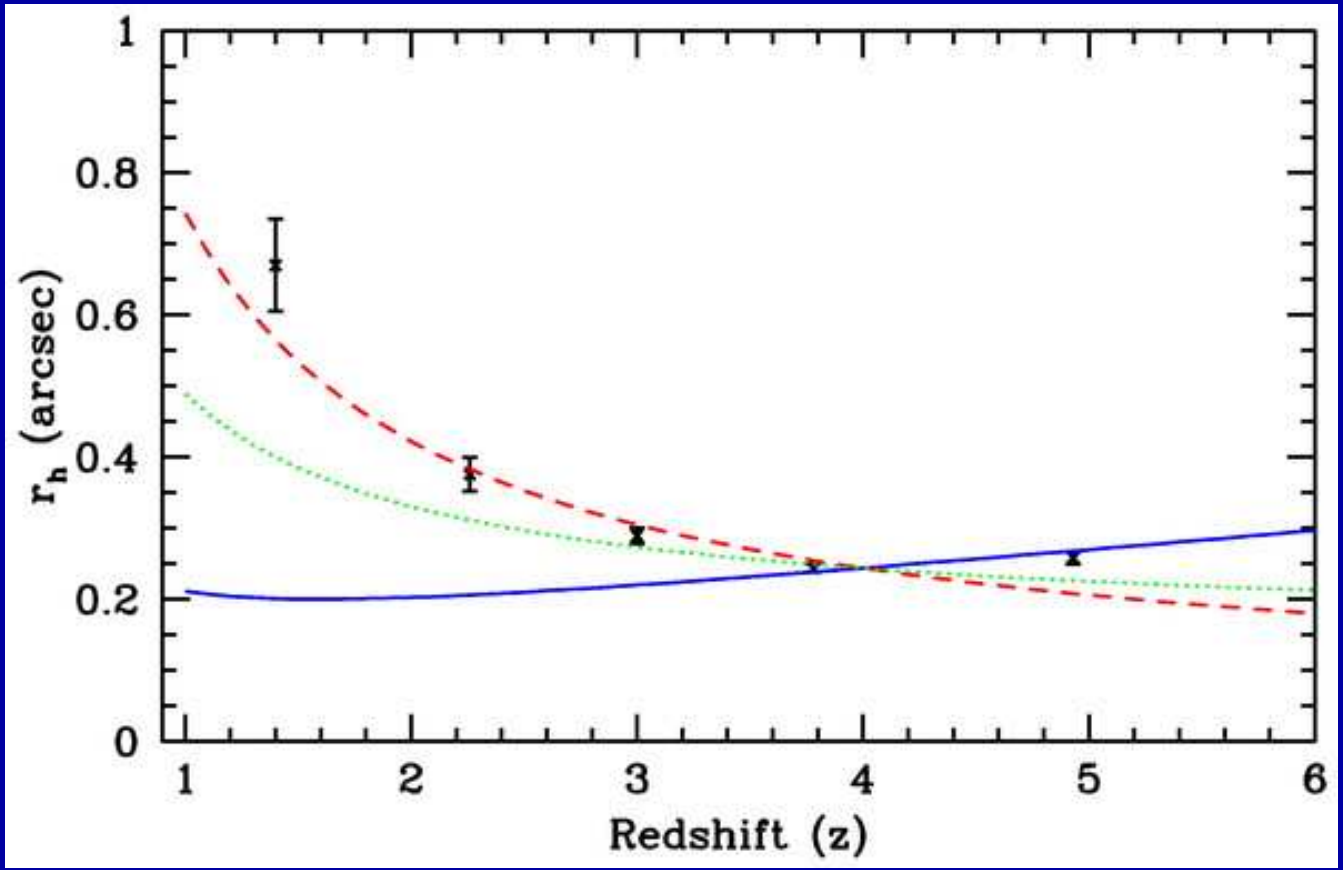

HST GOODS measured galaxy size evolution (Ferguson et al. 2004 ApJL):

- Median galaxy sizes decline steadily at higher redshifts, despite the cosmological Θ–z relation that minimizes at z$\simeq$1.6 for Λ-cosmology.
- Evidence of intrinsic size evolution: $r_{hl}(z) \propto r_{hl}(0)\ .\ (1+z)^{-s}$, $s \simeq 1$.
- Caused by hierarchical formation of galaxies, leading to intrinsically smaller galaxies at higher redshifts, where fewer mergers have occurred.
- SKA must anticipate the small $\lesssim 0\farcs15$ radio sizes of faint galaxies.

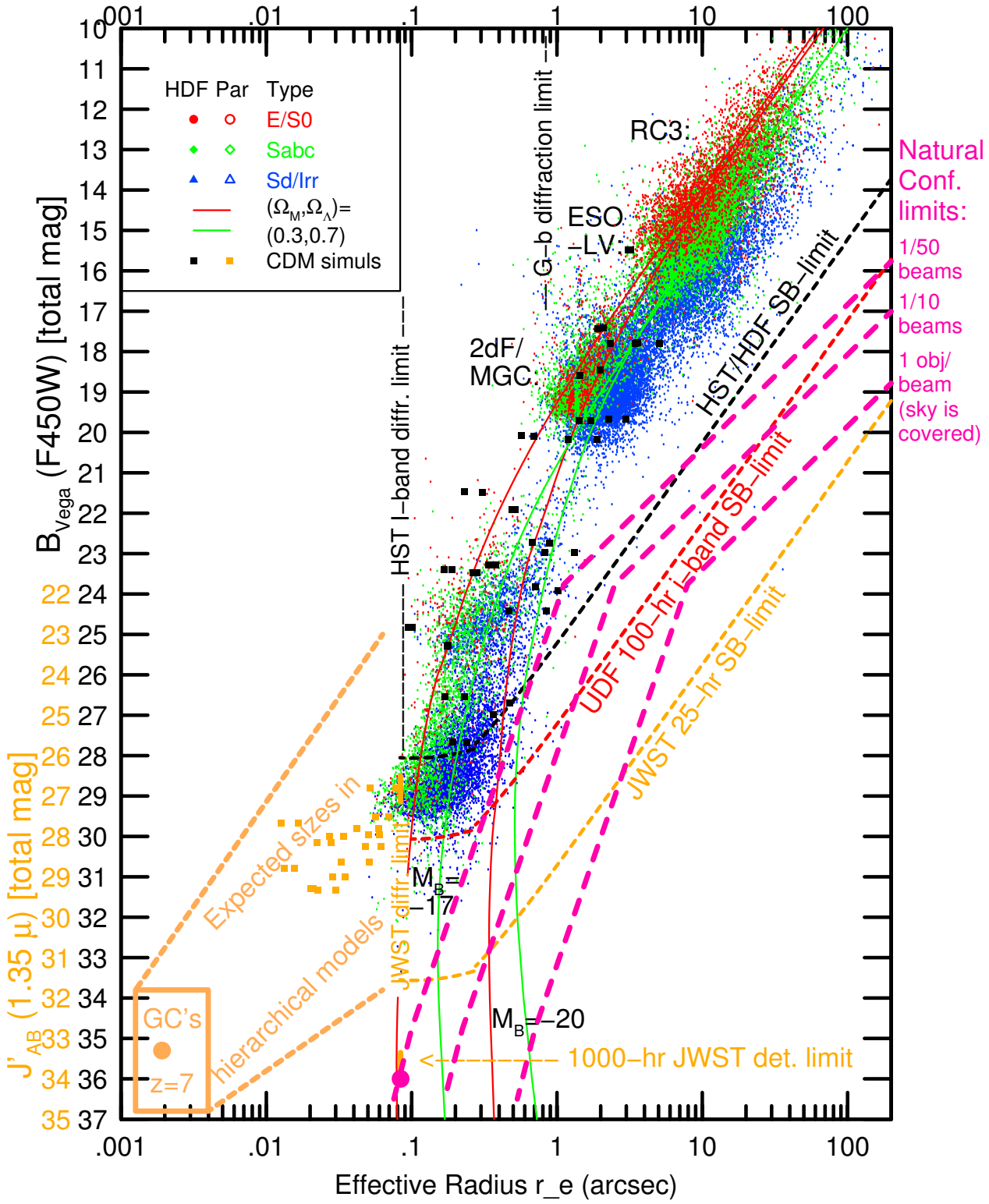
HDF Par Type
E/S0
Sabc
Sd/Irr
(Ω_M,Ω_Λ)=
(0.3,0.7)
CDM simuls
RC3:
ESO
–LV
2dF/
MGC
HST/HDF SB–limit
UDF 100–hr i–band SB–limit
JWST 25–hr SB–limit
HST I–band diffr. limit
G–b diffraction limit
JWST diffr. limit
Expected sizes in
hierarchical models
GC's
z=7
M_B=
–17
M_B=–20
1000–hr JWST det. limit
Natural
Conf.
limits:
1/50
beams
1/10
beams
1 obj/
beam
(sky is
covered)
B_Vega (F450W) [total mag]
J'_AB (1.35 μ) [total mag]
Effective Radius r_e (arcsec)
.001
.01
.1
1
10
100

Combination of ground-based and space-based HST surveys show:

- (1) Apparent galaxy sizes decline from the RC3 to the HUDF limits:
- (2) At the HDF/HUDF limits, this is not only due to SB-selection effects (cosmological $(1+z)^4$-dimming), but also due to:
- (2a) hierarchical formation causes size evolution: $r_{hl}(z) \propto r_{hl}(0)\,(1+z)^{-1}$
- (2b) increasing inability of object detection algorithms to deblend galaxies at faint mags ("natural" confusion $\neq$ "instrumental" confusion).
- (3) At AB$\gtrsim$30 mag, JWST and at $\gtrsim$10 nJy, SKA will see more than 2×10^6 galaxies/deg^2. Most of these will be unresolved ($r_{hl} \lesssim 0\farcs1$ FWHM (Kawata et al.2006). Since $z_{med} \gtrsim 1.5$, this influences how $(1+z)^4$-dimming affects the catalog completeness.
- For details, see Windhorst, R. A., et al.2007, in Proceedings of the 36^{th} COSPAR Scientific Assembly on "Challenges in High Resolution Space Astronomy: Astrophysics, Technology and Data", Eds. M. A. Shea et al. (Amsterdam: Elsevier), Advances in Space Research, Vol. xxx, p. 001–010, in press (astro-ph/0703171)

- (2) What instruments will JWST have?

The Near-Infrared Camera NIRCam made by an UofA + Lockheed + CSA consortium will do imaging from 0.6–5.3 μm using a suite of broad-, medium-, and narrow-band filters. NIRCam uses two identical and independently operated imaging modules, with two wavelengths observable simultaneously via a dichroic that splits the beam around 2.35 μm. Each of these two channels has an independently operated $2\farcm2 \times 4\farcm6$ FOV. Both channels are Nyquist-sampled: the short-wavelength channel at 2 μm with $0\farcs0317$/pixel, and the and long-wavelength at 4 μm with $0\farcs0648$/pixel. NIRCam's 10 2k×2k HgCdTe arrays will be passively cooled.

The Near-Infrared Spectrograph NIRSpec made by an ESA + GSFC consortium will do spectroscopy with resolving powers of R$\sim$100 in prism mode, of R$\sim$1000 in multi-object mode using a micro-electromechanical array system (MEMS) of micro-shutters that can open slitlets on previously imaged known objects, and of R$\sim$3000 using long-slit spectroscopy. All NIRSpec spectroscopic modes have a $\sim 3.4 \times 3.4'$ FOV.

- (2) What instruments will JWST have?

The Mid-Infra-Red Instrument MIRI made by an UofA + JPL + ESA consortium will do imaging and spectroscopy from 5–28 μm. MIRI is actively cooled by a cryocooler, which will cool it without using consumable gas.

The Fine Guidance Sensor (FGS) is made by CSA and provide stable pointing at the milli-arcsecond level. The FGS will have sufficient sensitivity and a large enough FOV to find guide stars with $\gtrsim$95% probability at any point in the sky. The FGS will have three simultaneously imaged fields of view of $2.3 \times 2.3'$, one of which feeds a pure guider channel, one feeding a guider channel plus a long-wavelength R$\sim$100 tunable filter channel with light split by a dichroic, and another feeding the short wavelength tunable filter R$\sim$100 channel.

JWST has fully redundant imaging and spectroscopic modes. It will not be serviced at L2, and therefore will undergo an extensive series of ground-testing and thermal vacuum testing in 2008–2009, after its main construction in 2004–2008. The main NASA contractor is Northrop Grumman Space Technology ("NGST") in Redondo Beach (CA).

Table 10. Predicted Performance of the JWST Observatory

Parameter	Capability
Wavelength	0.6 to 29 μm. Reflective gold coatings
Sensitivity	SNR=10, integration time = τ_i, R=$\lambda/\Delta\lambda$ and Zodiacal of 1.2 times that at north ecliptic pole
NIRCam	12 nJy (1.1μm, τ_i=10,000s, and $\lambda/\Delta\lambda = 4$)
NIRCam	10.4 nJy (2.0μm, τ_i=10,000s, and $\lambda/\Delta\lambda = 4$)
TFI	368 nJy (3.5μm, τ_i=10,000s, and $\lambda/\Delta\lambda = 100$)
NIRSpec	120 nJy (3.0μm, τ_i=10,000s, and $\lambda/\Delta\lambda = 100$)
NIRSpec	560 nJy (10μm, τ_i=10,000s, and $\lambda/\Delta\lambda = 5$)
MIRI	5000 nJy (21μm, τ_i=10,000s, and $\lambda/\Delta\lambda = 4.2$)
NIRSpec Med	5.2×10^{-22} Wm^{-2} (2 μm, τ_i=100,000s, R= 1000)
MIRI Spec	3.4×10^{-21} Wm^{-2} (9.2 μm, τ_i=10,000s, R= 2400)
MIRI Spec	3.1×10^{-20} Wm^{-2} (22.5 μm, τ_i=10,000s, R= 1200)
Spatial Resolution & Stability	Encircled Energy of 75% at 1 μm for 150mas radius Strehl ratio of ~ 0.86 at 2 μm. PSF stability better than 1%

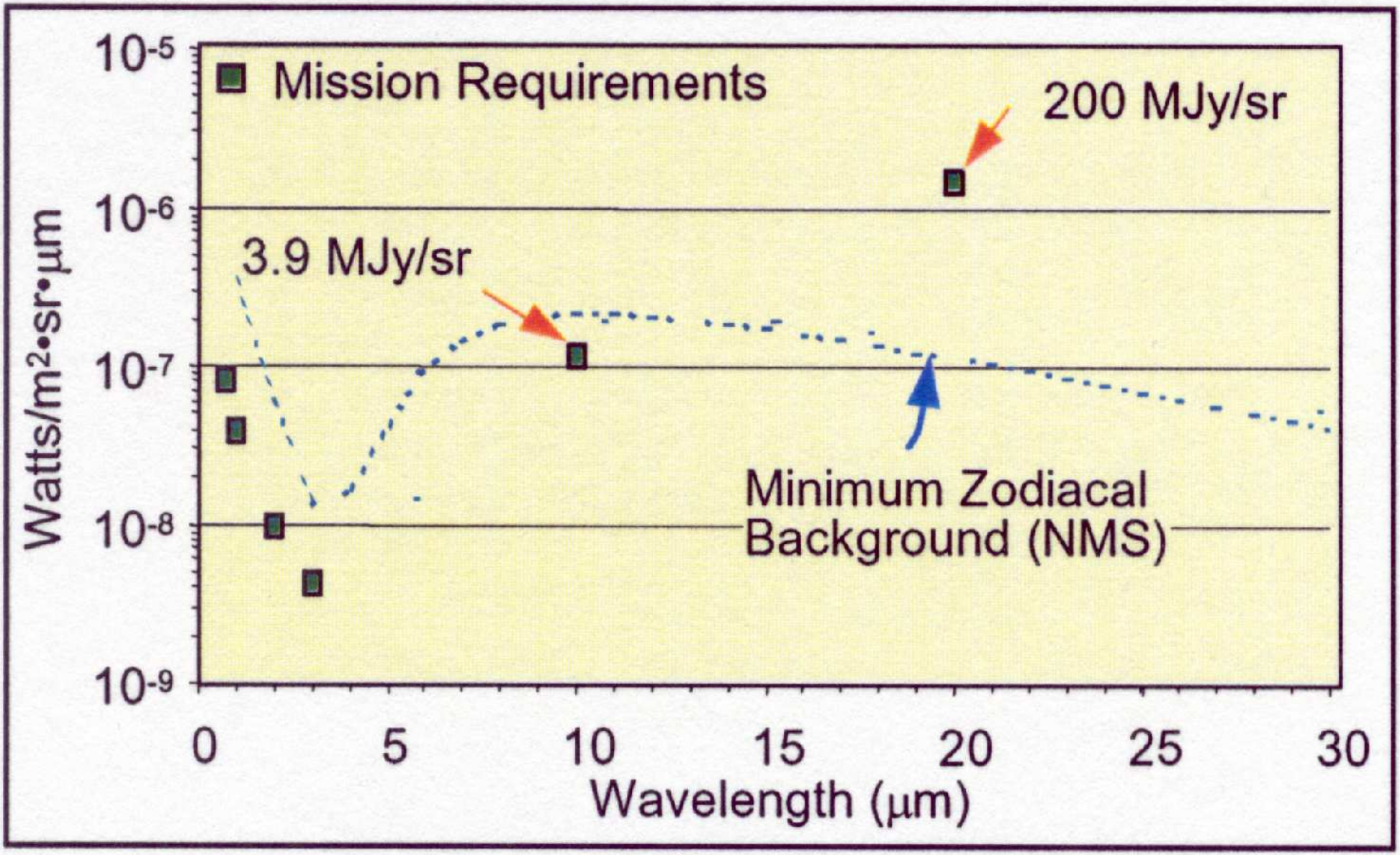

JWST L2 sky minimizes $\lambda \simeq 3$ μm: $\gtrsim 10^4\times$ fainter than ground-based sky.

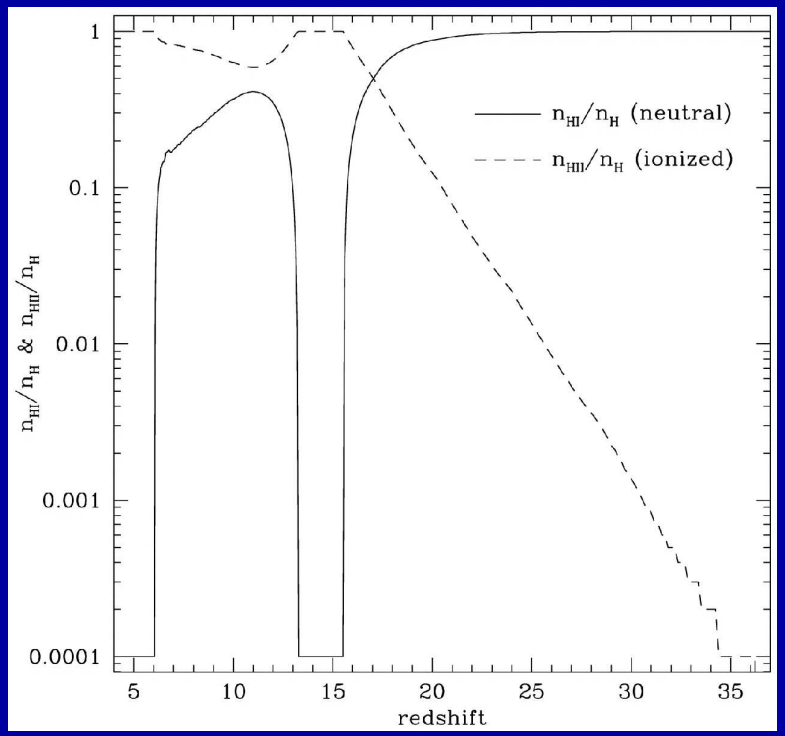

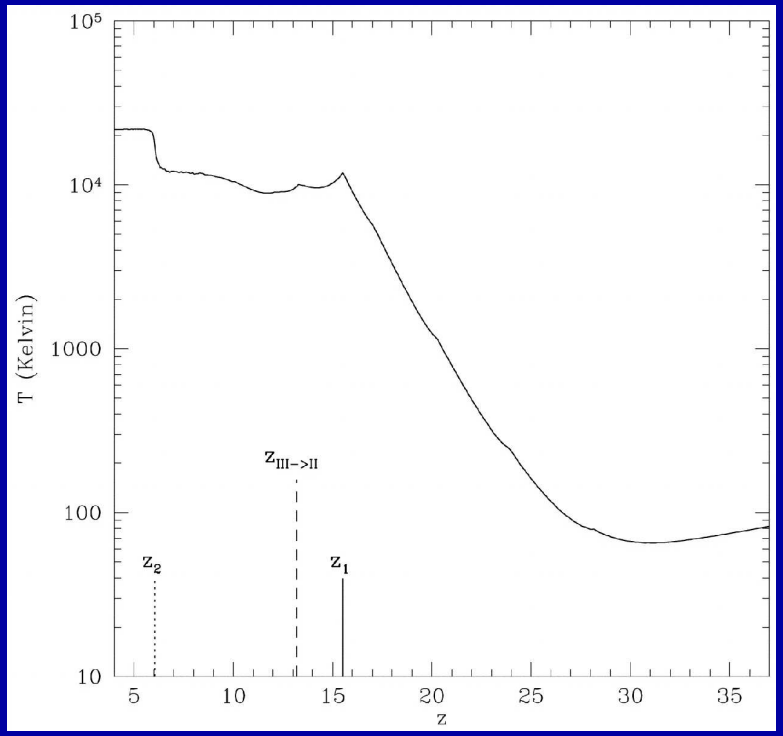

WMAP and detailed Hydrodynamical models (Cen 2003) suggest that:

- (1) Population III stars caused epoch of First Light at z≃11–20.
- (2) Pop III supernovae may have caused the Second Dark Ages at z=9–11, since they heated the IGM, which could not cool until:
- (3) The first Pop II stars started forming in dwarf galaxies with 10^7–10^9 $M_\odot$ at z≃6–9.

$\Rightarrow$ This will be visible to JWST in the luminosity function (LF) of the first star-forming objects at z≃20$\longrightarrow$6.

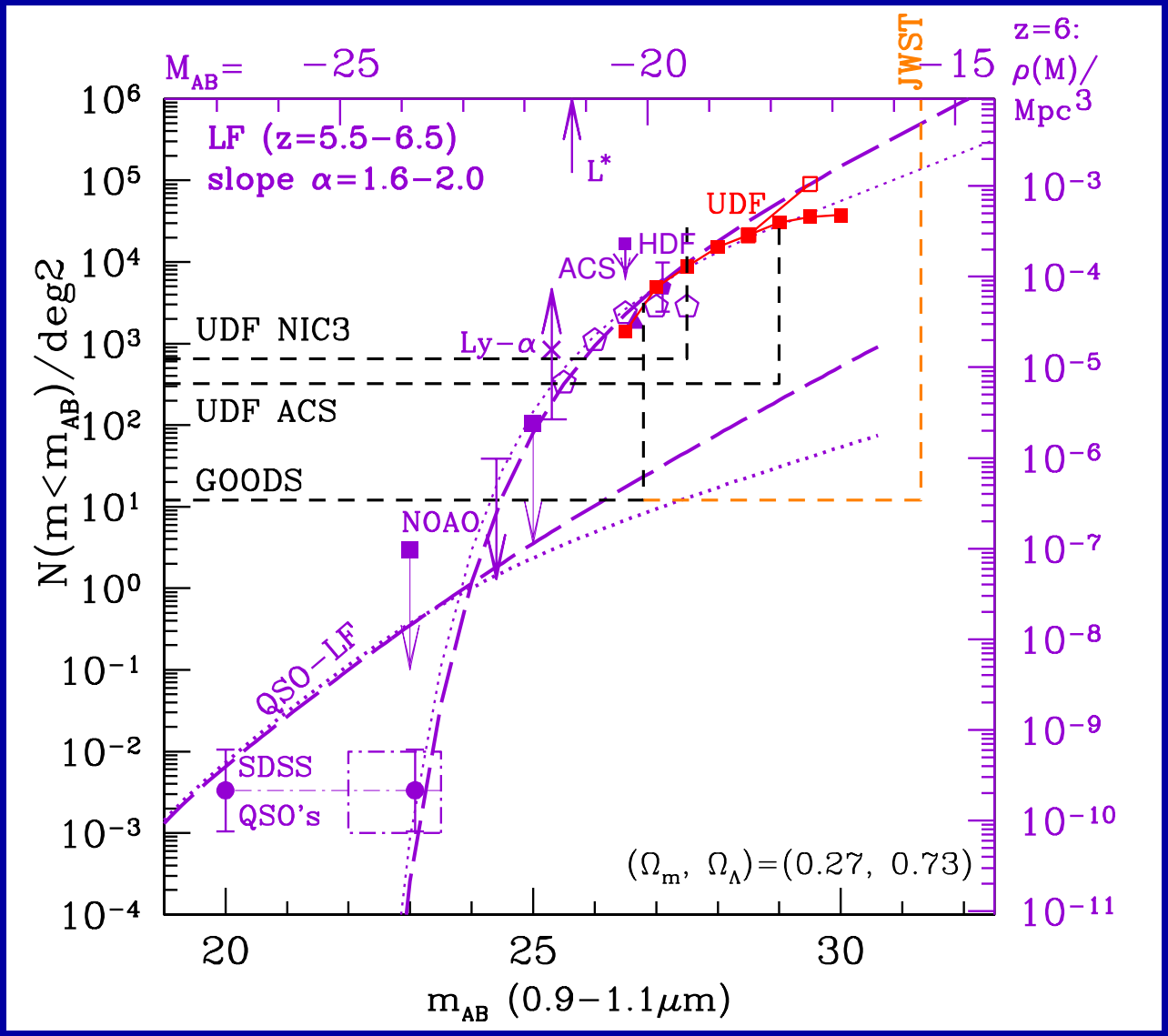

• HST/ACS has made significant progress at z$\simeq$6, surveying very large areas (GOODS, GEMS, COSMOS), or using very long integrations (HUDF). ACS can detect objects at z$\lesssim$6.5, but its discovery space A.Ω.Δlog(λ) cannot map the entire reionization epoch. NICMOS similarly is limited to z$\lesssim$8–10. JWST will be able to trace the entire reionization epoch.

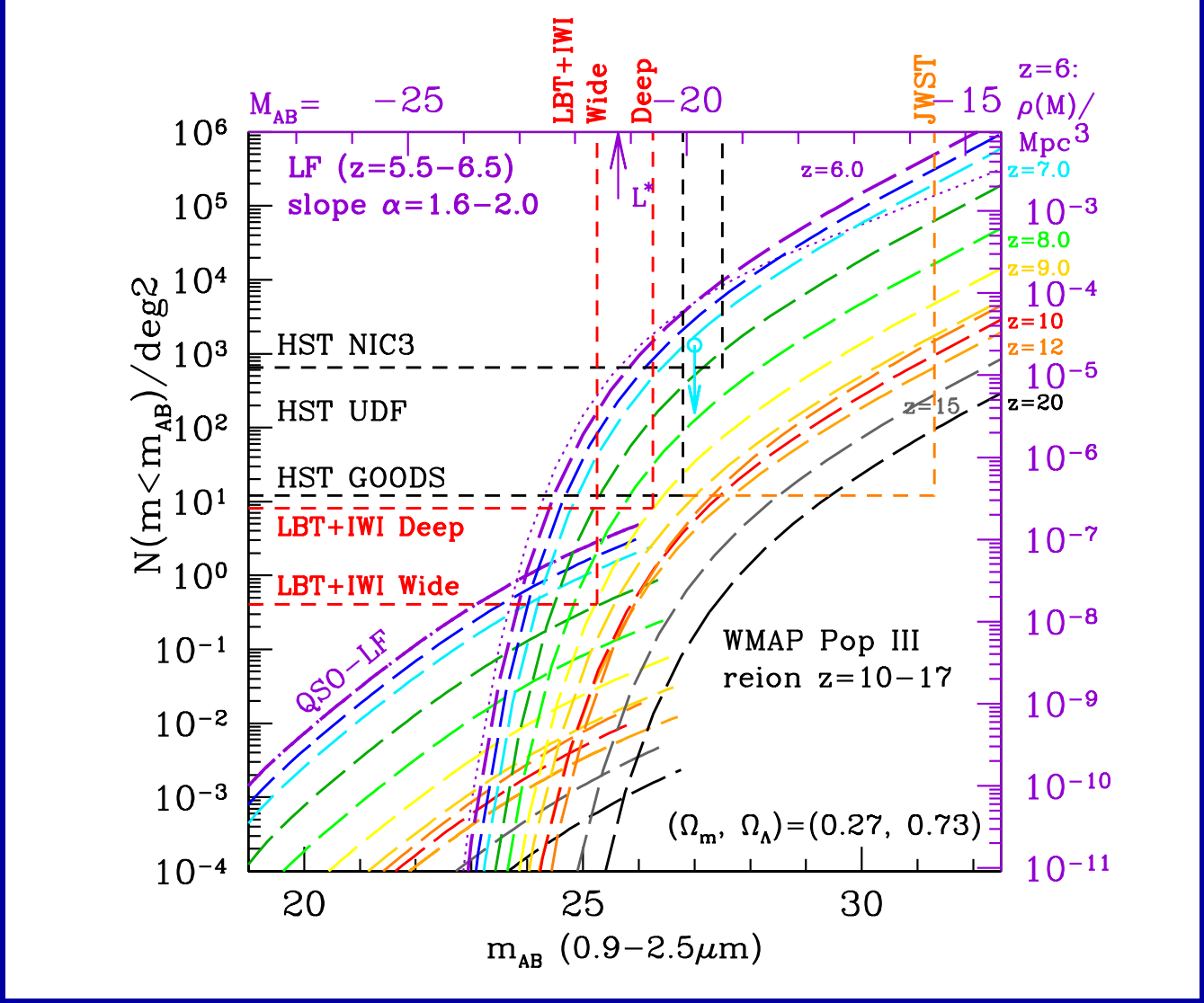

- Red boundaries indicate part of the galaxy and QSO LF that 4–10m class telescopes with WF IRCam can explore to z=10 and AB$\lesssim$25 mag.
- A ground-based wide-field near-IR survey to AB$\lesssim$25 mag z$\lesssim$10 is an essential complement to the JWST First Light studies:
- Co-evolution of supermassive black-holes and proto-bulges for z$\lesssim$10.

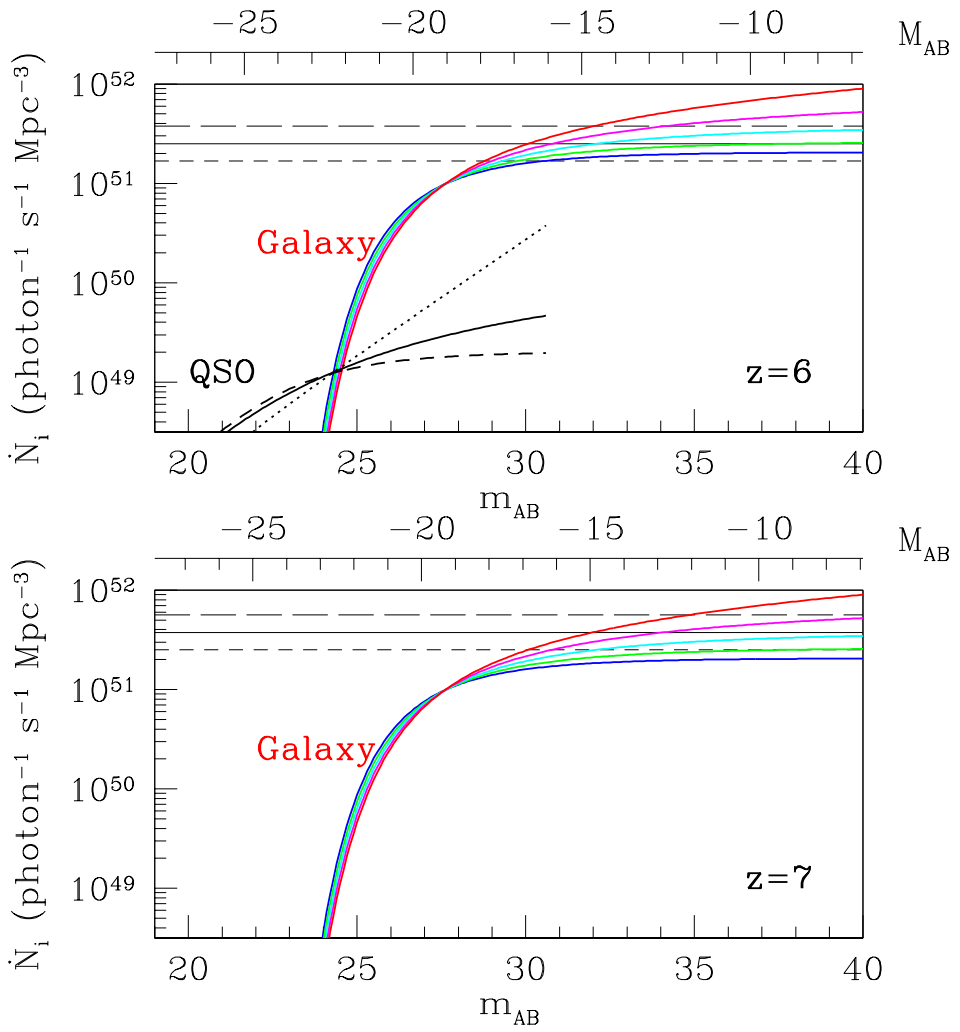

- A steep LF of z≃6 objects (Yan & Windhorst 2004a, ApJL, 600, L1) could provide enough UV-photons to complete the reionization epoch at z≃6.
- Pop II dwarf galaxies may not have started shining *pervasively* much before z≃7–8, or no H-I would be seen in the foreground of z≳6 quasars.
- JWST will measure this numerous population of dwarf galaxies from the end of the reionization epoch at z≃6 into the epoch of First Light (Pop III stars) at z≳10.

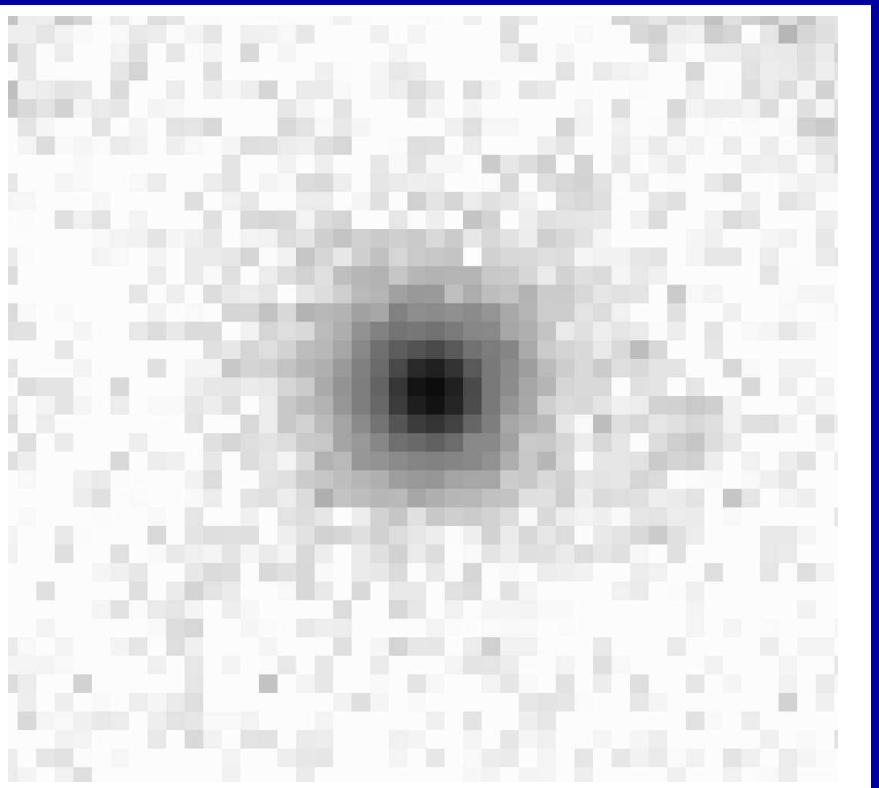

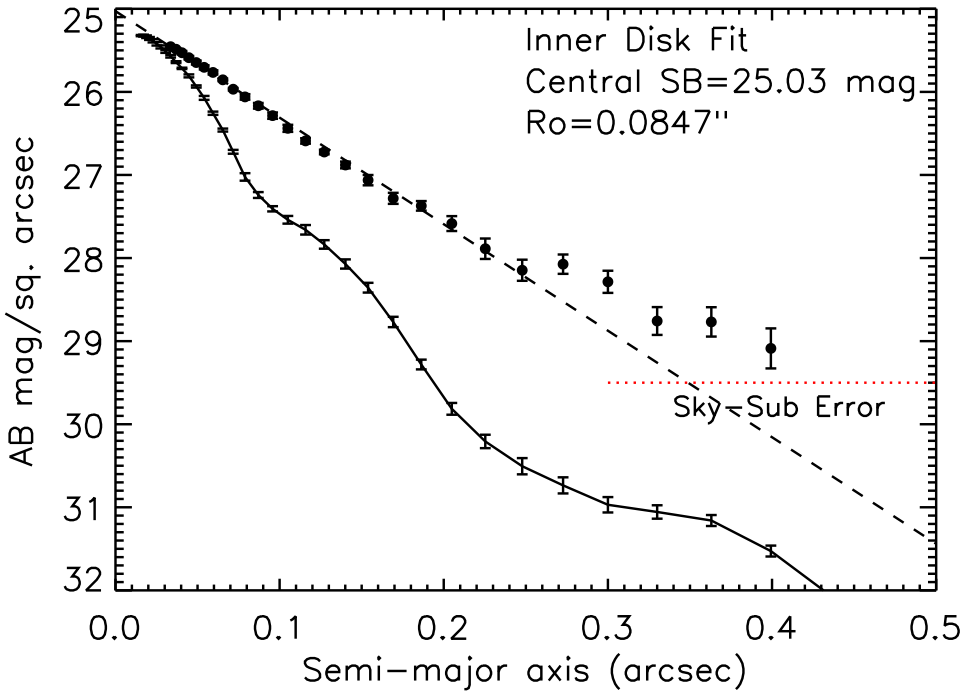

Sum of 49 isolated i-drops:
=5000 hrs HUDF z-band.
[$\simeq$ 330 hrs JWST 1 μm]

ACS light-profile, PSF and sky-error:
Deviates from exp. disk at $r_e \gtrsim 0''.25$
$\Rightarrow$ Dyn. age (z$\simeq$6) $\simeq$ 100-200 Myr
($cf.$ N. Hathi et al. 2006)

HST/ACS cannot accurately measure individual light-profiles at z$\simeq$6.

JWST can do this well for z$\gtrsim$6 in very long integrations.

Dynamical timescale $\simeq$ SED timescale $\Rightarrow$ Bulk of SF at $z_{form} \gtrsim$7.0??

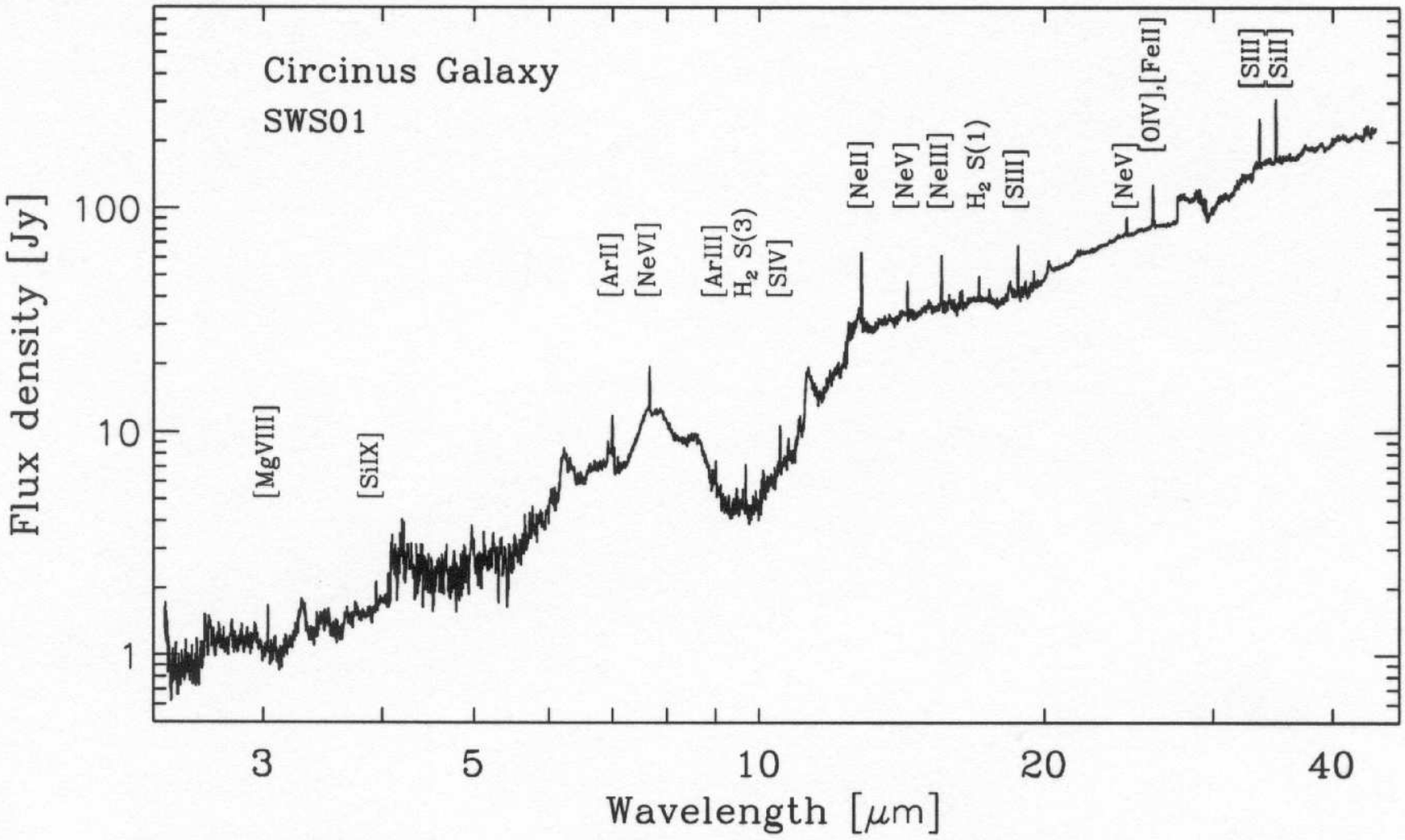

Figure 9. ISO Circinus Spectrum. Mid-infrared spectrum of the Circinus galaxy taken with ISO shows an abundance of emission lines useful for diagnosing the energy sources which power ULIRGs (From Moorwood et al. 1996).

Quantitative Morphology – We can numerically describe and identify m=1 galaxies!

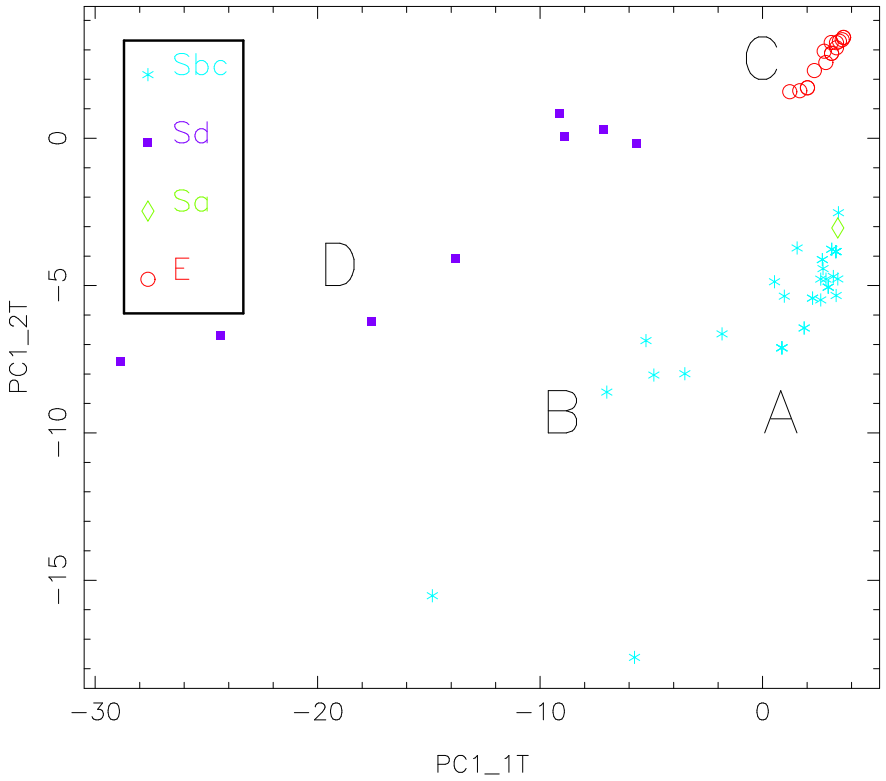

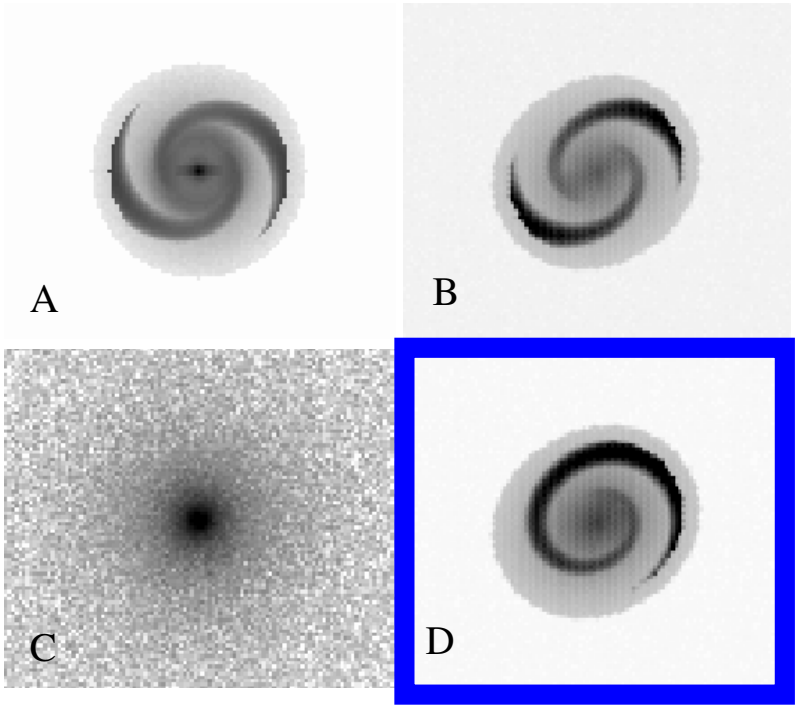

Odewahn et.al. 2002 ApJ, 568, 539

Fourier Decomposition is remarkably good in distinguishing and quantifying bars and (1-armed, 2-armed) spiral structure. JWST will be able to do this out to z=5 at least, hence enabling to quantitatively trace galaxy assembly.

Massive Star Formation: Near and Far

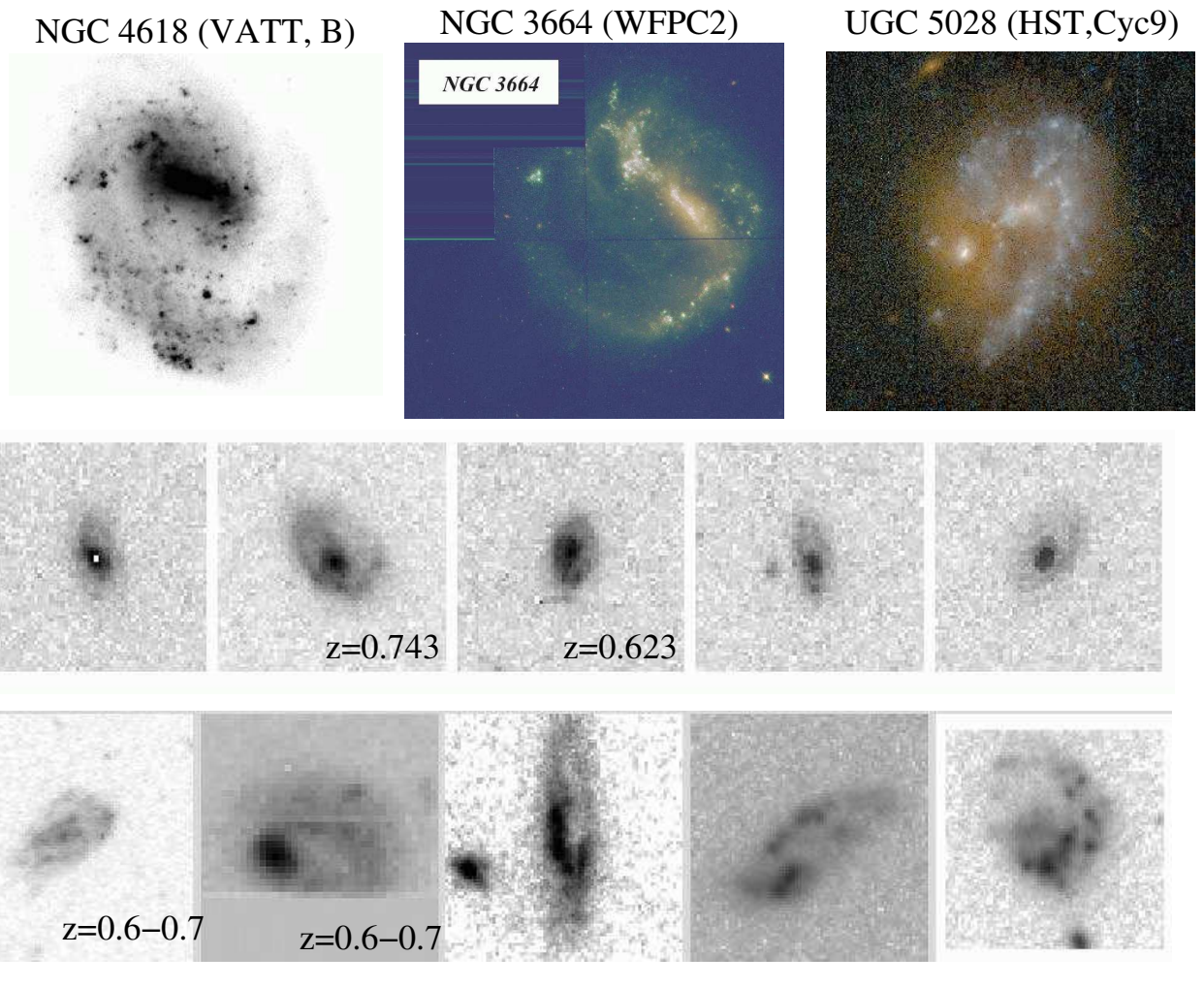

Fourier Decomposition of nearby and distant galaxies in JWST images will directly trace the evolution of bars, rings, spiral arms, and other structural features. This measures the detailed history of galaxy assembly in the epoch $z \simeq 1$–3 when most of today's giant galaxies were made.

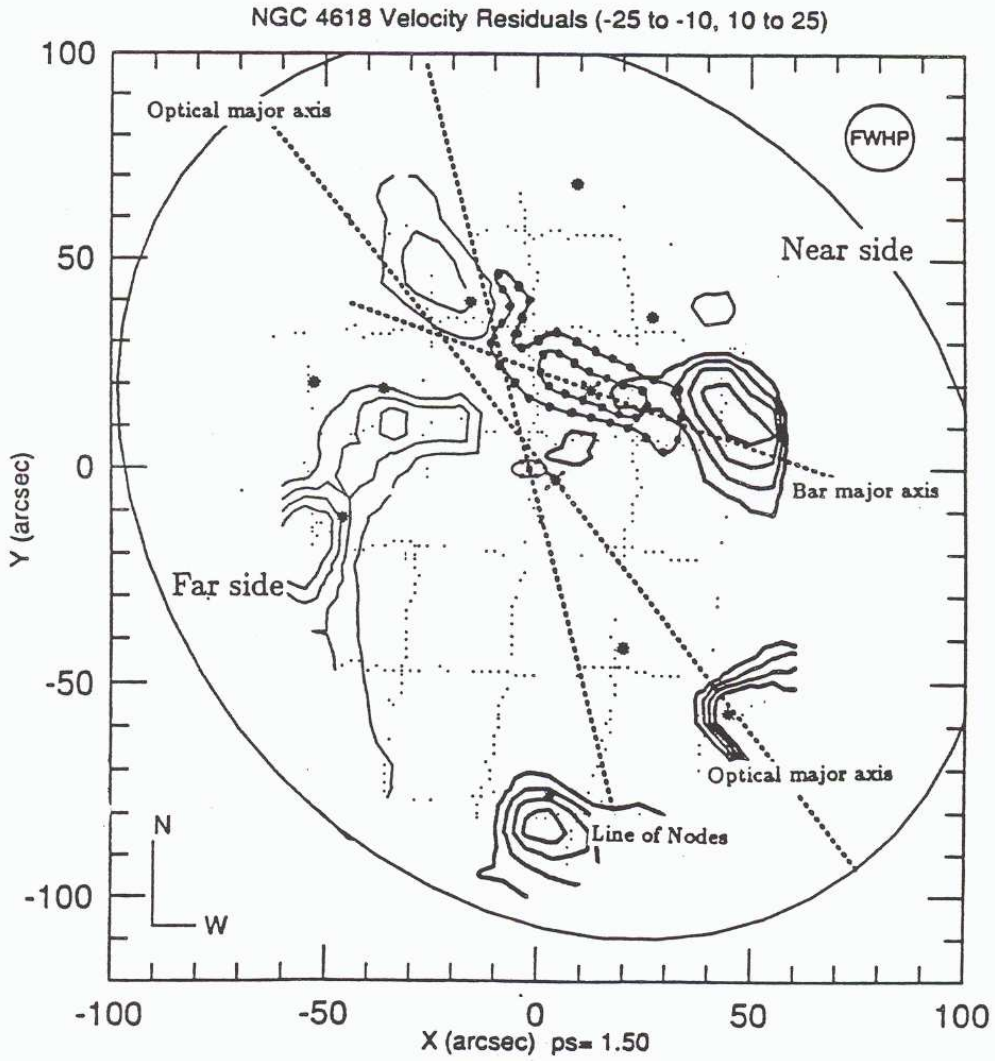

Hα Kinematics in NGC 4618 (Odewahn 1990)

Substantial departures from circular motion in m=1 arms, OFTEN accompanied by large OB associations (SSC?)

Spatially resolved NIRSpec and MIRI integral-field spectra of distant galaxies when compared to the quantitative structure from NIRCam Fourier Decompositions, will directly trace the physical causes of locally enhanced star-formation: infall, bulk velocities in excess of regular rotation, etc.

Hubble UV image of galaxy NGC 6782: spectacular star-forming rings

SPARE CHARTS ON JWST IMAGE SIMULATIONS

(5) Details on JWST image simulations:

- All based on HST/WFPC2 F300W images from the HST mid-UV survey of nearby galaxies (Windhorst et al. 2002,ApJ Suppl. 143, 113).
- WMAP COSMOLOGY: H_0=73 km/s/Mpc, Ω_m=0.24, Ω_Λ=0.76.
- INSTRUMENT: 6.0 m effective aperture, diffraction limited at $\lambda \gtrsim 2.0\mu$m, JWST/NIRCam, 0.″034/pix, read-noise=5.0 e^-, dark-current=0.02 e^-/s, NEP-Sky(1.6 μm)=21.7 mag/($''^2$) in L2, Zodi spectrum, t_{exp}=4×900s.

Row	Telesc.	Redshift	λ (μm)	FWHM ($''$)
1	HST	z∼0	0.293μm	0.″04
	JWST	z=1.0	0.586μm	0.″084
	JWST	z=2.0	0.879μm	0.″084
2	JWST	z=3.0	1.17 μm	0.″084
	JWST	z=5.0	1.76 μm	0.″084
	JWST	z=7.0	2.34 μm	0.″098
3	JWST	z=09.0	2.93 μm	0.″122
	JWST	z=12.0	3.81 μm	0.″160
	JWST	z=15.0	4.69 μm	0.″197

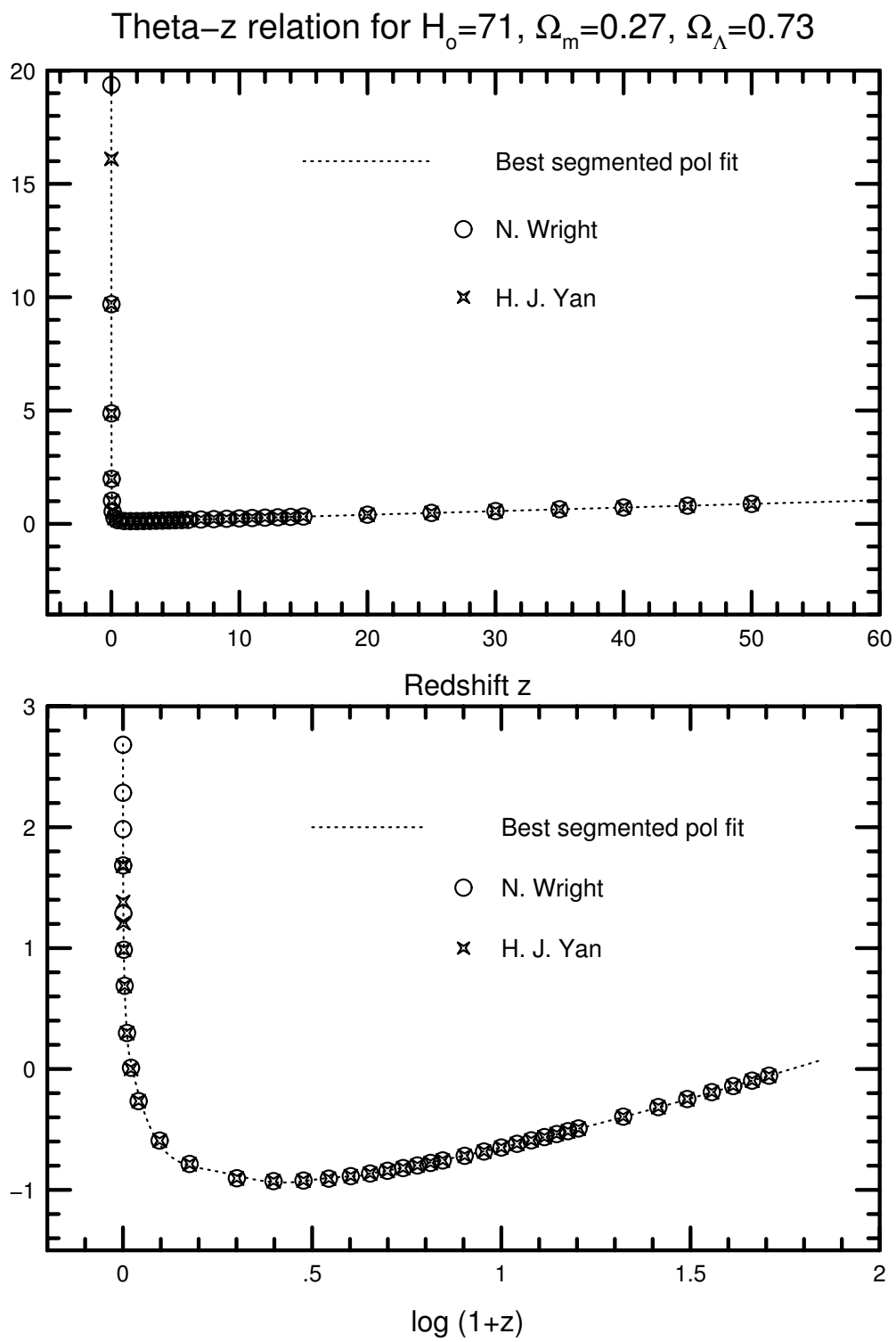

Angular size vs. redshift relation in a Lambda dominated cosmology of H_0 =73 $km\ s^{-1}\ Mpc^{-1}$, Ω_m=0.24, Ω_Λ=0.76.

In the top panel the relation is nearly linear in 1/z for z$\lesssim$0.05 (the small angle approximation) and linear in z for z$\gtrsim$3 (the Lambda dominated universe).

All curvature occurs in the range 0.05$\lesssim$z$\lesssim$3, which is coded up in the IRAF script that does the JWST simulations.

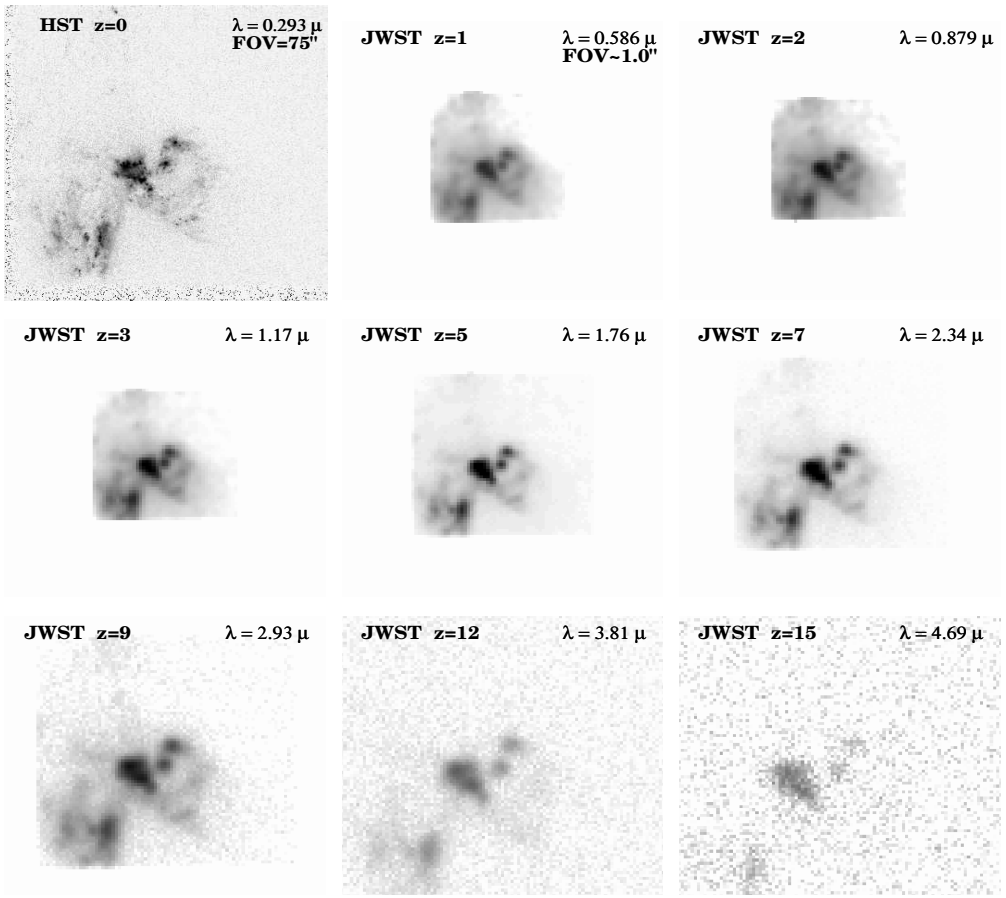

Fig. 4.06.a. JWST simulations based on HST/WFPC2 F300W images of the merger UGC06471-2 (z=0.0104). Note that the two unresolved star-bursting knots in the center remain visible until z∼12, beyond which the SB-dimming also kills their flux. This is the NOMINAL JWST [= (GOALS+REQUIREMENTS)/2].

ASSUMPTIONS: COSMOLOGY: H_0=71 km/s/Mpc, Ω_m=0.27, and Ω_Λ=0.73.

INSTRUMENT: 6.0 m effective aperture, JWST/NIRCam, 0.034″ /pix, RN=5.0 e^-, Dark=0.020 e^-/sec, NEP H-band Sky=21.7 mag/arcsec^2 in L2, Zodiacal spectrum, t_{exp}=1.0 hrs, read-out every 900 sec ("NOMINAL").

Row 1: z=0.0 (HST λ=0.293μm, FWHM=0.04″), z=1.0 (JWST λ=0.586μm, FWHM=0.084″), and z=2.0 (JWST λ=0.879μm, FWHM=0.084″). **Row 2:** z=3.0 (JWST λ=1.17μm, FWHM=0.084″), z=5.0 (JWST λ=1.76μm, FWHM=0.084″), and z=7.0 (JWST λ=2.34μm, FWHM=0.098″). **Row 3:** z=9.0 (JWST λ=2.93μm, FWHM=0.122″), z=12.0 (JWST λ=3.81μm, FWHM=0.160″), and z=15.0 (JWST λ=4.69μm, FWHM=0.197″)

The galaxy merger UGC06471-2 (z=0.0104) is a major and very dusty collision of two massive disk galaxies.

It shows two bright unresolved star-bursting knots to the upper-right of the center, which remain visible until z≃12, beyond which the cosmic SB-dimming kills their flux. These are more typical for the small star-forming objects expected at z≃10–15.

This is the NOMINAL JWST = (GOALS+REQUIREMENTS)/2.

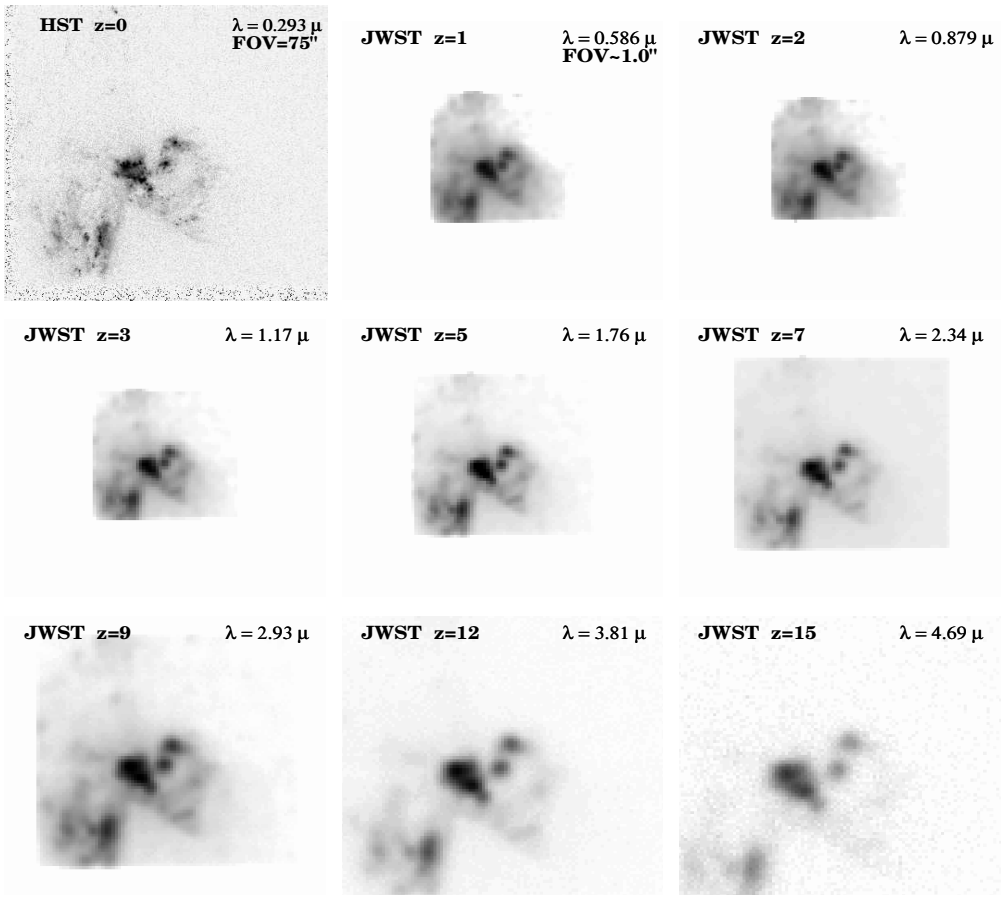

Fig. 4.06.c. JWST simulations based on HST/WFPC2 F300W images of the merger UGC06471-2 (z=0.0104). This is the BEST CASE JWST [meeting all GOALS, and t_{exp}=100 hrs]. The object is recognizable to z≃15.

ASSUMPTIONS: COSMOLOGY: H_0=71 km/s/Mpc, Ω_m=0.27, and Ω_Λ=0.73.

INSTRUMENT: 6.0 m effective aperture, JWST/NIR camera, 0.034″ /pix, RN=3.0 e^-, Dark=0.010 e^-/sec, NEP H-band Sky=21.7 mag/arcsec^2 in L2, Zodi spectrum, t_{exp}=100.0 hrs, read-out every 900 sec ("GOALS").

Row 1: z=0.0 (HST λ=0.293μm, FWHM=0.04″), z=1.0 (JWST λ=0.586μm, FWHM=0.084″), and z=2.0 (JWST λ=0.879μm, FWHM=0.084″). **Row 2:** z=3.0 (JWST λ=1.17μm, FWHM=0.084″), z=5.0 (JWST λ=1.76μm, FWHM=0.084″), and z=7.0 (JWST λ=2.34μm, FWHM=0.098″). **Row 3:** z=9.0 (JWST λ=2.93μm, FWHM=0.122″), z=12.0 (JWST λ=3.81μm, FWHM=0.160″), and z=15.0 (JWST λ=4.69μm, FWHM=0.197″)

The galaxy merger UGC06471-2 (z=0.0104).

This is the BEST CASE JWST. It assumes that all GOALS are met, and that t_{exp}=100 hrs. The whole object (including the two star-forming knots) is recognizable to z≃15.

This does not imply that observing galaxies at z=15 with JWST will be easy. On the contrary, since galaxies formed through hierarchical merging, many objects at z≃10–15 will be 10^1–$10^4\times$ less luminous, requiring to push JWST to its limits.

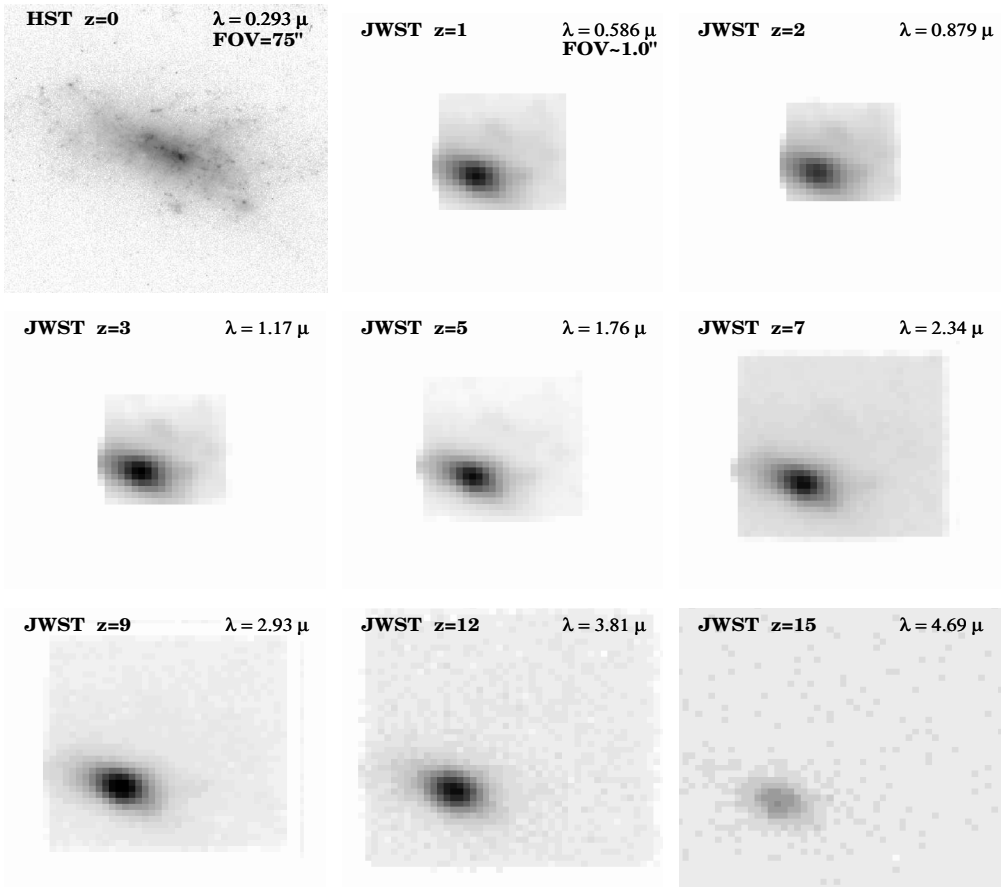

Fig. 4.01. JWST simulations based on HST/WFPC2 F300W images of the dwarf irregular NGC1140 (z=0.0050). This compact high SB object would be visible to z≃15, but hard to classify at all z≥1.

ASSUMPTIONS: COSMOLOGY: H_0=71 km/s/Mpc, Ω_m=0.27, and Ω_Λ=0.73.

INSTRUMENT: 6.0 m effective aperture, JWST/NIRCam, 0.034″ /pix, RN=5.0 e^-, Dark=0.020 e^-/sec, NEP H-band Sky=21.7 mag/arcsec^2 in L2, Zodiacal spectrum, t_{exp}=1.0 hrs, read-out every 900 sec.

Row 1: z=0.0 (HST λ=0.293μm, FWHM=0.04″), z=1.0 (JWST λ=0.586μm, FWHM=0.084″), and z=2.0 (JWST λ=0.879μm, FWHM=0.084″).

Row 2: z=3.0 (JWST λ=1.17μm, FWHM=0.084″), z=5.0 (JWST λ=1.76μm, FWHM=0.084″), and z=7.0 (JWST λ=2.34μm, FWHM=0.098″).

Row 3: z=9.0 (JWST λ=2.93μm, FWHM=0.122″), z=12.0 (JWST λ=3.81μm, FWHM=0.160″), and z=15.0 (JWST λ=4.69μm, FWHM=0.197″)

The compact high-SB dwarf irregular galaxy NGC1140 (z=0.0050).

With JWST, this object would be visible to z≃15, but it will be hard to classify at all redshifts z≥1.

Note that the object indeed reaches a minimum angular size at z≃1.7.

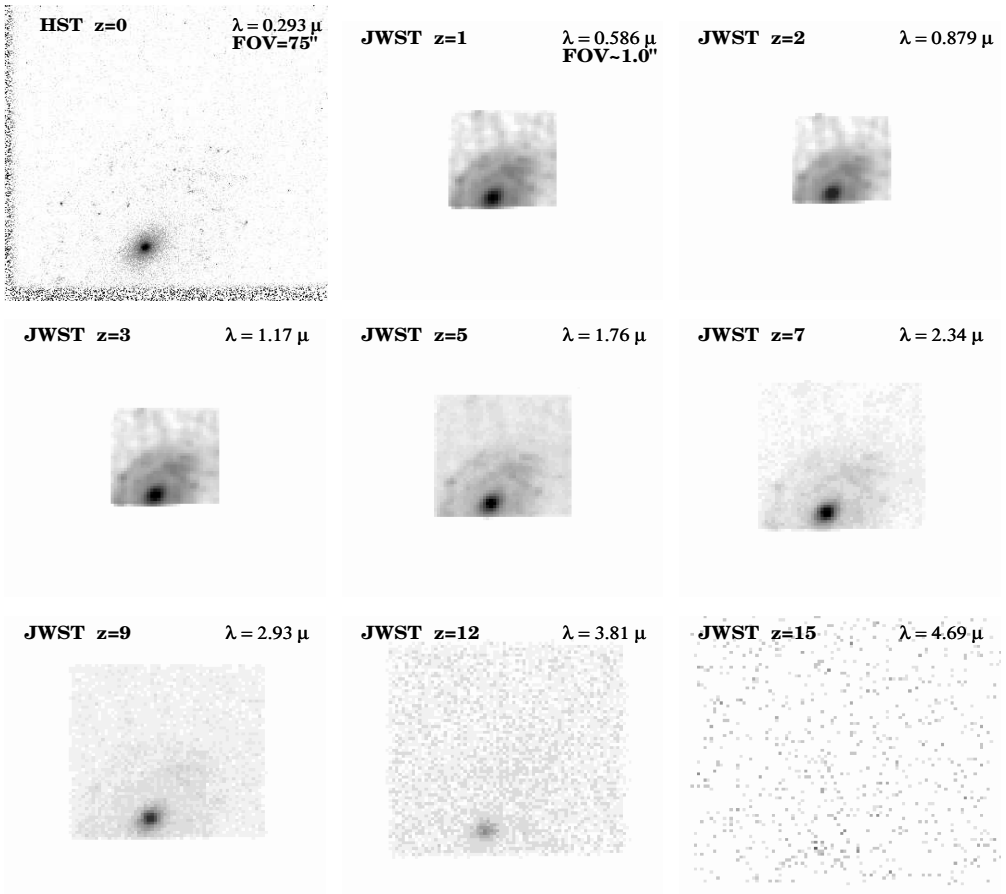

Fig. 4.02. JWST simulations based on HST/WFPC2 F300W images of the mid-type spiral NGC2551 (0.0078). Such an object would be visible to z≃10, but only recognizable to z≃7.

ASSUMPTIONS: COSMOLOGY: H_0=71 km/s/Mpc, Ω_m=0.27, and Ω_Λ=0.73.

INSTRUMENT: 6.0 m effective aperture, JWST/NIRCam, 0.034″ /pix, RN=5.0 e^-, Dark=0.020 e^-/sec, NEP H-band Sky=21.7 mag/arcsec^2 in L2, Zodiacal spectrum, t_{exp}=1.0 hrs, read-out every 900 sec.

Row 1: z=0.0 (HST λ=0.293μm, FWHM=0.04″), z=1.0 (JWST λ=0.586μm, FWHM=0.084″), and z=2.0 (JWST λ=0.879μm, FWHM=0.084″).

Row 2: z=3.0 (JWST λ=1.17μm, FWHM=0.084″), z=5.0 (JWST λ=1.76μm, FWHM=0.084″), and z=7.0 (JWST λ=2.34μm, FWHM=0.098″).

Row 3: z=9.0 (JWST λ=2.93μm, FWHM=0.122″), z=12.0 (JWST λ=3.81μm, FWHM=0.160″), and z=15.0 (JWST λ=4.69μm, FWHM=0.197″)

The mid-type spiral NGC2551 (z=0.0078) would be visible out to z≃10, but only recognizable out to z≃7.

Its disk is in principle visible to z$\gtrsim$5–7. Hence, if such objects are not seen by JWST at z$\lesssim$3, then disks likely form at z$\lesssim$3.

With HST we have seen glimpses of this, but with JWST these will become robust conclusions.

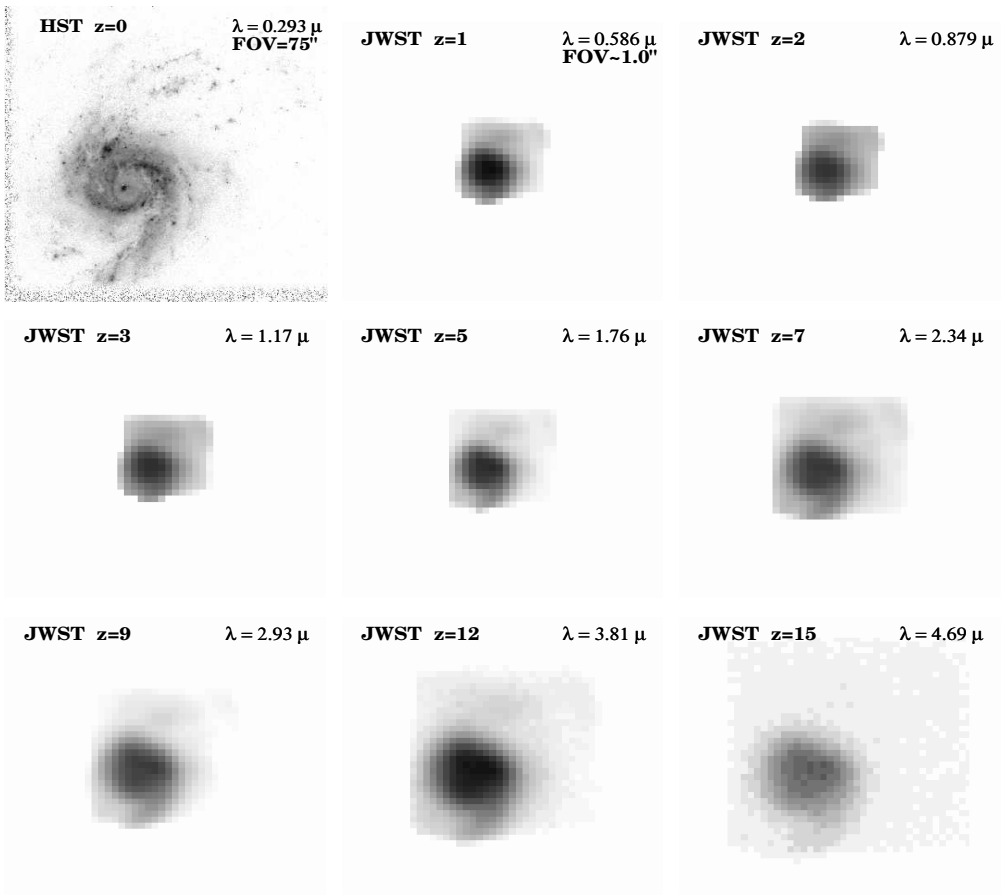

Fig. 4.03. JWST simulations based on HST/WFPC2 F300W images of the high-SB starbursting dwarf spiral galaxy NGC3310 (0.0033). The minimum in the Θ-z relation at z$\simeq$1.7 and the JWST diffraction limit at $\lambda \geq 2.2\mu$m — combined with the object's very high rest-frame UV SB — conspire to improve the effective JWST resolution on the mid-UV morphology of this object from z$\simeq$2 to z$\simeq$7.

ASSUMPTIONS: COSMOLOGY: H_0=71 km/s/Mpc, Ω_m=0.27, and Ω_Λ=0.73. INSTRUMENT: 6.0 m effective aperture, JWST/NIRCam, 0.034″ /pix, RN=5.0 e^-, Dark=0.020 e^-/sec, NEP H-band Sky=21.7 mag/arcsec^2 in L2, Zodiacal spectrum, t_{exp}=1.0 hrs, read-out every 900 sec.

Row 1: z=0.0 (HST λ=0.293μm, FWHM=0.04″), z=1.0 (JWST λ=0.586μm, FWHM=0.084″), and z=2.0 (JWST λ=0.879μm, FWHM=0.084″). **Row 2:** z=3.0 (JWST λ=1.17μm, FWHM=0.084″), z=5.0 (JWST λ=1.76μm, FWHM=0.084″), and z=7.0 (JWST λ=2.34μm, FWHM=0.098″). **Row 3:** z=9.0 (JWST λ=2.93μm, FWHM=0.122″), z=12.0 (JWST λ=3.81μm, FWHM=0.160″), and z=15.0 (JWST λ=4.69μm, FWHM=0.197″)

The very high-SB, compact starbursting dwarf spiral galaxy NGC3310 (z=0.0033).

The minimum in the Θ-z relation at z$\simeq$1.7 and the JWST diffraction limit at $\lambda \geq 2.2\ \mu$m — combined with the object's very high rest-frame UV-SB — conspire to improve the effective JWST resolution on the mid-UV morphology of this object from z$\simeq$2 to z$\simeq$7.

A rather exceptional case of where cosmology doesn't appear to cost you prohibitive sensitivity, but gains you resolution!

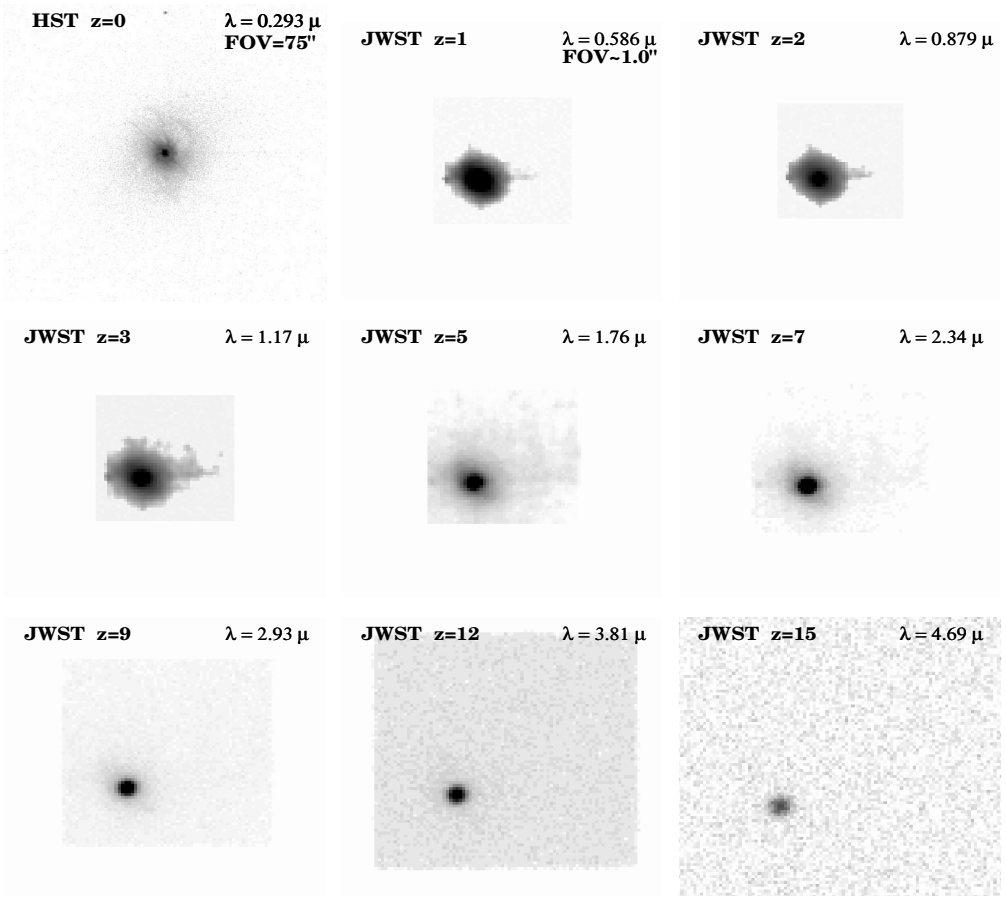

Fig. 4.04. JWST simulations based on HST/WFPC2 F300W images of the Seyfert galaxy NGC3516 (0.0088). Note that the faint nebulosity surrounding the AGN in the mid-UV at z=0 essentially disappears at z≥7, so that at high redshifts such objects would look like a pure AGN.

ASSUMPTIONS: COSMOLOGY: H_0=71 km/s/Mpc, Ω_m=0.27, and Ω_Λ=0.73.

INSTRUMENT: 6.0 m effective aperture, JWST/NIRCam, 0.034″ /pix, RN=5.0 e^-, Dark=0.020 e^-/sec, NEP H-band Sky=21.7 mag/arcsec^2 in L2, Zodiacal spectrum, t_{exp}=1.0 hrs, read-out every 900 sec.

Row 1: z=0.0 (HST λ=0.293μm, FWHM=0.04″), z=1.0 (JWST λ=0.586μm, FWHM=0.084″), and z=2.0 (JWST λ=0.879μm, FWHM=0.084″). **Row 2:** z=3.0 (JWST λ=1.17μm, FWHM=0.084″), z=5.0 (JWST λ=1.76μm, FWHM=0.084″), and z=7.0 (JWST λ=2.34μm, FWHM=0.098″). **Row 3:** z=9.0 (JWST λ=2.93μm, FWHM=0.122″), z=12.0 (JWST λ=3.81μm, FWHM=0.160″), and z=15.0 (JWST λ=4.69μm, FWHM=0.197″)

The Seyfert galaxy NGC3516 (z=0.0088) has a faint nebulosity surrounding its AGN in the mid-UV, while at longer wavelengths the surrounding elliptical galaxy is present (not shown here).

The nebulosity surrounding the AGN is essentially SB-dimmed away at z≥7, so that at high redshifts these objects would look like purely stellar objects ("quasars").

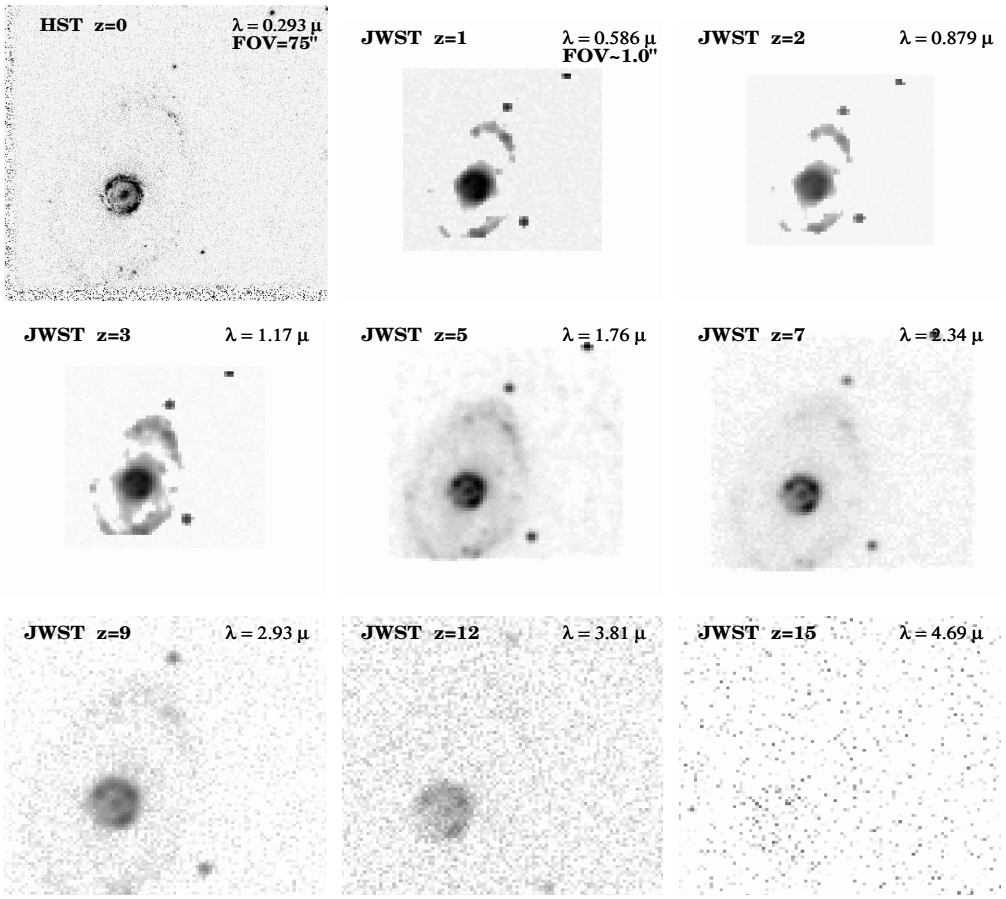

Fig. 4.05. JWST simulations based on HST/WFPC2 F300W images of the barred ring galaxy NGC6782 (0.0125). Note again that for z≃2–7, the effective resolution on the bright star-forming ring improves with increasing redshift, until the $(1+z)^4$-dimming completely kills it for z≳10.

ASSUMPTIONS: COSMOLOGY: H_0=71 km/s/Mpc, Ω_m=0.27, and Ω_Λ=0.73.

INSTRUMENT: 6.0 m effective aperture, JWST/NIRCam, 0.034″ /pix, RN=5.0 e^-, Dark=0.020 e^-/sec, NEP H-band Sky=21.7 mag/arcsec^2 in L2, Zodiacal spectrum, t_{exp}=1.0 hrs, read-out every 900 sec.

Row 1: z=0.0 (HST λ=0.293μm, FWHM=0.04″), z=1.0 (JWST λ=0.586μm, FWHM=0.084″), and z=2.0 (JWST λ=0.879μm, FWHM=0.084″). **Row 2:** z=3.0 (JWST λ=1.17μm, FWHM=0.084″), z=5.0 (JWST λ=1.76μm, FWHM=0.084″), and z=7.0 (JWST λ=2.34μm, FWHM=0.098″). **Row 3:** z=9.0 (JWST λ=2.93μm, FWHM=0.122″), z=12.0 (JWST λ=3.81μm, FWHM=0.160″), and z=15.0 (JWST λ=4.69μm, FWHM=0.197″)

The barred ring galaxy NGC6782 (0.0125) shows that at z≃2 to z≃7, the effective resolution on its high-SB bright star-forming ring improves with increasing redshift, until the $(1+z)^4$-dimming completely kills it for z≳10–12.

Another good case showing why cosmology is not "WYSIWYG".